FROG VIRUS 3: TRACKING VIRAL SPREAD USING MOLECULAR TOOLS

A thesis Submitted to the Committee on Graduate Studies in Partial Fulfillment of the Requirements for the Degree of Master of Science in the Faculty of Arts and Sciences

TRENT UNIVERSITY

Peterborough, Ontario, Canada

Environmental and Life Sciences M.Sc. Graduate Program

September 2018

ABSTRACT

Frog Virus 3: Tracking Viral Spread Using Molecular Tools

Samantha Adrianna Grant

Understanding the maintenance and spread of invasive diseases is critical in evaluating threats to biodiversity and how to best minimize their impact, which can by done by monitoring disease occurrences across time and space. I sought to apply existing and upcoming molecular tools to assess fluctuations in both presence and strain variation of frog virus 3 (FV3), a species of *Ranavirus*, across Canadian waterbodies. I explored the temporal patterns and spatial distribution of ranavirus presence across multiple months and seasons using environmental DNA techniques. Results indicate that ranavirus was present in approximately 72.5% of waterbodies sampled on a fine geographical scale (<10km between sites, 7,150 km^2), with higher detection rates in later summer months than earlier. I then explored the sequence variability at the major capsid protein gene (MCP) and putative virulence gene (vIF-2α) of FV3 samples from Ontario, Alberta, and the Northwest Territories, with the premise of understanding pathogen movement across the landscape. However, a lack of genetic diversity was found across regions, likely due to a lack of informative variation at the chosen genetic markers or lack of mutation. Instead, I found a novel FV3-like ranavirus and evidence for a recombinant between FV3 and a ranavirus of another lineage. This thesis provides a deeper understanding into the spatio-temporal distribution of FV3, with an idea of how widespread and threatening ranaviruses are to amphibian diversity.

Keywords: ranavirus, frog virus 3, amphibians, environmental DNA, phylogenetics, wildlife disease, disease surveillance, major capsid protein, vIF-2α

ACKNOWLEDGEMENTS

These past few years have been a roller coaster of ups and downs, from challenges and tears and frustration, to breakthroughs and laughter and relief, and I would like to thank everyone who brought me to my success, as well as those who supported me through my worst days. First, I would like to thank Dr. Christopher Kyle for his supervisory guidance, and for never giving up on me even when I felt like my work was a lost cause, and for pushing me to be the best that I can be. I would also like to thank my supervisory committee, Dr. Craig Brunetti, Dr. Chris Wilson, my defence committee member Dr. Christina Davy, and honourary mentions to Dr. Dennis Murray, Dr. Sibelle Vilaça, Dr. David Lesbarrères, Joe-Felix Bienentreu, and Meg Congram for their guidance, constant support, and their collaborative assistance in progressing my project further than I thought imaginable.

There were many people who helped me across all steps of my journey, from in the field, to the lab, to writing. I would like to thank past and present members of the Kyle lab for troubleshooting lab problems and keeping me sane with a good joke or two (or fifty). Thank you to members of the Murray lab, especially those on the eDNA project for their advice and encouragement when we were all discouraged, and reminding each other that we're going to make it out okay in the end. I'd also like to thank the many people who offered their assistance from the NRDPFC, Laurentian University, the Wilson fish lab, and the people who helped me with field work. And thank you to everyone in the Forensic Science department at Trent, who encouraged me as well as hired me as a TA which allowed me to afford to eat throughout my journey.

There are many friends who have shared with me laughter and adventures over the years here at Trent, all of which I'm very grateful for being in my life. A huge thank you to my friends who have been here from the beginning, Erin Prewer, Emilee Storfie, Mark Seegobin, Katelyn Jackson, and Kristi Goulet. To Adrian Borlestean, for his endless support, encouragement, and optimism, who makes me a better person. Also to my closest and oldest friends, Madison Bird, Laura Epp-Ruitenberg, and Sierra Barnes. To the many amazing people who went rock climbing with me, fellow TAs, fellow graduate students, and past and present roommates. And a special shout out to the can of peaches in my cupboard for always being my backup plan.

And of course, I'd like to thank my parents, Yvonne and Ian Grant, and my sister Rebecca. For being a phone call away in the middle of the night when I felt all hope was lost, for listening to my endless bouts of frustration, for sending me care packages when I was homesick, and for always having a big hug ready for me whenever I came home. Their endless love, encouragement, thoughtfulness, reassurance, assistance, devotion, and support helped bring me to where I am today. Thank you all for your endless support and love through this journey.

TABLE OF CONTENTS

LIST OF TABLES

LIST OF FIGURES

CHAPTER 1

GENERAL INTRODUCTION

1.1 Background

Biodiversity is important for the maintenance of healthy ecosystems (Stuart *et al.* 2004), yet biodiversity is being lost at an accelerating rate (Singh 2002; Romansic *et al.* 2009; Keesing *et al.* 2010). Factors undermining biodiversity are most often from anthropogenic influences such as pollution, habitat destruction, human translocation, climate change, and increased competition from invasive species (Daszak *et al.* 2001; Keesing *et al.* 2010). Alongside these threats, biodiversity is also threatened by emerging and invasive diseases (Daszak *et al.* 2000; Echaubard *et al.* 2014), such as in instances where climatic changes have led to increased temperatures or precipitation that facilitate disease persistence and dispersal (Kutz *et al.* 2005; Ariel *et al.* 2009). Monitoring invasive diseases, and understanding mechanisms of their maintenance and spread is critical in providing information on the extent of impact on biodiversity and how to best manage and minimize their impact (Belant & Deese 2010).

1.2 Amphibian Declines and Disease

Over the past twenty years, there have been increasing reports of declines in amphibian populations around the globe (Harp & Petranka 2006). These declines are thought to be linked to a number of anthropogenic factors, including habitat destruction, pollution, climate change, agriculture run-off, herbicides, pesticides, wildlife diseases, and wildlife trade (Harp & Petranka 2006; Gray *et al.* 2007; Schock *et al.* 2009; Duffus *et al.* 2015). Of note is that many of these factors increase stress on amphibians, which compromises their immune responses and makes them more susceptible to diseases (Gray *et al.* 2009; Reeve *et al.* 2013). In fact, emerging

infectious diseases are considered a major cause for amphibian population declines (Daszak *et al.* 2000). For example, Gray *et al.* (2007) found that *Rana clamitans* (green frog) tadpoles were 25% more likely to become infected with disease when inhabited in a wetland next to a cattle farm, where there was a high deposition of nitrogenous waste. The global dispersal of several amphibian pathogens has mainly been attributed to wildlife trade, as amphibians are marketed across the world for human consumption, as exotic pets, and as fishing bait (Picco *et al.* 2007; Schloegel *et al.* 2009; Kolby *et al.* 2014). The introduction of new pathogens to naïve populations of amphibians has been associated with massive die-off events across the globe, with initial infection often arising in trade facilities and then spreading to wild populations due to release or accidental escape (Zhang *et al.* 2001; Xu *et al.* 2010; Brunner *et al.* 2015; Duffus *et al.* 2015; Epstein & Storfer 2015).

Amphibians are affected by a myriad of pathogens including viruses, fungi, trematodes, parasites, and water molds. One example is *Saprolegnia ferax*, a fungus-like protist known as a water mold that lingers in moist habitats and primarily causes mortality in frog embryos and very early larval stages of some frog species (Romansic *et al.* 2009). While *S. ferax* is not a major threat to all life stages, water mold infection rates are associated with increasing UV-B exposure, caused by the thinning of the earth's ozone layer (Kiesecker *et al.* 2001). Another less common pathogen is the trematode *Ribeiroia* sp., a parasite whose larvae infect the hind limbs of amphibians, forming subcutaneous cysts and causing malformations (Johnson *et al.* 2002; Daszak *et al.* 2003; Huver & Koprivnikar 2015). Malformations include missing limbs, extra limbs, and skin webbings, all of which decrease survivorship in adults (Johnson *et al.* 2002). While these diseases have negative impacts on amphibians, other pathogens have more direct and pronounced effects, having higher mortality rates. Specifically *Batrachochytrium*

dendrobatidis (*Bd*) and *Batrachochytrium salamandrivorans* (*Bsal*), are chytrid fungi that are highly lethal to amphibians (Gray *et al.* 2015b; James *et al.* 2015); and ranaviruses are a group of highly infectious viruses that systemically infect amphibians at all life-stages and can cause mortality rates upwards of 90% in juveniles (Greer *et al.* 2005; Gray *et al.* 2009).

Bd was first recognized in the 1990s and was listed as a notifiable disease by the World Organization of Animal Health (OIE) in 2009 (Longcore *et al.* 1999; Olson *et al.* 2013), meaning that reports of this pathogen are required by law to be notified to government authorities. While *Bd* was first described in the 1990s, the earliest records of the effects of this disease were documented in 1974, collected in North American *Lithobates pipiens* (Carey *et al.* 1999). *Bd* is present on all continents except Antarctica, infects over 350 amphibian species (Skerratt *et al.* 2007), and is responsible for ongoing rapid amphibian declines around the globe in both captive and wild populations (Carey *et al.* 1999; Boyle *et al.* 2004). In Australia, the emergence of *Bd* has been associated with an absence of observations for six native species of frog now assumed to be extinct (García-Díaz *et al.* 2016). Infection of *Bd* often causes a fatal and rapidly progressing disease known as chytridiomycosis (Fisher *et al.* 2009). Attributing host death to *Bd* is sometimes difficult as *Bd* does not present easily noticeable symptoms (Fisher *et al.* 2009). However, the fungus is known to target keratinized regions such as mouthparts in tadpole and cause hyperkeratosis on the skin of metamorphic frogs, suggesting that amphibians suffocate due to thickened skin (Fisher *et al.* 2009). While keratinised mouthparts on tadpoles is not always fatal, infected individuals following metamorphosis often maintain the infection and succumb as an adult (Boyle *et al.* 2004).

Bsal primarily threatens salamander species, whereas *Bd* is more infectious in frog species (Gray *et al.* 2015b). While *Bd* causes hyperkeratosis which is difficult to see, *Bsal* tends

to form skin ulcerations and epidermis degradation, which are easier to observe macroscopically (Gray *et al.* 2015b). The *Bsal* fungus originated from Asia, and was introduced to the Netherlands likely through international trade of salamanders and newts (Martel *et al.* 2014). Since its introduction, fire salamander (*Salamandra salamandra*) populations within the Netherlands have been extirpated, and the fungus has been introduced in Germany, Belgium, and the United Kingdom (Martel *et al.* 2013, 2014; Gray *et al.* 2015b). While *Bsal* is currently not considered to be in North America, introduction through international trade could cause extreme threats to salamander biodiversity, as North America houses 48% of all known salamander species (Yap *et al.* 2015).

1.3 Ranaviruses

Ranaviruses are a group of double stranded DNA viruses within the family *Iridoviridae* (Bayley *et al.* 2013). *Iridoviridae* are amongst a group of families of nucleocytoplasmic large DNA viruses (NCLDV) that infect eukaryotes ranging from single-celled organisms all the way to humans. Other families within this group include *Mimiviridae* that infect amoeba, and *Poxviridae*, the family that includes human smallpox virus (Claverie *et al.* 2009; Yutin & Koonin 2012). Specifically, *Iridoviridae* family is made up of five genera that infect insects (*Iridovirus and Chloriridovirus*) and cold-blooded vertebrates (*Megalocytivirus, Lymphocytivirus,* and *Ranavirus*) (Tan *et al.* 2004; Forzán *et al.* 2017). As of 2015, ranaviruses have been documented to infect over 175 ectothermic vertebrates across all continents except Antarctica (Goorha & Murti 1982; Duffus *et al.* 2015). Ranaviruses only replicate at 32 ^{o}C or lower, largely explaining why they only infect ectothermic vertebrates and not warm blooded species (Granoff *et al.* 1965).

There are currently over 20 ranaviruses described under the genus *Ranavirus*, however, based on genetic similarity and host species, only seven are recognized by the International Committee on Taxonomy of Viruses (ICTV) as distinct virus species. Iridoviruses were grouped by the ICTV based on capsid properties, virion size and symmetry, and 26 shared core genes (Eaton *et al.* 2007). The seven recognized species are frog virus 3 (FV3), *Bohle iridovirus* (BIV), *Ambystoma tigrinum* virus (ATV), *Epizootic hematopoietic necrosis virus* (EHNV), European catfish virus (ECV), Santee-Cooper ranavirus (SCRV), and Singapore grouper iridovirus (SGIV) (Jancovich *et al.* 2012; Gregory Chinchar *et al.* 2017). While there are more ranaviruses beyond these seven, the remaining viruses are grouped within distinct lineages, based on sequence relatedness, host species, genome size, protein profiles, and restriction fragment length polymorphisms (RFLP) (Figure 1, Tan *et al.* 2004; Jancovich *et al.* 2012, 2015b). Many of these ranaviruses are also named based on the species they were isolated from, e.g., Spotted salamander Maine (SSME), tiger frog virus (TFV), and *Rana grylio* virus (RGV), etc. All of these fall within the lineage of FV3, suggesting that they may be isolates of the same species, rather than species of their own (Figure 1.1, Chinchar *et al.* 2017).

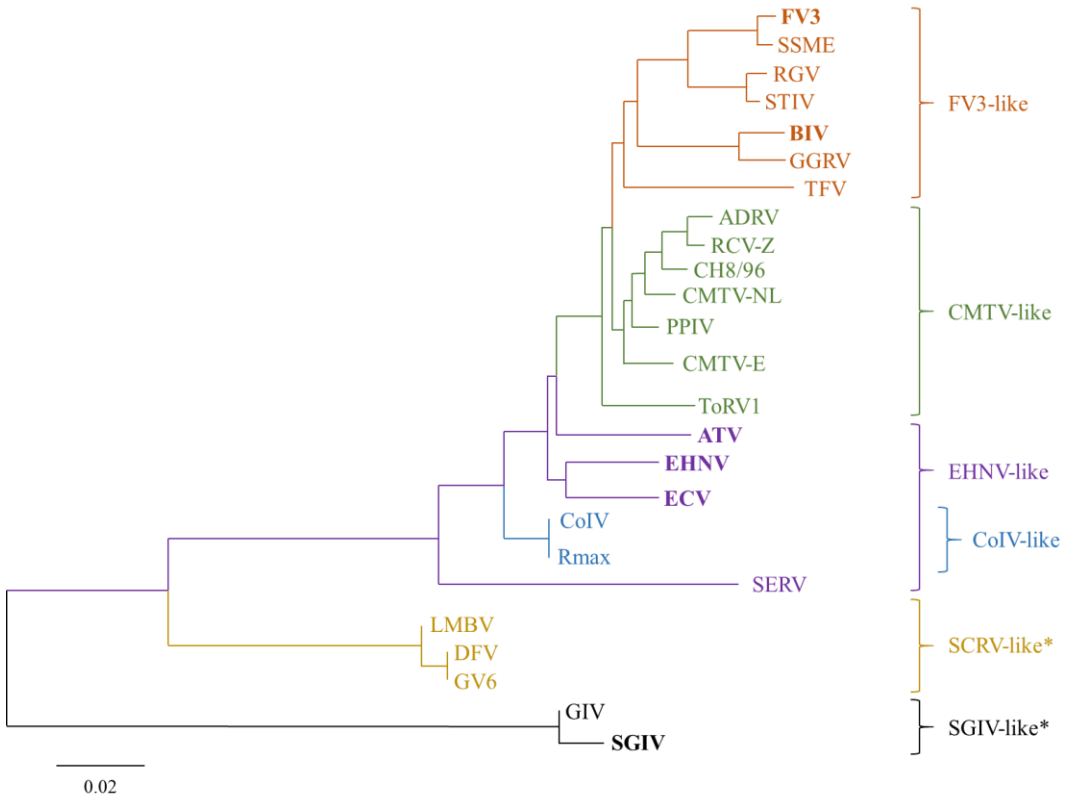

Figure 1.1: Phylogram showing evolutionary relationships and lineages between 25 ranaviruses based on their aligned genomes. The lineages include FV3-like: Frog virus 3 (FV3), spotted salamander Maine (SSME), Rana grylio virus (RGV), soft-shelled turtle iridovirus (STIV), Bohle iridovirus (BIV), German gecko ranavirus (GGRV), tiger frog virus (TFV); CMTV-like: *Andrias davidianus* ranavirus (ADRV), Rana catesbiana virus (RCV-Z), Testudo hermanni ranavirus (CH8/96), common midwife toad virus (CMTV-NL, CMTV-E), pike-perch iridovirus (PPIV), and tortoise ranavirus 1 (ToRV1); CoIV-like: Cod iridovirus (CoIV), and ranavirus maximus (Rmax); EHNV-like: *Ambystoma tigrinum* virus (ATV), epizootic hematopoietic necrosis virus (EHNV), European catfish virus (ECV), and short-finned eel ranavirus (SERV); SCRV-like (a combination of viruses under the Santee-Cooper ranavirus): Largemouth bass virus (LMBV), doctor fish virus (DFV), and guppy virus 6 (GV6); and SGIV-like: Grouper iridovirus (GIV), and Singapore grouper iridovirus (SGIV). Viruses in bold are recognized as species of ranavirus. Lineages with an asterisk denote clusters of ranaviruses that are highly divergent and may be classified as independent genera from ranaviruses. Phylogenetic tree was referenced based on figures from (Jancovich *et al.* 2015b; Chinchar *et al.* 2017; Claytor *et al.* 2017).

1.4 Frog Virus 3

The best characterized species of ranavirus is frog virus 3 (FV3). FV3 was first isolated in a northern leopard frog (*Lithobates pipiens*) in the Midwest United states in 1965, but it was initially assumed not to have a major impact on the environment due to a lack of reported outbreaks (Granoff *et al.* 1965). Since then, FV3 has been isolated from many species that include: amphibians, reptiles, and fish (Chinchar *et al.* 2011; Jancovich *et al.* 2015b). FV3 was the first ranavirus species described. Since then, many FV3 species and isolates have been isolated from wild and captive populations due to increased surveillance and study (Chinchar 2002). The genome structure of FV3 was first investigated in the early 1980s (Goorha & Murti 1982), and later sequenced (Tan *et al.* 2004) to learn more about ranaviral organization and molecular mechanisms of replication.

1.5 Etiology of FV3

FV3 as well as other ranaviruses cause systemic infections that spread to multiple organs, starting with the kidney, then liver, gastrointestinal tract, and skin (Gantress *et al.* 2003). Clinical symptoms of the virus include lethargy, erythema, edema, hemorrhaging, limb and body swelling, and ultimately death (Greer *et al.* 2005; Harp & Petranka 2006; Miller *et al.* 2015). The virus can be transmitted in one of three ways: direct contact of an infected individual to a susceptible one, indirect contact through the water, or by cannibalising an infected animal (Harp & Petranka 2006; Brunner *et al.* 2007; Cunningham *et al.* 2007; Brenes *et al.* 2014). The gastrointestinal tract is likely the primary point of entry of ranaviruses, with virus detection occurring after 3 hours of waterborne exposure by healthy individuals (Robert *et al.* 2011). Many amphibians secrete antimicrobial peptides from their skin, which combat against ranaviruses

from easily entering their system through their skin (Chinchar *et al.* 2001; O'Rourke 2007; Gray *et al.* 2009), but contact transfer is not impossible, especially direct contact on tadpoles (Brunner *et al.* 2007).

Onset of mortality of infected larvae is usually rapid, often only taking a matter of days before thousands of previously healthy larvae have died (Green *et al.* 2002). Amphibians are most likely to succumb to FV3 when they are larvae or in metamorphosis (Green *et al.* 2002). Infected tadpoles can have >90% mortality rates, especially in naïve populations exposed to an initial outbreak of FV3 (Gray *et al.* 2009). This is likely due to the fact that tadpoles, like many juvenile animals, have a less developed immune system and a lack of adaptive immunity (Bayley *et al.* 2013; Grayfer *et al.* 2015). Most amphibian outbreaks and mortality events occur during the summer months, especially in the mid-to-late summer when many species are going through metamorphosis (Green *et al.* 2002). FV3 infection within a waterbody is not restricted to one species, as it can infect any amphibian (frog or salamander) inhabiting the same site (Wheelwright *et al.* 2014). In captivity, FV3 mortality rates of amphibians at any life stage are also very close to 100% (Green *et al.* 2002; Greer *et al.* 2005). This is likely due to high density of hosts, increased stress in enclosed environments, and the continuous addition of new (often wild caught) hosts, resulting in guaranteed transmission (Waltzek *et al.* 2014). Between 1996 and 2001, 57% of all reported mortality and morbidity events of amphibians were reported as viral infections, most likely ranaviruses (Green *et al.* 2002).

1.6 Global Distribution of FV3

FV3 is widespread across Canada and the United States, although the exact distribution is unknown as a matter of limited surveillance (Figure 1.2; Duffus *et al.* 2015). Most studies on

FV3 and notable outbreaks have occurred in either North America or Europe, where both anurans (frogs and toads) and urodeles (salamanders and newts) have been reported with infection (Hyatt *et al.* 2000; Ariel *et al.* 2009; Duffus *et al.* 2015). There have been reports of FV3 in Central and South America, including Costa Rica (Whitfield *et al.* 2013), Nicaragua (Stark *et al.* 2014), and Brazil (Mazzoni *et al.* 2009). The few reports from Asia include FV3 outbreaks within multiple forestry farms and wild waterbodies in China (Xu *et al.* 2010), and a mass die-off event at a wild pond in Japan (Une *et al.* 2009). There have been very few documented cases of ranaviruses infecting frogs in Africa, but ranavirus species identification methods were either not used or PCR amplification was too weak, therefore it is unclear whether FV3 was present (Duffus *et al.* 2015; Kolby *et al.* 2015). As mentioned previously, the leading cause of global spread of amphibian disease is thought to be legal trade. A species of high demand in the pet trade are North American bullfrogs (*Lithobates catesbeiana*), a known carrier of FV3 both in captivity and the wild (Gray *et al.* 2007; Mazzoni *et al.* 2009; Schloegel *et al.* 2009). With the increasing demand of American bullfrogs in global trade, the risk of ranavirus outbreaks in otherwise healthy frog farms is expected to rise, and if individual bullfrogs are released into the wild then there is a greater risk of infecting naïve wild populations (Xu *et al.* 2010).

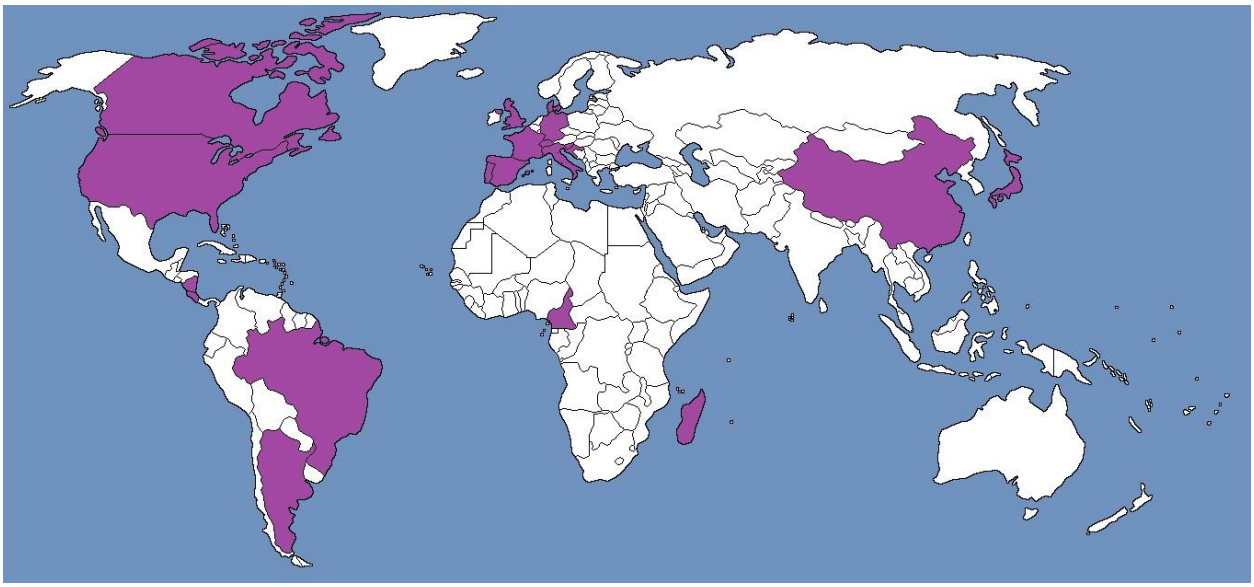

Figure 1.2: Countries with documented reports of Frog virus 3. Modified from Duffus *et al.* (2015).

1.7 Phylogeny of Ranaviruses and FV3

When confronted with a new genetic variant of ranavirus, the ICTV determines whether it should be its own species or a strain falling under a distinct lineage (such as FV3-like, or EHNV-like, for example) (Jancovich *et al.* 2012). How the ICTV determines that a virus is a distinct species depends on several criteria, including host species, protein profiles, gene synthesis by open reading frame (ORF) alignment, and restriction fragment length polymorphism (RFLP) profiles of genomic DNA (Tan *et al.* 2004; Jancovich *et al.* 2012, 2015b). Of these criteria, one of the most useful methods is a phylogenetic analysis of various genes (Tan *et al.* 2004; Jancovich *et al.* 2012; Stöhr *et al.* 2015). Iridoviruses all share 26 core genes that are often used for phylogenetic and order comparison, and have been used to distinguish lineages of ranavirus species as mentioned previously (Figure 1.1): FV3-like, CMTV-like, EHNV-like, CoIV-like, SCRV-like, and GIV/SGIV-like (Jancovich *et al.* 2015b; Chinchar *et al.* 2017; Claytor *et al.* 2017). The FV3-like lineage is the only lineage that infects amphibians, fish, and reptiles (Jancovich *et al.* 2015b). Among the core genes used for phylogeny, the most common regions are the major capsid protein gene (MCP), DNA polymerase, RNA-α and -β, and vIF-2α (Chen *et al.* 2011; Stöhr *et al.* 2015).

Characterization of ranaviruses is often done via the MCP gene; a highly conserved gene within species. Since the MCP is conserved between species, it is also used to identify novel ranavirus isolates and categorize them into the appropriate lineage (Allender *et al.* 2013a; Duffus & Andrews 2013; Kolby *et al.* 2014; Waltzek *et al.* 2014). When determining the species or isolate of a ranavirus using the MCP, most studies only consider a 500 bp fragment of the 1,392 bp gene using published primers and for ease of amplification when DNA has degraded (Mao *et al.* 1997; Greer *et al.* 2005; Duffus & Andrews 2013). However, many closely related species of

ranavirus can be up to 99% identical in sequence, therefore looking at a small portion can sometimes misidentify an isolate (Duffus & Andrews 2013). While using the MCP is an excellent starting point for ranavirus phylogeny among lineages, there remains a lack of understanding as to the intra-specific genetic variability of ranaviruses. An increased genetic resolution could potentially be applied to understanding the evolution of the disease over space and time.

1.8 Ranavirus Genetics

Analyses of open reading frames (ORFs) are often used to understand the pathogenicity and cell replication of ranaviruses (Chen *et al.* 2011; Morrison *et al.* 2014; Jancovich *et al.* 2015a; Claytor *et al.* 2017). One marker linked to pathogenicity is the α-subunit of the eukaryotic initiation factor 2 (eIF-2α) gene. This gene is found within eukaryotes, poxviruses, and iridoviruses (Essbauer *et al.* 2001). Within ranaviruses, there is a varying degree of homology compared to the eIF-2α gene in eukaryotes, denoting the viral homolog as vIF-2α. Some ranavirus species do not carry the vIF-2α gene (e.g., GIV and SGIV), while others have a truncated version of the gene (FV3, STIV, and RGV) lacking three-quarters of the N-terminal (Chen *et al.* 2011; Grayfer *et al.* 2015). Complete knockout of this gene results in lower host death rates and increased time until death, suggesting that it plays a role in virulence (Jancovich & Jacobs 2011). There is evidence that the lack of the N-terminal region in FV3 and STIV causes the viruses to be less virulent than viruses with the complete gene (Majji *et al.* 2006). Examining the length of the vIF-2α gene in ranaviral isolates is performed to estimate virulence, as well to determine the relationship of new isolates to ranavirus species, as done with phylogeny (Essbauer *et al.* 2001; Stöhr *et al.* 2015).

A recent study has compared the genomes of closely related species of ranavirus isolated within a spotted salamander, and determined genes or regions that might contribute to virulence (Morrison *et al.* 2014). Morrison et al. (2014) looked at the virulence between three isolates of FV3 by infecting tadpoles, and found that one isolate known as SSME had a lower mortality rate than the other two. The genome of the less virulent isolate was then sequenced to compare genes and determine what genetic differences may be linked to increased virulence. Compared to the wild-type FV3 (wt-FV3) isolate, there was a 98.79% sequence identity, with a genome length of 105,070 bp, opposed to the 105,903 bp that the wt-FV3 isolate contains. Further analyses showed a number of differences between the SSME and wild-type FV3 (wt-FV3) isolates, including a 757 bp deletion, completely deleting ORF 65L and the majority of 66L, and numerous 1 bp deletions in 43R, 46L, and 50L causing frameshift mutations often resulting in the loss of the original stop codons. A 139 bp insertion within ORF 66L was also found when comparing the SSME with the genomes of other FV3-like strains; RGV, STIV, and TVF. The SSME genome also had 24 bp substitutions and a 27 bp insertion found within ORF 19R, possibly denoting a hypervariable region that could be used for phylogeographic purposes. The MCP for reference only had a single variable base between SSME and wt-FV3 (99.92% identity). Finally, there was also variability within repeated segments; not only between virus species, but also between environmental samples taken from the same waterway (Morrison *et al.* 2014), thus providing evidence that there is intra-specific genetic variation on a small geographical scale.

1.9 Detection Methods of FV3

FV3 is a systemic virus which quickly manifests the kidney, gastrointestinal tract, and liver (Gantress *et al.* 2003; Forzán *et al.* 2017). As such, when sampling an individual suspected to be infected for FV3, hepatic tissue is the preferred tissue to test for virus presence or absence (Robert *et al.* 2011; Duffus & Andrews 2013; Brenes *et al.* 2014; Miller *et al.* 2015; Forzán *et al.* 2017). The problem with using the liver is that it requires euthanizing the suspected individual. Non-lethal sampling methods used to obtain virus cells from a specimen, such as toe clips of adults, tail clips of larvae, and swabs in the mouth or cloaca (Gray *et al.* 2012; Kolby *et al.* 2014) are likely to give less reliable results than sampling from the liver and are all relatively invasive. For example, Gray *et al.* (2012) found that tail clips had a 20% false-negative and 6% false positive rate, and swabs had a 22% false negative and 12% false-positive rate when compared to hepatic tissue.

Two of the most common detection methods for testing specimens for FV3 involve quantitative real-time PCR (qPCR) or conventional PCR using primers specific to the MCP gene (Mao *et al.* 1997; Hyatt *et al.* 2000; Allender *et al.* 2013a). qPCR visualizes the amplification of target DNA in real-time, and gives a concentration of DNA when compared to a standard curve. Conventional PCR is not as sensitive or accurate as qPCR, as qPCR reports the exact quantity of the target DNA at each cycle of the PCR relative to reference standards with the additional specificity of a 3rd tagged oligonucleotide, whereas conventional PCR only provides an end point estimate of the degree of amplification. Since the MCP is a highly conserved gene within ranaviruses, it is the best target for not only diagnosing a ranaviral infection, but also to determine a ranavirus species (or strain) (Mao *et al.* 1997). Conventional PCR methods often use primers targeting regions around 500 bp in length that include variable regions in order to

determine the species of virus. qPCR methods often use primers for shorter regions (50-70 bp) and target regions that are conserved across all ranavirus species (Picco *et al.* 2007; Allender *et al.* 2013a; Hall *et al.* 2015). For this reason, qPCR is often only used to detect presence and viral load of an infection, as opposed to determining species of virus.

1.10 Environmental DNA

There has been a growing investment in developing detection assays using environmental DNA (eDNA), allowing for aquatic species and pathogen detection without the need for invasive sampling (e.g., Turner *et al.* 2014; Valentini *et al.* 2016). eDNA eliminates specimen sampling by instead capturing free-floating cells in water or soil, which is then filtered, extracted, and tested for the presence of a specific organism by targeting DNA fragments with species-specific PCR primers (Lodge *et al*. 2012). eDNA has been used to detect invasive species of fish such as bluegill sunfish (*Lepomis macrochirus*) and Asian bigheaded carp (*Hypophthalmichthys* spp.) (Takahara *et al*. 2013; Turner *et al*. 2014; Wilson *et al*. 2014), endangered species of fish, plants, and amphibians (Bronnenhuber & Wilson 2013; Rees *et al*. 2014; Laramie *et al*. 2015; Boothroyd *et al*. 2016), aquatic pathogens including parasites and fungi (Huver & Koprivnikar 2015; Kolby *et al*. 2015), and common aquatic species for improved monitoring programs (Goldberg *et al*. 2011; Veldhoen *et al*. 2016). Traditional tissue sampling requires time, resources, and effort to capture a target specimen (Spens *et al.* 2017), which is often stressful and occasionally lethal to the host (Hall *et al.* 2015). Many studies have found that eDNA detection methods are more sensitive and inexpensive than traditional sampling methods, especially in cases when surveying for rare or invasive species that may be low in density (Goldberg *et al*. 2011; Jerde *et al*. 2011; Dejean *et al*. 2012; Valentini *et al*. 2016). eDNA can be used to survey a

single species, but it can also be used to identify multiple taxa of a waterbody using high throughput sequencing (HTS) and metabarcoding (Valentini *et al.* 2016). Metabarcoding allows for amplification and sequencing of all species within an ecosystem without the need for prior knowledge of what organisms may live there, although there are many issues with preferential amplification among different species and as such, direct testing is still the gold standard for species detection from eDNA.

1.11 eDNA and Ranavirus

There are only two reports on eDNA use for ranavirus detection: Hall *et al.* (2015) detected ranavirus at sites where there were known infections, while Kolby *et al.* (2015) attempted to detect pathogens in a region where ranaviruses had never been reported before. Hall *et al.* (2015) used eDNA in wood frog ponds where known die-off events were occurring and compared virus titres in the water to titres in tadpoles. They found that there was a significant correlation to virus titres in water and larvae, and found that eDNA had a 92% diagnostic sensitivity when comparing to sites with infected larvae. They also found that titres of FV3 could be detected around 15 days before die-off events began, and continue detecting 25 days after observed mortality events (Hall *et al.* 2015). Kolby *et al.* (2015) conducted an investigation across Madagascar testing for *Bd* and ranavirus in both wild habitats and commercial facilities. Part of their investigation also included eDNA sampling, where they found ranavirus within two amphibian trade facilities included in the survey (Kolby *et al.* 2015).

Currently, we know that eDNA can successfully capture ranaviral DNA, however the capacity or usefulness of this technique has not been fully explored. Preliminary studies compared titres in water to that in larvae (Hall *et al.* 2015), but there has yet to be a study that

demonstrates the effectiveness of eDNA viral surveillance across multiple months and years. Detection of ranavirus has been limited to the visual observation of epidemics, often within ponds of metamorphizing amphibians (Green *et al.* 2002; Brunner *et al.* 2015). Ranavirus appears to become more active during summer months (Kolby *et al.* 2015): some possible explanations for this seasonality include detection biases by surveying shallow, accessible waters; viral introduction by carrier adults in breeding grounds; increased susceptibility throughout development as metamorphosis is energetically costly (Rollins-Smith 1998); and increased susceptibility due to high temperatures (Brunner *et al.* 2015). Using eDNA sampling methods might help disprove or strengthen the different hypotheses as to why ranavirus outbreaks are seasonally driven.

1.12 What is still Unknown – eDNA and Ranavirus

There is a need to develop an assay for efficient ranavirus surveillance that can detect the pathogen in a systematic, rigorous, and cost-effective way in order to further understand the epidemiology of the disease. Effective disease surveillance requires rapid collection and processing of results using diagnostic assays that maximize the probability of detecting the pathogen (Thurmond 2003; Stallknecht 2007) while minimizing false positives and negatives. eDNA is an ideal candidate for ranavirus surveillance within waterbodies in North America, as the virus has been found to persist outside of a host for varying amounts of time depending on temperature. Munro *et al*. (2016) found that FV3 lasted longer in water then in sediment at all temperatures, and also lasted longer in colder (35 days at 4 °C) versus warmer temperatures (5 days at 30 °C). In order to maximize diagnostic sensitivity and efficiency, eDNA sampling should be tested across multiple months in a season to determine which month is most likely to

have virus present in the water. One possibility is that FV3 would most likely be present when environmental temperatures are at its highest, causing increased stress on amphibians and faster replication rates of the virus (Bayley *et al.* 2013). Another possibility is during the early summer when most amphibian species are in larval stages, and are most susceptible to disease (Greer *et al.* 2005).

The application of quantitative eDNA testing can also allow for assessment of potential environmental variables or features that influence ranavirus outbreaks and spread. With rapid and ongoing detection of the virus across multiple seasons, fluctuations in presence or absence can be attributed to factors such as rainfall frequency and volume, water temperatures, pH levels, salinity, or anthropogenic factors such as pollution or human traffic. Adequate disease surveillance is the first step in disease management; once the extent of a disease is determined, then subsequent steps can be taken to control infection levels, prevent further outbreaks, and eradicate pathogens from the environment (Belant & Deese 2010).

1.13 What is still Unknown – Intraspecific Variation of FV3

Genomic evidence suggests that different isolates of FV3 exist in North America (Morrison *et al.* 2014), and that genetic variation is not limited to a 500 bp MCP fragment targeted for phylogenetic analyses. Different presentations of genes can be used for understanding levels of virulence, possible host specificity, and fine-scale phylogenetic comparison. The putative vIF-2α gene can be used to better understand expected levels of virulence of newly discovered virus isolates based on the size of the gene. Variation found within these two genes may provide insight into new FV3-like isolates that could be studied on a genomic scale to further understand intra-species variation and patterns of spread.

1.14 My Thesis

The goal of my thesis was to further understand the spread and management of ranaviruses in the Canadian environment by assessing prevalence in time and space, as well as evaluating samples of FV3 at two of its genes. In chapter 2, I aimed to investigate the effectiveness of eDNA detection by sampling multiple months across two summer field seasons, assessing the patterns of disease prevalence and abiotic factors that may contribute to these patterns. In chapter 3, I performed a finer scale genetic analysis to screen for intraspecific variants of FV3 across Ontario as well as Alberta and Northwest Territories. I focused on the MCP and vIF-2α genes to determine if there is variability that can further our understanding of the relatedness and suspected virulence of any newly discovered variants.

In chapter 2, my questions are:

1. Is ranavirus present in water with similar environmental patterns, or is ranavirus presence random over time? Should viral presence follow environmental patterns (waterbody size, water temperature, pH, etc.) then locations with similar conditions may allow for the virus to thrive longer, and allow for a greater understanding of ranavirus preservation.
2. Are there fluctuations in the presence of ranavirus in water over multiple summer months? The presence and preservation of the virus in water may follow a pattern where it is most commonly detectable at one point in the season, suggesting that ranavirus sampling via eDNA methods should be performed at the time when the chances of detection are at its highest.
3. What is the estimated prevalence of ranavirus across a finer scale in Ontario waterbodies? The distribution of ranaviruses in the environment are currently unknown, however with

reliable eDNA sampling methods we may be able to gain an understanding of how common or uncommon ranaviruses are in Ontario.

In chapter 3, my questions are:

1. Are there multiple genetic isolates of FV3 found across Canada or is there only one FV3 haplotype in surveyed areas based on the MCP and vIF-2α genes?
2. Is there evidence for ranavirus variability within Canada by comparing FV3 samples taken from varying locations and distances across the landscape?

1.15 Hypotheses and Predictions

In chapter 2, my hypotheses were as follows:

1. Are there patterns of ranavirus presence in water based on a temporal scale? If there is a temporal pattern in ranavirus presence across multiple summers, then eDNA methods will be an ideal method for capturing ranavirus DNA and detect the presence of the virus at various frequencies from multiple sites depending on the month of the summer season.
2. Are there abiotic factors (i.e. water temperature, pH, salinity, conductivity) that effect the likelihood that ranavirus will be present in a waterbody? If there are abiotic factors that influence the presence of ranavirus in the water, then waterbodies with similar factors may be more likely to carry ranavirus.
3. Is ranavirus presence ubiquitous around central Ontario? eDNA can be used to determine the prevalence of ranavirus based on a small geographical scale in Ontario. If many waterbodies are sampled for ranavirus on a finer distribution, then the fraction of positive

sites may provide an idea of general abundance across larger scales throughout the rest of Ontario and possibly Canada.

In chapter 3, my hypotheses were as follows:

1. Is there variability of FV3 found across sites in various provinces and territories within Canada? If there is intraspecific variation of FV3, then the MCP gene in its completion will be an ideal marker for initial evidence on a large-scale due to its conservation.
2. Are there vIF-2α variants of FV3 that could reflect differences in virulence? If there are multiple vIF-2α variants in FV3 samples across Canada, then there may be selective pressures influencing the virulence of the various FV3 haplotypes.

CHAPTER 2

SPATIAL AND TEMPORAL DISTRIBUTION OF RANAVIRUS USING ENVIRONMENTAL DNA DETECTION

Preface

Contributions: Water samples filtered via cellulose nitrate filters were collected and processed by Samantha Grant. Water samples were filtered via Sterivex capsules and site abiotic factors were collected by Megan Congram and Carly Marie Scott, and extracted by Megan Congram and Audrey Wilson. Frog virus 3 control samples were cultured in Dr. Craig Brunetti's lab. Statistical model analysis was scripted by Lynne Beaty.

Abstract

Amphibians are experiencing widespread population declines associated with emerging diseases such as chytrid fungus and ranaviruses which cause rapid onset epidemics and often mass die-offs. Providing insight into the extent of pathogen distribution, temporal patterns in disease presence, and environmental factors that allow for pathogen persistence allow for enhanced disease surveillance. Disease surveillance in aquatic habitats is often invasive, costly, and time consuming, and environmental DNA (eDNA) detection tools are increasingly being used to address these issues and provide enhanced pathogen detection. In this study, we applied eDNA detection tools to survey for the spatial and temporal distribution of ranaviruses by sampling 126 waterbodies in Ontario, Canada. We also evaluated various eDNA amplification procedures that enhanced pathogen detection and minimize PCR inhibitors.

At a coarse geographic scale (>30 km between sites, 73,100 km^2), 33 waterbodies were sampled across three sampling periods (June, July, August), where we found ranavirus in 24 sites collectively over two years, with detection most prevalent in later months of the season. An

additional 93 sites were sampled on a finer scale (<10km between sites, 7,150 km^2) where we found ranavirus in 65% and 80% of sites in May and July respectively, suggesting an approximate prevalence of infection within 72.5% of waterbodies in the region.

Our results suggest that ranaviruses can persist at detectable levels across months and years in some waterbodies, and can be detected using eDNA despite a lack of observable die-off events. The virus was also more prevalent in water in later summer months, however not all field sites followed this trend. This is important, as die-off events often have a rapid onset, where carcasses are either quickly scavenged or degraded, likely leading to a lack of observation for most die-offs. These results strengthen the validity of eDNA as a surveillance tool for ranaviruses, and suggest that eDNA sampling should occur multiple times throughout a season to ensure adequate surveillance.

Keywords: environmental DNA, amphibian, ranavirus, pathogen surveillance, frog virus 3

2.1 Introduction

Anthropogenic influences have been associated with changing disease dynamics, such as human translocation and the global pet trade, which has assisted the spread of pathogens into formerly naïve populations (Daszak *et al.* 2000; Schloegel *et al.* 2009; Echaubard *et al.* 2014; Kolby *et al.* 2014). Emerging infectious diseases pose significant threats to biodiversity as a result of drastic population declines in many species (Daszak *et al*. 2001; Kutz *et al*. 2005; Keesing *et al*. 2010). Enhancing our understanding of the life history of pathogens through disease surveillance and factors that influence disease maintenance are key to developing mitigating actions to lessen the negative impacts from emerging diseases (Belant & Deese 2010). To this end, optimizing cost-effective, reliable, and sensitive methods for pathogen detection are crucial (Duffus *et al.* 2015).

There has been a growing investment in the development of detection assays using environmental DNA (eDNA) that have been notable in allowing for aquatic species and pathogen detection without the need for invasive sampling (e.g., Goldberg *et al.* 2011; Turner *et al.* 2014; Laramie *et al.* 2015; Boothroyd *et al.* 2016; Valentini *et al.* 2016). Aquatic eDNA eliminates specimen sampling by instead capturing DNA and cells in water, which is then filtered, extracted, and tested for the presence of a specific organism by use of species-specific PCR primers (Lodge *et al.* 2012). eDNA has been used to detect invasive species of fish such as bluegill sunfish (*Lepomis macrochirus*) and Asian bigheaded carp (*Hypophthalmichthys* spp.) (Takahara *et al.* 2013; Turner *et al.* 2014; Wilson *et al.* 2014), endangered species of fish, plants, and amphibians (Bronnenhuber & Wilson 2013; Rees *et al*. 2014; Laramie *et al.* 2015; Boothroyd *et al.* 2016), and aquatic pathogens including parasites and fungi (Huver & Koprivnikar 2015; Kolby *et al.* 2015). Many studies have found that eDNA methods of detection

are more effective than traditional sampling methods, especially in cases when surveying for rare or invasive species that may be low in density (Goldberg *et al.* 2011; Jerde *et al.* 2011; Dejean *et al.* 2012; Valentini *et al.* 2016).

In context of pathogen detection, traditional sampling may inaccurately portray the absence of a pathogen should a limited sample size of captured specimens be uninfected (Cooch *et al.* 2012), further, low disease prevalence can greatly influence the required sample sizes for surveillance to be effective (Cameron & Baldock 1998; Hall *et al.* 2015; Spens *et al.* 2017). While eDNA tools can allow for more extensive sampling regimes and enhanced sensitivity in detecting pathogens in cases of low prevalence in the environment (Guy *et al.* 2003; Jane *et al.* 2015; Boothroyd *et al.* 2016), eDNA surveillance needs to be placed in context of extensive validation and sensitivity tests. Careful controls are needed to minimize cross-contamination of low DNA template samples, false positives, and false negatives that may result from low test sensitivity or variables in the samples themselves, such as PCR inhibitors (Jane *et al*. 2015; Veldhoen *et al*. 2016; Spens *et al*. 2017). For example, organic and inorganic compounds such as urea, humic acids, phenolic compounds, heavy metals, polysaccharides from algae, sewage, bacterial cells, non-target DNA, and pollen can hamper PCR amplification and result in false negatives (Wilson 1997; Converse *et al.* 2009).

While there are numerous pathogens that are harmful to amphibians (e.g., *Saprolegnia ferax, Ribeiroia* sp.; Kiesecker *et al.* 2001; Johnson *et al.* 2002; Daszak *et al.* 2003; Romansic *et al.* 2009; Huver & Koprivnikar 2015), two pathogens are primarily linked to global amphibian population declines: *Batrachochytrium dendrobatidis* (*Bd*) and ranaviruses (Boyle *et al.* 2004; Stuart *et al.* 2004; Fisher *et al.* 2009; Price *et al.* 2014; D'Aoust-Messier *et al.* 2015; James *et al.* 2015). *Bd* is an aquatic fungus that causes a rapidly progressing disease known as

chytridiomycosis (Fisher *et al.* 2009), whereas *Ranavirus* is a genus of viruses that circulate in the bloodstream of its host, causing systemic infections of the kidney, liver, gastrointestinal tract, and skin (Gantress *et al.* 2003). While *Bd* is more detrimental to adult amphibians, ranaviruses are a larger threat to larvae and metamorphosing amphibians, with mortality rates of infected tadpoles around 90% (Green *et al.* 2002; Greer *et al.* 2005).

Ranaviruses such as frog virus 3 (FV3) are presumed to be widespread across North America, however the exact distribution is unknown as most observations are opportunistic, as opposed to a systematic surveillance of this pathogen (Duffus *et al.* 2015). The ephemeral nature of the die-offs, however, likely leads to underreporting of this disease, as deceased larvae are scavenged or quickly decompose, leaving little evidence of a die-off event, making the presence of disease difficult to detect (Harp & Petranka 2006; Skerratt *et al.* 2007; Brunner *et al.* 2015). Documented cases of ranavirus presence are normally from observations of a mass mortality event in waterbodies under study, or due to accidental observation (Green *et al.* 2002; Greer *et al.* 2005; Mazzoni *et al.* 2009; Duffus & Andrews 2013; Stark *et al.* 2014; Wheelwright *et al.* 2014). The dynamics of ranavirus in a waterbody are not entirely understood. Ranaviruses may remain at low levels in the water due to hosts which did not clear infection, yet failed to succumb to the disease, which would allow for future epidemics once conditions were ideal (i.e. high host density, introduction of naïve larvae, etc.) (Roy & Kirchner 2000; Brunner *et al.* 2015). eDNA may allow us to detect ranavirus at these low concentrations and provide more accurate portrayal of pathogen abundance in any given area without the need to rely on capturing infected specimens or carcasses, so long as there are individuals carrying and shedding the virus into the water (Hall *et al.* 2015).

Recently, eDNA-based methods have been adopted to capture ranaviruses from water (Kolby *et al.* 2015, Hall *et al.* 2015). Kolby *et al.* (2015) used eDNA-based detection methods to discover if ranaviruses and *Bd* had been introduced to Madagascar, and found that *Bd* was not present in any samples, while ranavirus was present in water samples from two commercial amphibian export facilities. Hall *et al.* (2015) reported a correlation between viral titers of infected larvae to titers in wood frog ponds via eDNA sampling. They also found that ranavirus titers were detectable with eDNA ~15 day before and ~30 days after initial die-off, suggesting that the virus is detectable in water for at least a ~45-day timeframe, even if mortality events are not occurring at the time. While eDNA appears to be a viable method of ranavirus monitoring, there lacks a more extensive, systematic, spatial and temporal survey of ranavirus in the environment to better understand the maintenance of the disease. For example, viral titer levels may be the highest during the early summer, when there are many susceptible tadpoles emerging in the waterbody (Greer *et al.* 2005; Bayley *et al.* 2013), or it may be in the late summer when amphibians are in later stages of metamorphosis – a taxing stage which is also highly susceptible to pathogens (Green *et al.* 2002).

The application of eDNA can also allow for assessment of potential environmental variables or features that influence ranavirus outbreaks and spread. With rapid and ongoing detection of the virus across multiple seasons, fluctuations in presence or absence may be attributed to abiotic factors such as water temperatures, pH levels, conductivity, salinity, or estimated waterbody size. Understanding underlying factors for disease outbreak can allow us to take first steps in disease management; once the extent and cause of disease preservation is determined, then subsequent steps can be taken to control infection levels, prevent further outbreaks, and eradicate diseases from the environment (Belant & Deese 2010).

In this study, we investigated the use of eDNA as a surveillance tool for ranavirus across two groups of various waterbodies with unknown ranavirus presence status. The first group had widespread field sites (>30 km between sites, 73,100 km^2) sampled over three summer months spanning two years, while the second group had field sites on a finer scale (<10km between sites, 7,150 km^2) and was sampled across two months for one summer. The goals were to; (i) outline the most reliable protocol for ranavirus detection using eDNA-based methods that maximize the yield of viral DNA while minimizing inhibitors, (ii) determine if there is an optimal period for eDNA-based ranavirus detection by assessing the fluctuation of presence over time, (iii) determine if abiotic factors influence the presence of ranavirus in a waterbody, and (iv) estimate the presence of ranavirus based on a fine-scale geographic analysis.

2.2 Materials and methods

2.2.1 Field collections – Cellulose nitrate filtration

This study was conducted in the summers of 2016 and 2017 across south-central Ontario, Canada (Figure 2.1). During 2016, 18 waterbodies were visited for eDNA collection. The sites were selected based off previous tissue sampling studies (Echaubard, *unpublished data*) surveying for ranavirus and *Batrachochytrium dendrobatidis* (*Bd*) in 2012, where selected sites had positive detection for ranavirus (Rv). In 2017, 25 sites were visited for eDNA sampling; 10 sites with positive Rv detection in 2016, and 15 additional sites. The subsequent 15 sites for 2017 sampling followed one of two criteria: Rv positive specimens collected within last 3 years, or isolated pools of stagnant water such as ponds, marshes, or ephemeral pools.

At each study site, three water samples of 250 mL were collected for in-lab eDNA filtering. Points of sampling varied based on layout and size of waterbody, however points were a minimum of three meters apart in any given waterbody. Water was collected at approximately 10 cm below surface level to avoid contaminants on the surface. Locations where water was standing and surrounding vegetation were favoured to maximize the chances of collecting amphibian and virus DNA. Each bottle was dried with a paper towel before placed in a cooler around 4 °C for transport back to the lab. Each site was revisited three times during the two summers (June, July, and August). At each site, additional information was recorded on type of waterbody, weather, air temperature, and time collected. All equipment was decontaminated between sites (boots, hip waders) using 10% bleach and left to sit for 15 minutes before rinsing with deionized water (Hall *et al.* 2015). Water samples were held in a cooler at 4 °C until arriving at Trent University where they were kept in a fridge until filtration.

eDNA samples were filtered within 24 hours of collection through 0.2 μm cellulose nitrate filters (Whatman, CAT# 10401312; GE Healthcare Life Sciences, Mississauga, ON, Canada) using a powered vacuum pump (EMD Millipore Corporation) and magnetic funnels (Pall Corporation). Once filtered, filters were removed using flame sterilized forceps, then placed in 1.5 mL microcentrifuge tubes and stored at -20 °C. Pre-filter blanks were run with deionized water through each funnel and cup prior to filtering samples, followed by post-filter blanks after samples were run to ensure materials were properly decontaminated. Equipment (bottles, caps, funnels, cups) was decontaminated in 10% bleach for 15 minutes and then rinsed with deionized water between each site. A cooler negative with deionized water was included each day of water collection, and coolers were decontaminated with 10% bleach between sampling days.

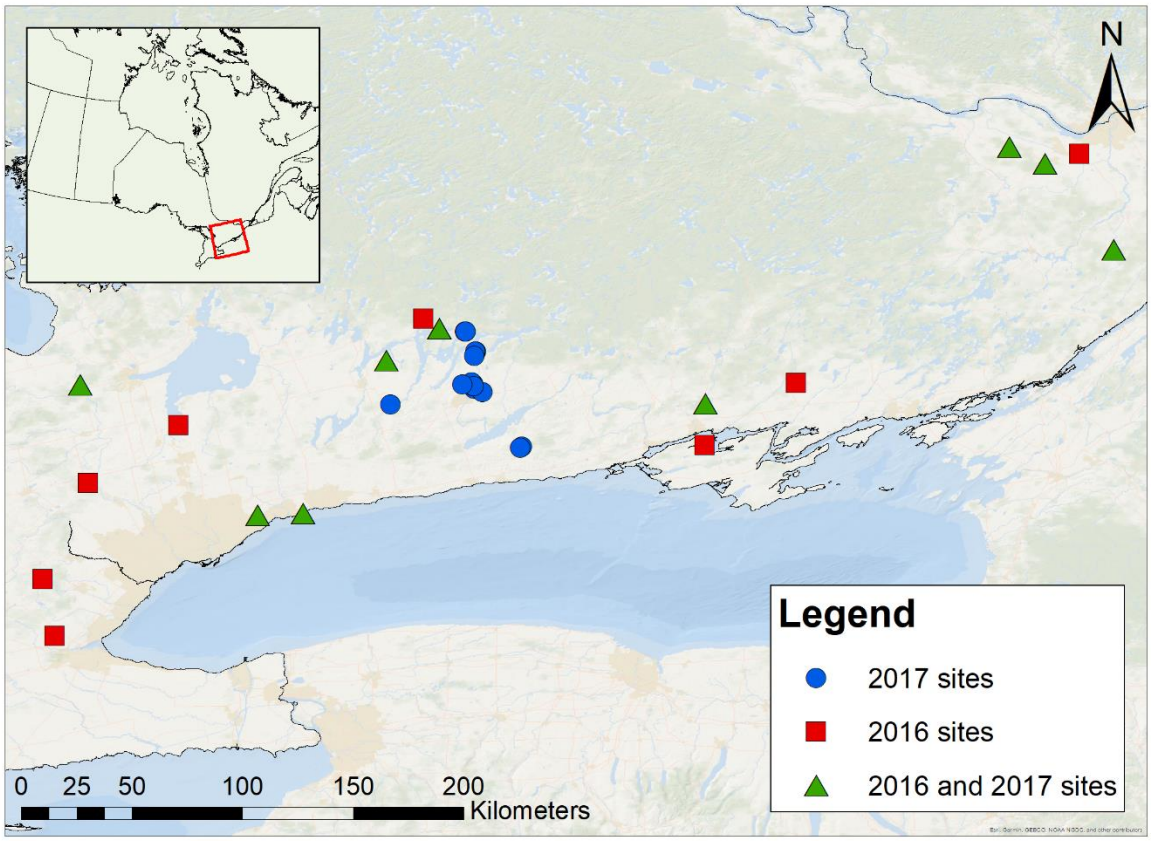

Figure 2.1: Map of southcentral Ontario, Canada field sites for cellulose nitrate filter eDNA collection. eDNA samples were taken three times in summer seasons (June, July, August). Points indicate the year the sites were sampled. Green triangles: 2016 and 2017; Red squares: 2016 only; Blue circles: 2017 only.

2.2.2 Field collections – Sterivex capsule filtration

In 2017, an additional 93 sites were sampled in parallel with a separate study for the presence of *Bd* in the surrounding region of Peterborough, Ontario, Canada (unpubl. data), and had water samples collected during two sampling rounds between late May and July (Figure 2.2). Each site was sampled from five points around the waterbody and filtered through Sterivex 0.22-μm capsule filters, following sampling protocol described in Chestnut *et al.* (2014). Samples were drawn into 60 mL syringes that had been rinsed three times in native water, then pushed through a 0.22-μm Sterivex capsule until clogged with natural debris. Volumes ranged from 60 mL to 500 mL, averaging around 250 mL. Capsules were then flushed with 50 mL of 0.01 M phosphate buffered saline (PBS) followed by an additional expiration of air to drain all liquid. The outflow end of the capsule was closed with Hematocrit sealant clay and 0.9 mL of lysis buffer solution was injected for preservation before being capped. Capsules were then sealed and labeled in individual plastic bags and kept in a cooler at 4 °C until returned to the lab where they were refrigerated at 4 °C until extraction.

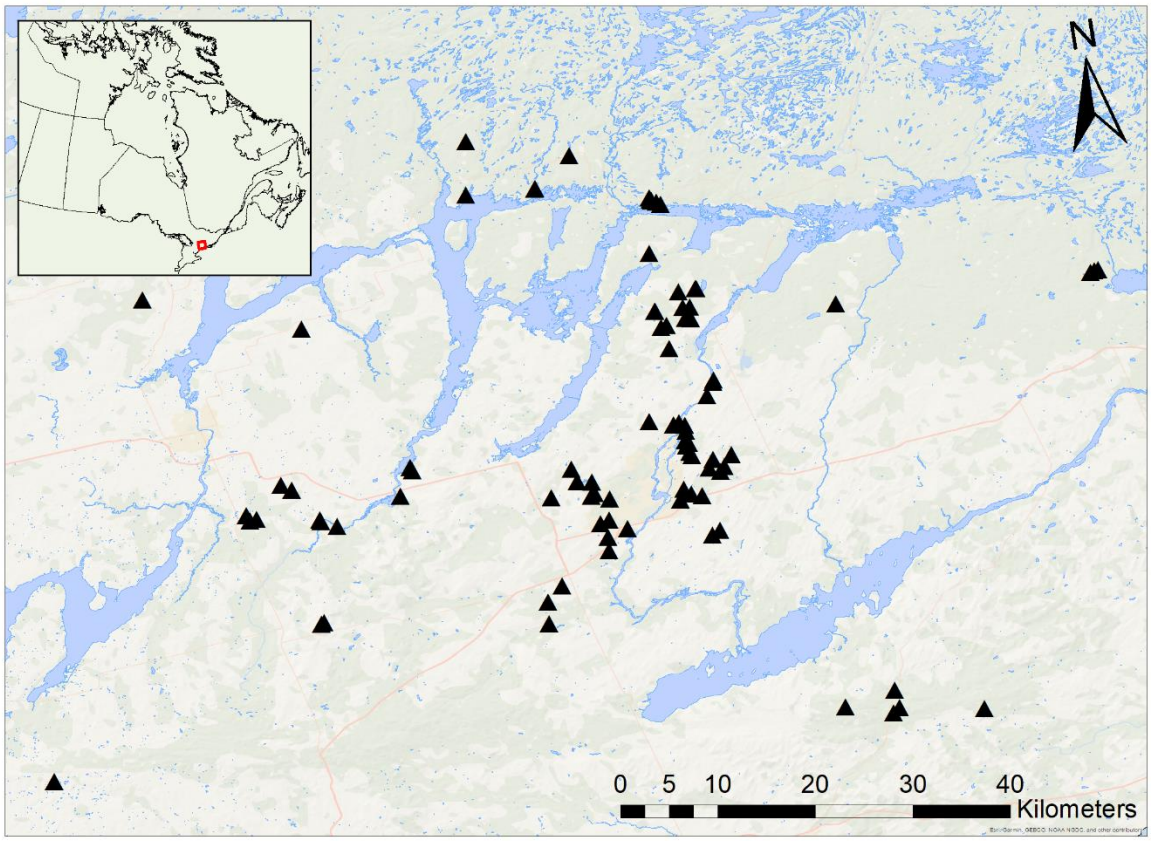

Figure 2.2: Map of 2017 eDNA field sites that were collected via Sterivex capsule filters, surrounding Peterborough, Ontario, Canada.

2.2.3 Extraction eDNA sample extraction

eDNA filters (n=111) had 280 μL of 1X lysis buffer (4 M urea, 0.2 M NaCl, 0.5% *n*-lauroyl sarcosine, 10 mM 1,2-cyclohexanediaminetetraacetic acid and 0.1 M Tris-HCl, pH 8.0) and 20 mg/mL proteinase K (Qiagen Inc.) added and incubated at 56 °C. Samples were vortexed every 30 minutes for the initial three hours of incubation then left them overnight at 56 °C (Goldberg *et al.* 2011). The following day, samples were spun down and the filter papers were removed using forceps sanitized in a concentrated (50%) solution of DECON (Decon Laboratories Limited, East Sussex, UK) and rinsed in deionized water. 230 μL of lysate was transferred to a clean deep well plate and submitted to the NRDPFC for magnetic bead extraction (MagneSil). One filter negative control and one filter positive control was included with each set of extractions. Filter positives were 250 mL of deionized water spiked with $2x10^3$ pfu/μL of frog virus 3 (FV3) filtered through a 0.2 μm cellulose nitrate filter.

Capsule filters (n=930) were extracted following the $SX_{CAPSULE}$ protocol from Spens *et al*. (2017). Each set of extractions were completed along with a negative to ensure no contamination of samples. All equipment (caps and syringes) were decontaminated between samples and days by soaking in 10% bleach for 15 minutes.

2.2.4 qPCR Master Mix comparison

To further reduce inhibitors that may present false negative results, two TaqMan Master Mixes were compared on a subset of eDNA samples to determine which had the highest recovery of DNA. The two master mixes were TaqMan Universal Master Mix, and TaqMan Environmental Master Mix 2.0 (Applied Biosystems, Foster City, California, USA). A qPCR was prepared with standards of synthetic FV3 dilutions of 10^7, 10^6, 10^5, 10^4, 10^3, and 10^2 copies

run in triplicate. The synthetic DNA sequence was a 500 bp fragment of the major capsid protein gene (MCP) from FV3 with an 18 bp insert for a synthetic probe (Wilson *et al.* 2015). A subset of 33 eDNA samples were run in duplicate and spiked with a synthetic FV3 virus in a one-to-one ratio. Each subset was run twice with the different master mix. Each reaction was run with 2.5 μL template eDNA, 2.5 μL of $4x10^4$ copies synthetic FV3, 1X TaqMan of either PCR Master Mix, 0.3 μM of forward (5'-ACACCACCGCCCAAAAGTAC-3') and reverse (5'-CCGTTCATGATGCGGATAATG-3') primers, and 0.25 uM fluorescent probe (5'-VIC-GGATCCAAGCTTAGGCCT-MGB-3') for a total of 20 μL. Reactions were run at 58 °C annealing temperature for 50 cycles. Two PCR negatives and four synthetic positives were included in a 1:1 ratio with deionized water. eDNA samples following this experiment were run using the Environmental Master Mix (see results).

2.2.5 qPCR assay

Standard curves were generated using dilutions of 10^4, 10^3, 10^2, 10^1, 10^0, and 10^{-1} pfu/μL of FV3 cultured in epithelioma papulosum cyprini (EPC) cells (Fijan *et al.* 1983), provided by Dr. Craig Brunetti of Trent University (Peterborough, Ontario). Standards and eDNA samples were run in triplicate in reaction volumes of 20 μL. Primers targeted a 70 bp segment of the MCP within all known ranavirus species found in North America (Picco *et al.* 2007). Each reaction was run with 5 μL of unknown concentrations of template DNA, 1X TaqMan Environmental PCR Master Mix 2.0 (Applied Biosystems, Foster City, California, USA), 0.3 μM of forward and reverse primers (above), and 0.15 μM fluorescent probe (5'-FAM-CCTCATCGTTCTGGCCATCAACCAC-MGB-3'). Reactions were run with an initial holding stage of 50 °C for 2 minutes, then 95 °C for 10 minutes, followed by a cycling stage of 95 °C for

15 seconds and 58 °C for 1 minute for 50 cycles. All runs were conducted using the Applied Biosystems 7900 detection system, and data analysis was conducted using the Applied Biosystems StepOnePlus™ system following the protocols for standard curve experiment.

2.2.6 Statistical analysis

To minimize the chance of calling false positives and false negatives, we established qPCR thresholds including a limit of detection (LOD) and limit of quantification (LOQ). LOD was determined using the Ct values of the qPCR standard dilution series of all sample runs and plotting them using R code and method from Hunter *et al.* (2017). The purpose of calculating LOD was to determine the lowest amount of ranavirus DNA that is both detectable and distinguishable from the concentration plateau (Hunter *et al.* 2017). For LOQ, receiver operating characteristic (ROC) curve analyses was performed to estimate the performance of qPCR assays (Fan *et al.* 2006; Nutz *et al.* 2011). ROC curves generate a value based on the area under the curve (AUC), where an AUC of 1.0 would represent the qPCR assay having a 100% accuracy rate of distinguishing a true detection (positive control, sample) and a non-detection (negative control, true negative), whereas an AUC of 0.5 would represent that the assay had no power of distinguishing between the two (Nutz *et al.* 2011; Serrao *et al.* 2017). Sensitivity and specificity values of unknown samples and negative controls were assessed as LOQ thresholds 0.01, 0.02, 0.03, 0.04, 0.05, and 0.07 pfu/µL following methods described in Serrao et al. (2017).

Based on LOD and LOQ, capsule samples were ranked as positive or negative on two calling methods: a more conservative method where two of three qPCR replicates were required to pass the threshold, and a less conservative method where only one of three replicates required to pass the threshold. This offered a range for calling a site positive, as Sterivex capsules have

yet to be applied to ranavirus sampling. To determine the efficiency of using five biological replicates for Sterivex capsules, samples were plotted as a barplot to compare the number of biological replicates tested for positive Rv against the percentage of positive sites. The purpose was to determine if the number of positive sites plateaus when using less than five biological replicates per site.

To test whether there was a temporal pattern of ranavirus presence in eDNA samples over time, samples filtered with cellulose nitrate filters across 2016 and 2017 were analyzed using a logistic regression using the *glm* function following a binomial distribution with logit-link function.

For the capsule filters, to evaluate whether abiotic factors predicted pathogen richness at a site, we used a generalized linear mixed model (GLMM). Abiotic predictors included water temperature, water pH, conductivity, and estimated size of waterbody. Predictors were standardized and tested for collinearity before assessed as numeric random effects. The number of virus-positive qPCR replicates (n=15 per site visit) were the response count data, using a Poisson distribution with log-link function. Models were examined as single interactions and two-way interactions with both additive and multipliable effects. The sixteen resulting models were ranked using Akaike's information criterion (AIC) and I selected the model with the lowest AIC (Johnson & Omland 2004). All analyses were performed in R version 3.4.2 (R Core Team 2017).

Spatial and temporal variation in ranavirus prevalence were visualized by interposing the intensity of ranavirus presence across each month of capsule sampling, among field sites using the inverse distance weighting (IDW) method (Shepard 1968). Ranavirus intensity was based on the number of replicates (n=15) that passed the threshold determined by LOD and LOQ. IDW

considers the geographical distance between sampled sites and interprets closer sites as having a stronger weight on ranavirus prevalence, with weight diminishing as distance between sites increases (Bataille *et al.* 2013). Interpolation was performed in ArcMap version 10.6 considering for each site the 12 closest geographical sites for ranavirus prevalence across each month.

2.3 Results

2.3.1 qPCR Master Mix comparison

Environmental DNA (eDNA) samples that had been spiked with 10^5 copies of synthetic virus had an average recovery of 19%, with 18 samples showing total inhibition when using the Universal Master Mix (Figure 2.3). However, the levels of inhibition significantly decreased when using the Environmental Master Mix, resulting in a 90% recovery rate (Figure 2.3). Due to the significant increase in DNA recovery, eDNA samples were subsequently processed with the Environmental Master Mix.

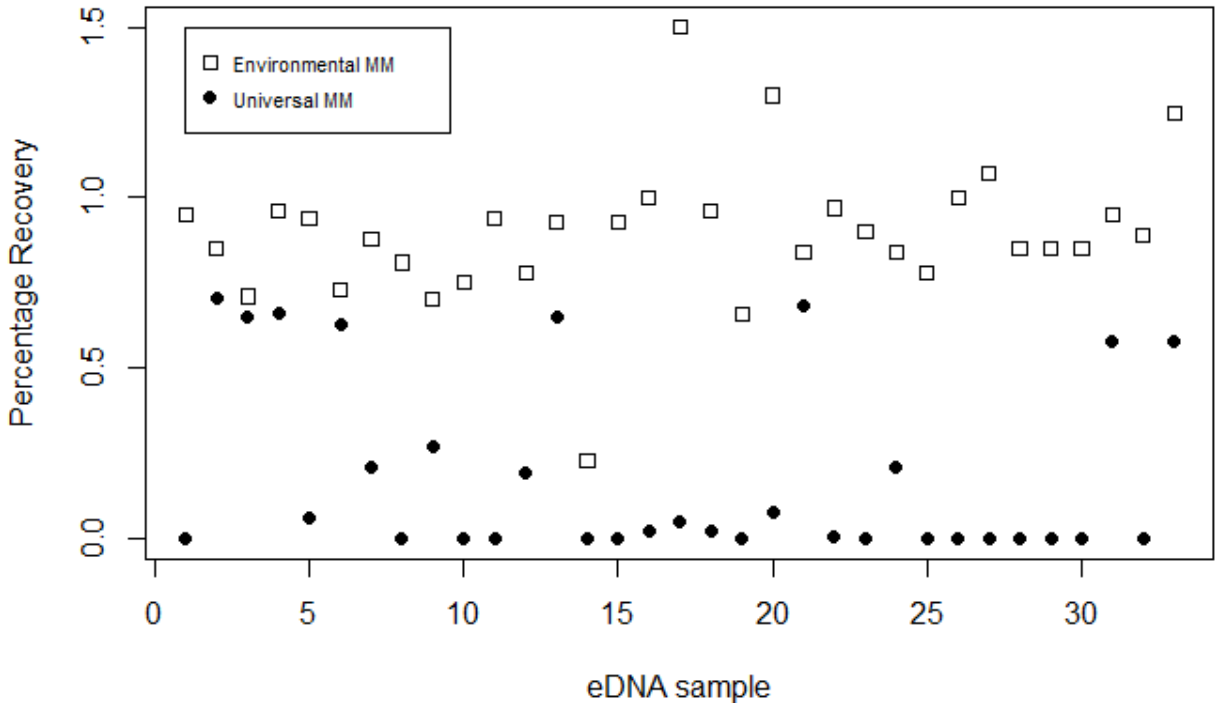

Figure 2.3: Recovery comparison of 33 samples using Universal Master Mix (filled circles) versus Environmental Master Mix (open squares)

2.3.2 Ranavirus presence in 2016 – Cellulose nitrate filters

Standard curves of cultured FV3 ranged from 10^4 to 0.1 pfu/μL and had slopes averaging at -3.5 with R^2 values around 0.99. Nine of the 18 waterbodies were positive for ranavirus (Rv) in eDNA samples (Figure 2.1). Among these nine, two sites were positive only during the May/June sampling period (KEN1, MIN), two sites were positive only during August sampling (KEN2, MOA), three sites were positive during July and August sampling (EDU, K3, RCA), and two sites were positive for all three sampling periods (BEA, K1, Table 2.1). 4 sites were positive in June (22%), 5 were positive in July (36%), and 7 were positive in August (53%). Percentages were calculated excluding sites that dried up. Due to an inability to access, two of the three sites positive during July and August were not sampled in June. Only KEN1 had observed signs of infection (lethargic tadpoles observed swimming near the water's surface), which resulted in high pfu values of ranavirus (average 90.92 pfu/5 μL of all technical replicates for this site). A parallel study was performed that required the collection of swabs of tadpoles from the sites sampled in 2016. A total of 51 swabs from tadpoles had been taken from the 10 sites sampled across both summers (Table 2.1). It was found that all lethargic tadpoles from KEN1 sampled in June were positive for Rv. One site (MOA) had one tadpole (n=7) positive for ranavirus during the August sampling period, and was positive for Rv from eDNA with an average of 0.23 pfu/μL. Only one site (STL) was positive in two tadpoles (n=7) yet negative in all eDNA samples for that sampling round. All sites (with exception of KEN1) had concentrations ≤1.46 pfu/μL, with no observed signs of mortality or infection.

2.3.3 Ranavirus presence in 2017 – Cellulose nitrate filters

Of the 25 sites visited in 2017, 24 were positive for Rv at least once throughout the three sampling periods (Table 2.1, 2.2). 10 of the 24 positive sites were sampled in both 2016 and 2017 (Table 2.1). 15 sites were positive in June (60%), 18 were positive in July (72%), and 16 were positive in August (70%). Percentages were calculated excluding sites that dried up. Nine of the 10 sites sampled across both years were positive across both years, and only one was negative during 2016, but positive during 2017 (STL). Out of the remaining 14 positive sites, four were positive for Rv during all three months, eight were positive during two of the three months, and two sites were positive for one month; with one of those sites having dried up before August (Table 2.2). There were signs of ranavirus infection at only one site (DEN2), where a single tadpole was found with a reddened body. This site had been positive for Rv during all three sampling months. Out of the eight sites where Rv was detected during two of three months, five were negative during June, one was negative in July, and two were negative in August.

Table 2.1: Plaque-forming unit (pfu/µL) averages for all positive sites during 2016 and 2017. Data includes number of positive tadpole swab samples taken in 2016 at the same time as a parallel study.

Site	Month	Tadpole swabs +/total*	Signs of infection		eDNA +/total		eDNA average Rv (pfu/5 µL)	
			2016	2017	2016	2017	2016	2017
BEA	June	N/A	No	No	2/3	3/3	0.31	2.56
	July	N/A	No	No	2/3	2/3	0.27	0.13
	August	N/A	No	No	2/3	3/3	0.41	0.15
EDU	June	N/A	No	No	N/A***	3/3	N/A	0.06
	July	N/A	No	No	2/3	0/3	0.13	-
	August	N/A	No	No	3/3	0/3	0.14	-
K1	June	N/A	No	No	1/3	0/3	1.44	-
	July	N/A	No	No	1/3	2/3	0.04	0.12
	August	N/A	No	No	2/3	3/3	0.05	1.57
K3	June	N/A	No	No	0/3	0/3	-	-
	July	0/1	No	No	2/3	1/3	0.13	0.1
	August	N/A	No	No	1/3	2/3	0.03	0.09
KEN1	June	6/6	**Yes**	No	3/3	3/3	90.92	12.18
	July	N/A	No	No	N/A**	3/3	N/A	1.04
	August	N/A	No	No	N/A**	N/A**	N/A	N/A
KEN2	June	0/1	No	No	0/3	3/3	-	0.17
	July	0/4	No	No	0/3	1/3	-	0.09
	August	0/7	No	No	3/3	2/3	0.89	0.56
MIN	June	0/3	No	No	1/3	0/3	0.04	-
	July	N/A	No	No	0/3	0/3	-	-
	August	N/A	No	No	N/A**	1/3	N/A	0.07
MOA	June	0/7	No	No	0/3	2/3	-	0.12
	July	0/6	No	No	0/3	0/3	-	-
	August	1/7	No	No	2/3	0/3	0.23	-
RCA	June	N/A	No	No	N/A***	1/3	N/A	0.10
	July	0/1	No	No	1/3	0/3	0.18	-
	August	N/A	No	No	1/3	0/3	1.46	-
STL	June	N/A	No	No	0/3	1/3	-	0.07
	July	N/A	No	No	0/3	2/3	-	0.24
	August	2/8	No	No	0/3	3/3	-	100.1

* Tissue sampling was only performed during 2016
** Sites that dried up
*** Sites that were not sampled due to inability to access water

Table 2.2: Monthly comparison of sites sampled using cellulose nitrate filters, not including the 10 sites sampled during both 2016 and 2017 (Table 2.1).

Site	Filter type	Year	Rv concentration (pfu/5 uL)		
			June	July	August
ACT	CN	2016	-	N/A	N/A
DM2	CN	2016	-	-	-
ELM	CN	2016	-	-	-
GL1	CN	2016	-	-	-
MUR	CN	2016	-	N/A	N/A
NHA	CN	2016	-	N/A	N/A
SAL	CN	2016	-	-	-
SS	CN	2016	-	-	-
ARCH	CN	2017	0.09	-	0.51
DANCE	CN	2017	0.30	0.11	-
DEN1	CN	2017	-	5.90	107.2
DEN2	CN	2017	59.2	1.20	4.15
DUMP2	CN	2017	0.05	3.42	0.12
DUMP4	CN	2017	333.9	10.6	3.32
GOLD	CN	2017	-	-	-
NORW	CN	2017	20.7	0.14	-
OMOM	CN	2017	0.12	0.07	4.05
SHARP	CN	2017	0.51	-	-
TRN2	CN	2017	-	8.78	0.15
TRN3	CN	2017	-	2.54	N/A
UNIP	CN	2017	-	0.39	0.16
WDM	CN	2017	-	0.72	0.09
WDP	CN	2017	-	0.06	0.05

N/A: Indicates that sites dried up throughout season.
- : Indicates sites that were negative for ranavirus (0.00 pfu/5 uL)

2.3.3 Limit of detection and quantification

The best statistical model for limit of detection (LOD) was determined for serial-dilution points from 10^4 to 10^{-1} pfu/µL (Supplementary Figure S2.1) where LOD was estimated to be 0.0301 pfu/µL (0.021-0.041 95% CI). However, values below 0.03 pfu/µL were detected with quantitative PCR instrumentation. A total of 910 environmental samples were taken with the capsules, along with 89 control negatives. 627 samples (68.9%) had a value over 0.01 pfu/µL and were used to assess the sensitivity and specificity. Based on the LOD, the limit of quantification (LOQ) thresholds from 0.01 to 0.03 were considered inadmissible, and specificity and sensitivity were considered at 0.04 pfu/µL. A threshold of 0.04 pfu/µL had a sensitivity of 57.2% (TP=50.1%, FN=37.4%) and a specificity of 96.6% (TN=12.0%, FP=0.42%).

The ROC curve was generated from 627 field samples and 89 negative controls, and had an area under the curve (AUC)=0.92, suggesting a relatively high (>0.96) discriminatory power between true-negatives and false-positives (Supplementary Figure S2.2, Fan *et al.* 2006).

2.3.5 Temporal eDNA analysis

eDNA samples taken via cellulose nitrate filters across three months in 2016 and 2017 were analyzed in a logistic regression with a binomial model to determine if there was variation in the likelihood of presence depending on the time of the season. Sites that passed the threshold of acceptance in two or more qPCR replicates were assigned the value of 1, and negative samples were 0. Samples were plotted using the Julian calendar. There was significance where detection in August was more likely to be positive than in June or July (Figure 2.4; logistic regression: d.f. = 1, $P = 0.0424$), determining that ranavirus is more likely to be at detectable quantities in the later summer months as opposed to earlier in the summer season.

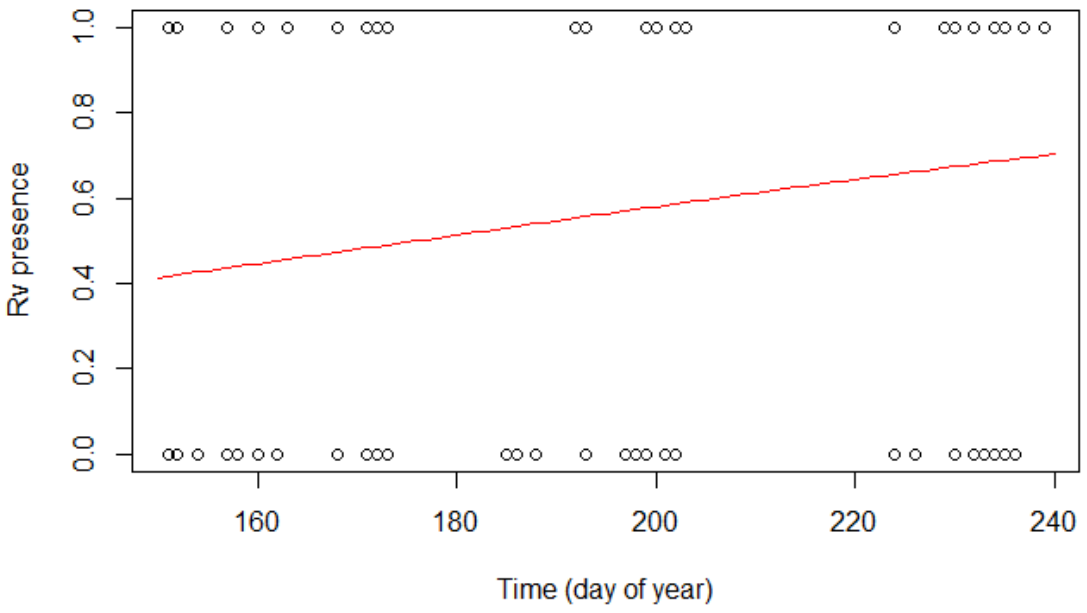

Figure 2.4: Ranavirus presence at 33 sampling sites using eDNA methods across the summer months of 2016 and 2017. Positive sites were assigned a value of 1 while negative sites were 0 (y-axis). Time was portrayed using Julian calendar days (x-axis). Line of best fit reflects the fluctuation of ranavirus presence in water over time.

2.3.6 Ranavirus prevalence in central Ontario – Sterivex capsules

Pathogen abundance data were analyzed based on the threshold established by the LOD and LOQ, in order to classify findings as a range rather than a set percentage to offer room for variation. In the conservative method, capsule samples were called positive if two or more qPCR replicates were equal to or greater than 0.04 pfu/µL (Hall *et al.* 2015). In the less conserved method, capsules were considered positive if one qPCR replicate passed the threshold. A site was considered positive if one of the five capsules were positive.

Out of 93 sites, 54-76% were positive in May, and 67-91% were positive in July, with 35-66% positive across both months (Figure 2.5). Of these sites, there was only one with signs of die-offs, where a number of dead metamorphic frogs were collected and tested positive for ranavirus (data not shown). Between 4-19% were negative for both months, and in July, 10 sites had dried up. Positive samples ranged from 0.04 pfu/µL to 229.6 pfu/µL, where the highest site was found to be going through a mass die-off event.

The number of sites positive for Rv increased as the number of biological replicates (n=5) increased (Figure 2.6). When comparing both May and July samples separately, the number of biological replicates required to call positives plateaued at around 4 capsule samples. Four capsules had positives in 64% and 78% of sites per month, whereas five capsules had 65% and 80% respectively.

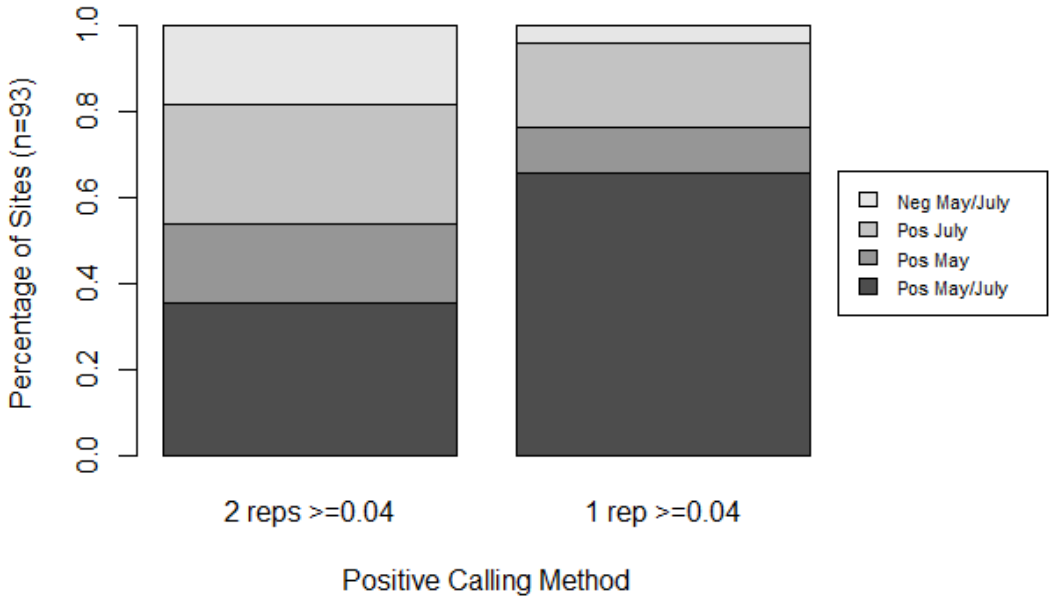

Figure 2.5: Breakdown of positive Sterivex capsules sampled in May and July. Samples are presented with conserved (minimum of two qPCR replicates ≥0.04 pfu/µL per sample per site) and less conserved (minimum of one qPCR replicates ≥0.04 pfu/µL per sample per site) thresholds, to determine a range.

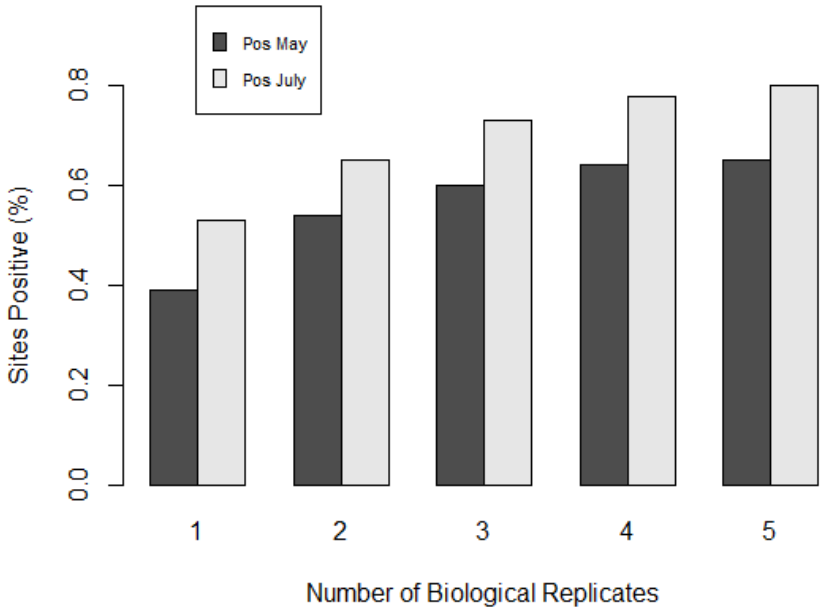

Figure 2.6: Comparison of the percentage of sites called positive based on the number of analyzed replicates per site. Values were determined based on the average of both positive calling methods seen in Figure 2.5.

Between May and July, the prevalence of ranavirus in eDNA samples varied between the two sampling periods, with seemingly more prevalence in July based on the IDW analysis (Figure 2.7, red denotes prevalence between 50-100%). Presence and intensity of virus varied among numerous regions (top left, bottom right) across sampling months, with a greater portion of the July heatmap being yellow (25-37% prevalence) and above compared to May. The greater number of replicates that were positive had a positive correlation to the concentration of Rv within eDNA samples (Supplementary Figure S2.3).

While there was a temporal pattern with ranavirus prevalence, the GLMM results showed that there were no significant predictors in terms of abiotic factors with positive ranavirus replicates as the response (Table 2.3). The highest-ranked model was the water temperature*conductivity interaction but had weak AIC and R^2 values (K=5, AIC=1038.29, R^2= 0.099).

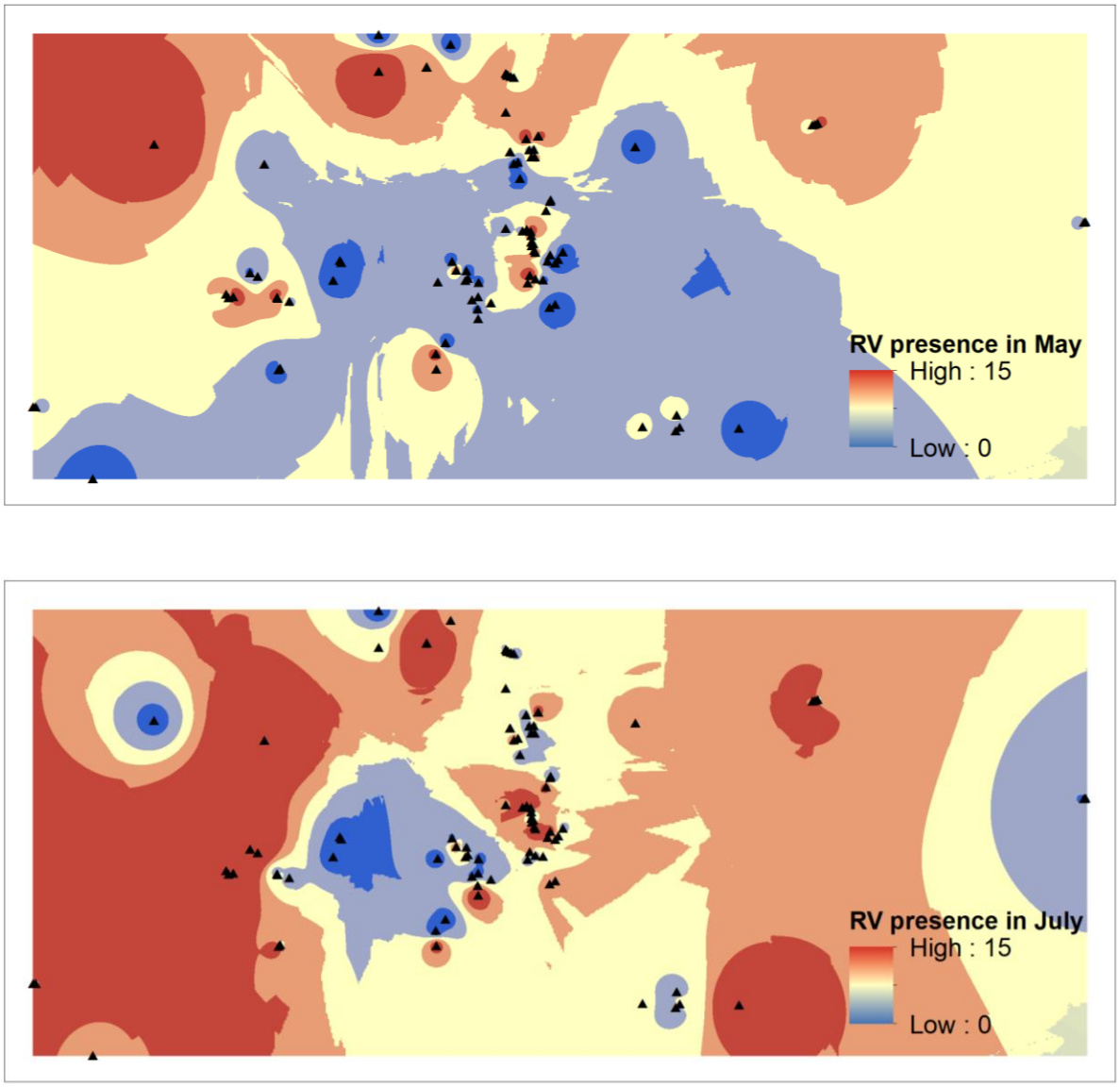

Figure 2.7: Spatial and temporal variation in ranaviral prevalence in the greater Peterborough region, Ontario, Canada. Heatmaps were generated with an inverse distance weighting method of capsule samples taken from 93 sites in 2016 (indicated by triangles), portraying the interpolated prevalence depicted as heatmaps. Intensity values were based on the number of positive qPCR replicates from each site out of 15 (five capsules per site, with three qPCR replicates per capsule). Colour-coded values follow a gradient from blue (0-12%), light blue (12-25%), yellow (25-37%), orange (37-50%), and red (50-100%).

Table 2.3: Generalized linear mixed model (GLMM) where abiotic factors taken during sampling period were predictors to abundance of ranavirus in eDNA samples. Strength of predictor models was determined by Akaike's information criterion (AIC) and R^2 values.

Variable	K	AIC	Delta AIC	R^2
Water temp * Conductivity	5	1038.29	0	0.099
Water temp + pH	4	1046.54	8.24	0.065
Water temperature	3	1046.82	8.52	0.061
Water temp * pH	5	1047.19	8.89	0.075
Water temp + Waterbody size	4	1048.15	9.85	0.063
Water temp * Waterbody size	5	1048.39	10.1	0.066
Water temp + Conductivity	4	1048.61	10.32	0.061
pH * Waterbody size	5	1059.71	21.42	0.045
pH	3	1060.65	22.36	0.026
pH + Conductivity	4	1061.56	23.26	0.028
pH + Waterbody size	4	1062.16	23.87	0.031
pH * Conductivity	5	1062.95	24.65	0.029
Null	2	1065.18	26.89	0
Conductivity	3	1066.43	28.14	0.005
Conductivity * Waterbody size	5	1066.83	28.53	0.032
Waterbody size	3	1066.86	28.57	0.003
Conductivity + Waterbody size	4	1068.23	29.93	0.008

2.4 Discussion

Ranavirus detection from eDNA was successful in an attempt to replicate similar methods from Hall *et al.* (2015) for waterbodies with no obvious signs of disease. There were also variable patterns of ranavirus presence when surveying multiple sites across two summer seasons, suggesting that there is a slight trend where ranavirus is more detectable in later summer months. Notably, there were low levels of virus detected continuously across multiple months even without the presence of die-offs, suggesting that presence of the virus may go unnoticed even though there are no obvious signs of infection or mortality, making eDNA-based methods a valuable detection tool for surveillance of ranavirus in the environment.

Ranaviruses such as frog virus 3 (FV3) are supposedly widespread across North America, but the exact extent is unknown as a matter of limited surveillance (Duffus *et a*l. 2015). On a coarser geographic scale (>30 km between sites, 73,100 km^2), ranavirus was detected in 24 of 31 sites sampled with cellulose nitrate filters (77%), with 9 of 18 sites positive in 2016 (50%) and 24 of 25 sites in 2017 (96%). On a finer geographic scale (<10km between sites, 7,150 km^2), we found that ranavirus was detected in 54-76% sites in May, and 64-91% sites in July, with 25-66% of sites being positive during both sampling rounds. Considering the capsule sampling alone, 81-96% of the 93 sites were positive at some point throughout the two sampling periods, suggesting a high rate of ranavirus presence in this fine-scale region. While ranavirus presence found in the region does not necessarily translate to the rest of Ontario or North America, it is worth applying eDNA-based surveillance methods on other regions to achieve a greater understanding of abundance with a higher degree of certainty.

There was a general trend within our results which suggested that later summer months are more likely to have detectable levels of ranavirus than earlier months. For the cellulose

nitrate filters, this trend was observed with the logistic regression, detecting more positive sites as the summer progressed (Figure 2.4). For capsule data, a total of five eDNA samples were taken at each site, with each having three qPCR replicates, leaving a total of 15 replicates per site, per sampling period. Based on the inverse distance weighting (IDW) maps, there was an increased number of replicates which were positive for Rv in July, where more of the region was yellow (25-37%) and above. However, it is important to note that not all sites followed this trend. For the cellulose nitrate filter sites, there were 6 sites that were positive only in June, and 3 that were positive in all months except August. While it is more likely to detect the virus in later months, some sites only have detectable levels early in the season, meaning that eDNA sampling should be performed multiple times in a season.

When looking at the predictor models, abiotic factors were not strong predictors. As such, biotic factors may be stronger predictors for ranavirus presence and intensity, such as taxonomic richness, species presence, and predator presence (Tornabene *et al.* 2017). While none of the abiotic factors were strong predictors, temperature is very likely tied to the trend seen with Rv presence across various months, as demonstrated in the results of this study. Host-pathogen dynamics can be influenced by temperature, as viruses replicate faster at their ideal temperatures (Brunner *et al.* 2015). In our capsule samples, the average water temperature taken during May was 14.9 ^{o}C, and in July the average was 20.5 ^{o}C (data not shown), where more sites had detectable levels of Rv in July (77.5% positive compared to 65% in May). By comparison, in Ariel *et al.* (2009), various ranavirus isolates were propagated *in vitro* and found that FV3 had an optimal temperature of 24 ^{o}C. Bayley *et al.* (2013) also found that FV3-infected tadpoles had a mortality rate of 96% at 20 ^{o}C, compared to only 32% mortality at 15 ^{o}C. A similar trend was seen in red-eared slider turtles (*Trachemys scripta elegans*) infected with FV3, where mortality

rates were 100% at 22 ºC, but only a 50% mortality rate at 28 ºC (Allender *et al.* 2013b). However, Echaubard *et al.* (2014) found a different trend in northern leopard frogs (*Rana pipiens*), where tadpoles infected with an FV3-like ranavirus (Morrison *et al.* 2014) had a higher likelihood of death at 14 ºC (67% mortality) compared to 22 ºC (51%). These studies suggest that Rv replication is likely ideal around 20 ºC, however mortality may also be host- and strain-dependent, as the virus used in Echaubard *et al.* was an FV3-like isolate, not FV3 itself (Echaubard *et al.* 2014; Morrison *et al.* 2014; Brunner *et al.* 2015).

Another possible explanation for this seasonal trend may be based on the density-dependent transmission model of wildlife disease, where transmission is theorized to be directly related to an increase in susceptible host density (McCallum *et al.* 2001). In the later summer months, more taxa (amphibian and other vertebrates such as fish or reptiles) are at higher densities due to emergence from hibernation, reproduction, and decreased water volumes, providing increased host density. However, this hypothesis has been tested with ranavirus previously, and found that this model does not reflect what is seen with infected tadpoles (Greer *et al.* 2008; Brunner *et al.* 2017), possibly disproving it. A more likely explanation for this trend may be the presence of more metamorphic amphibians within the waterbodies (Brunner *et al.* 2015). In wood frog tadpoles for example, the odds of mortality when exposed to ranavirus increased with each Gosner (1960) development stage (Warne *et al.* 2011). Epidemics are often observed in amphibians that are going through metamorphosis, as it is an energy-taxing process that causes immunosuppression (Speare & Smith 1992; Rollins-Smith 1998; Carey *et al.* 1999; Green *et al.* 2002; Greer *et al.* 2005).

One of the key concerns when working with eDNA is minimizing inhibitory effects that can cause false negatives. In this study, MagneSil magnetic beads were the preferred method of

extraction as it eliminated an initial collection of inhibitors that would have been present if extracted using DNeasy (data not shown). A subsequent test found that the Environmental Master Mix worked to eliminate almost 100% of remaining inhibition from the water samples tested (Strand *et al.* 2011; Jane *et al.* 2015), resulting in a greater number of positives that would have otherwise gone undetected. Should these methods have not been compared, it is very likely that many positives found in this study would have appeared as false negatives instead. False negative reporting rates can lead to numerous issues in terms of disease surveillance. For example, high false negatives may lessen the demand for surveillance or preventative measures as the pathogen would seem like less of a threat than it is; patterns that allow for disease persistence may be overlooked, such as water pollutants or anthropogenic stressors; and should preventative measures be put in place, sites resulting in false negatives may be missed, causing unforeseen die-offs and allow for further movement of the pathogen.

Hall *et al.* (2015) used three water samples taken per site, and each sample was run in triplicate for qPCR. Our cellulose nitrate filter samples followed the same protocol, and positives were only accepted if two of three technical replicates passed the threshold. In our study, we established a limit of detection (LOD) and a limit of quantification (LOQ) to determine a threshold of detection to strengthen the validity of true positives. First, the LOD was estimated to be 0.0301 pfu/µL (0.021-0.041 95% CI) based on the standard dilutions of each qPCR run (Hunter *et al.* 2017). However, qPCR instrumentation could detect lower than 0.03 pfu/µL, therefore the application of this method to our results may not be accurate. LOQ was then determined to be 0.04 pfu/µL, as it had a conserved sensitivity (57.2% of samples above threshold) and strong level of specificity (96.6% of controls under threshold, Nutz *et al.* 2011; Serrao *et al.* 2017). For capsule results, we accepted positives on a conserved and less conserved

method (Figure 2.5). The conserved method required two qPCR replicates to pass the 0.04 pfu/µL threshold, whereas the less conserved required only one to pass the threshold. This was performed to determine a range of calling positives for capsule samples, as this method of eDNA collection has never been performed for Rv surveillance. It is important to note that our results were based on our ability to detect the virus, and that a site that is considered negative may merely be a failure to detect.

While this study did not develop a new collection or extraction protocol with Sterivex filters, this was the first attempt at quantifying ranavirus from eDNA captured within an enclosed filter, suggesting that there is more than one effective way to sample for Rv using eDNA methods. In this study, we analyzed results based on five biological replicates per site for capsule sampling. Many eDNA studies take a total of three biological replicates per site (Chestnut *et al.* 2014; Wilson *et al.* 2014; Hall *et al.* 2015; Kolby *et al.* 2015; Laramie *et al.* 2015; Serrao *et al.* 2017), however in our study, five samples were taken per site, as there is 95% confidence of positive detection if the target is present (Chestnut *et al.* 2014). In our study, we found that positive sites plateaued around fourth biological replicates with 64% positive in May and 78% positive in July. By comparison, with five biological replicates there were 65% positive sites in May, and 80% in July. For three replicates, the number of sites positive were 60% and 73%. Should we have used three biological replicates, we would have misdiagnosed four and six sites per month, whereas with four, one and two sites would have been misdiagnosed. The number of samples taken per sites should be considered as additional samples are costly, despite being more accurate. While we were successful in detecting ranavirus using Sterivex capsules, future studies should consider a direct comparison of titers between cellulose nitrate filters and enclosed filters, to strengthen the validity of enclosed filters for ranavirus detection.

During the time of this study, another study was done which required sampling frogs at all life stages using body swabs. From this study, there was a total of 141 swabs of adults and 51 swabs from tadpoles (Table 2.1). All adult swabs returned negative for ranavirus, though it is possible that some may have been false positives as there is a 22% false negative rate when comparing oral cavity and cloacal swabs to liver samples, and the swabs for this study were only body swabs (Gray *et al.* 2012). When comparing between traditional specimen sampling and eDNA sampling during 2016, there were a higher number of Rv-positive sites identified with eDNA (n=9) than with swabs (n=3). Only one site was negative for ranavirus from eDNA samples, yet positive for tissue sampling (STL, Table 2.1). Initially, it was speculated that this was because the waterbody was a stream, suggesting that the viral DNA moved further downstream and was not captured. However, when sampling the same site in 2017, this site was positive for Rv across all three sampling months, with August having a high concentration of 100.1 pfu/µL. It is possible that low viral titers within bodies of moving water may be more difficult to detect comparatively to stagnant water, and that higher titers are required within moving water in order to be detected.

Higher rates of viral presence in eDNA sampling compared to traditional sampling is likely due to three non-mutually exclusive hypotheses. First, body swabs have a high rate of false-negative results for a systemic ranavirus, and many of the sites were limited to adult swabbing as tadpoles were unable to be found (Gray *et al*. 2012). Second, when an outbreak is not occurring, it is likely that not all specimens are carrying the virus, and that the specimens collected happened to be uninfected by chance (Cooch *et al.* 2012). And finally, while sub-lethal doses of virus are likely present in specimens that were not captured, infected specimens are likely releasing virus into the water, which was picked up via eDNA sampling. These factors

should be considered when determining an optimal method for ranavirus surveillance, seeing as ranavirus was detected in three times as many sites using eDNA as opposed to swab and tissue sampling.

When surveying for ranaviruses, eDNA appears to be an effective alternative to traditional sampling methods, and is less time consuming and costly, as well as non-invasive to host species. While Hall et al. (2015) was first to successfully amplify ranavirus from eDNA, our study worked to advance the validation of eDNA-based methods as a surveillance tool by documenting the spatio-temporal patterns of presence over multiple months and seasons, and determine factors which predicted ranavirus presence. While eDNA is more likely to detect Rv in later summer months, eDNA-based sampling is most optimal when used across multiple months, as ranavirus outbreaks and detectability is sporadic across the season. Waterbodies where there are constant low levels of ranavirus should be further studied to understand what causes the preservation and re-emergence each season. As a final note, as amphibian pathogens are a growing concern across Ontario and North American waters, the application of eDNA surveillance should be seriously considered in order to track how widespread these diseases impend.

2.5 Acknowledgements

I would like to thank Megan Congram for collecting the 93 Sterivex capsule field samples and allowing me to use them and their data, along with Audrey Wilson for aiding in extracting and running the samples. I would also like to thank Dr. Lynne Beaty for advice on the statistical analysis of predictor models. Finally, I thank Dr. Sibelle Torres Vilaça for her help in the lab and data analyses.

CHAPTER 3

INTRASPECIFIC VARIATION OF FROG VIRUS 3 AT TWO DISTANT CANADIAN REGIONS PROVIDING EVIDENCE FOR NOVEL AND POSSIBLE RECOMBINANT FV3-LIKE RANAVIRUSES

Preface

Contributions: Ontario samples were collected and extracted by Samantha Grant. Northwest Territories and Alberta samples were collected, extracted, and pre-screened for frog virus 3 by Joe-Felix Bienentreu of Laurentian University. Frog virus 3 control samples were cultured in Dr. Craig Brunetti's lab at Trent University.

Abstract

Frog virus 3 (FV3) and FV3-like ranaviruses can infect a variety of cold-blooded aquatic species and present a primary threat to amphibians across the globe. Previous studies of FV3-like viruses have largely investigated higher-level phylogenetic distinctions of these pathogens via portions of the conserved major capsid protein (MCP), and the putative virulence gene vIF-2α. Few studies however, have investigated the spatial distribution of FV3 variants at the population level – data that can be used to further understand the spatial epidemiology of this disease. In this study, we sequenced the MCP and vIF-2α of 127 FV3-positive amphibians sampled from Canadian waterbodies in Ontario, North-eastern Alberta, and southern Northwest Territories to explore if intraspecific genetic variation exists within FV3. There was a lack of variation at the two markers across these regions, suggesting that there is a lack of FV3 sequence diversity in Canada and may hint at a single source of infection that has spread. However, an undocumented variant termed WBRV was detected in samples from three sites in Alberta and Northwest

Territories that clustered within the FV3-like lineage with 99.3% sequence homology. For vIF-2α, all sequences were the expected truncated variant except for six samples in Ontario. Sequences from these samples were suggestive of recombination with common midwife toad virus (CMTV). Our lack of variation suggests higher resolution genome analyses may be required to further explore the spatial spread and intraspecific variation of the disease.

Keywords: frog virus 3, ranavirus, amphibians, major capsid protein, vIF-2α, phylogenetic, wildlife disease

3.1 Introduction

Spatio-temporal phylogeographical analyses of infectious diseases are important sources to the understanding of pathogen dispersion (Lemey *et al.* 2009). Gene sequences from pathogen isolates sampled across different years and geographical locations can be used to identify means of transmission (i.e. environmental barriers or bridges, anthropogenic influences), and therefore help develop conservation efforts which target these sources of pathogen movement (Wallace & Fitch 2008; Cullingham *et al.* 2009). For example, phylogeographic studies have been employed to zoonotic and human diseases, such as HIV (Leitner *et al.* 1996), rabies (Bourhy *et al.* 2008; Lemey *et al.* 2009), and influenza (Wallace & Fitch 2008; Lemey *et al.* 2009), by exploring the intraspecific genetic variation of viral strains over space and time to infer pathogen spread, movement, and maintenance in their host.

Over the past twenty years, there have been increasing reports of declines in amphibian populations around the globe (Singh 2002; Stuart *et al.* 2004; Harp & Petranka 2006). Combined with anthropogenic stressors such as habitat destruction, pollution, climate change, agriculture run-off, herbicides, pesticides, and wildlife trade (Harp & Petranka 2006; Gray *et al.* 2007; Schock *et al.* 2009; Duffus *et al.* 2015), there have been upsurges in amphibian mortality from disease. Two prominent and broadly dispersed diseases associated with mass epidemics and significant population declines include the fungal disease, *Batrachochytrium dendrobatidis*, and ranaviruses, such as frog virus 3 (FV3) (Green *et al.* 2002; Greer *et al.* 2005; Gray *et al.* 2009, 2015; James *et al.* 2015).

Ranavirus is a genus of the family *Iridoviridae* that is made up of over 20 systemically infectious species and isolates that target ectothermic vertebrates (Tan *et al.* 2004, Brunner *et al.* 2015, Duffus *et al.* 2015, Forzán *et al.* 2017). Within this genus, eight viruses are recognized as

distinct species by the International Committee on Taxonomy of Viruses (Chinchar *et al*. 2017). One of the most prevalent and best characterized species of *Ranavirus* is FV3 (Granoff *et al.* 1965). Although FV3 is considered a species, other ranaviruses are grouped within the same lineage as FV3 based on factors that include amino acid and nucleotide sequence relatedness, host species, genome size, genetic co-linearity, gene content and GC content (Tan *et al.* 2004, Jancovich *et al.* 2012, 2015). Examples of FV3-like viruses include, but are not limited to: Soft-shelled turtle iridovirus (STIV), *Rana grylio* virus (RGV), and tiger frog virus (TFV), all isolated within various species in China (He *et al.* 2002, Huang *et al.* 2009, Lei *et al.* 2012), bohle iridovirus (BIV), isolated from *Limnodynastes ornatus* (Ornate burrowing frog) in Australia (Marsh *et al.* 2002), German gecko ranavirus (GGRV) isolated in Germany (Stöhr *et al.* 2015), and spotted salamander Maine (SSME) isolated in the USA, that has 98.79% sequence identity to FV3 (Morrison *et al.* 2014). Many other FV3-like ranavirus isolates have been identified, either in other regions of the globe other than the region of its initial isolation, or within different species or taxa. FV3 has been identified within *Scaphirhynchus albus* (pallid sturgeon) within USA (T. B. Waltzek unpubl. data), and within *Rana catesbeiana* (American bullfrog) and *Rana temporaria* (Common frog) in Brazil and the UK respectively (R. A. Mazzoni *et al.* unpubl. data, S. J. Price *et al.* unpubl. data). Another FV3-like virus known at *Rana catesbeiana* virus (RCV) has also been isolated in American bullfrogs within Japan, Taiwan, and USA, likely through international trade (Une *et al.* 2009, Claytor *et al.* 2017, C. -Y. Hsieh *et al.* unpubl. data).

Ranavirus research has primarily focused on phylogenetics of isolates with vast global distances between one another (different continents), or different taxonomic host origin (e.g., Hyatt *et al.* 2000; Chinchar 2002; Holopainen *et al.* 2009; Stöhr *et al.* 2015), however, little work has been done investigating intraspecific variation of a single strain itself, such as FV3. A

thorough analysis of the intraspecific genetic variability of FV3 may provide insight on its environmental maintenance and movement which can be used to predict its future spread. Many ranavirus studies focus on the major capsid protein gene (MCP, ORF 90R) and the viral homolog of eIF-2α (vIF-2α, ORF 26R) due to their conservation and individuality between lineages (Mao *et al.* 1997; Hyatt *et al.* 2000; Stöhr *et al.* 2015). The MCP gene is genetically conserved within ranavirus and is often used to identify and categorize ranavirus isolates into their appropriate lineage (Allender *et al.* 2013; Duffus & Andrews 2013; Kolby *et al.* 2014; Martel *et al.* 2014; Waltzek *et al.* 2014). However, literature and databases suggest that the MCP can show evidence of variation within FV3 when sampled across continents and taxonomic classes of hosts (Tan *et al.* 2004; Holopainen *et al.* 2009; Mazzoni *et al.* 2009; Saucedo *et al.* 2017).

In this study, I investigated the intraspecific genetic variability among isolates of FV3 samples across three Canadian regions over three years to shed light on the spatio-temporal genetic diversity present in FV3 within Canada. I assessed intraspecific FV3 variation by examining the full MCP gene sequence (1,392 bp) for higher resolution to detect haplotypes at this commonly profiled locus. Along with comparison of haplotypes within Canada, I also compared haplotypes in our study to other FV3 isolates from previous studies. I chose to sample at both fine and coarse geographical scales, with samples taken from Ontario, Alberta, and Northwest Territories. Further, given the importance of vIF-2α in pathogenicity (Jancovich & Jacobs 2011) I also screened for size variants and sequenced this gene to estimate virulence, as well to determine the relationship between our haplotypes to pre-existing ranaviruses (Essbauer *et al.* 2001; Stöhr *et al.* 2015). These results should help to elucidate the intraspecific variation within FV3 and its spatio-temporal spread, which provides predictors into future movement of the virus.

3.2 Materials and Methods

3.2.1 Sample Collection

Sixteen field sites were visited across central Ontario in June and August of 2016, with only four sites having FV3 positive specimens (Table 3.1, Figure 3.1). Tadpoles were euthanized by submersion in ethanol and stored in 95% ethanol. Nitrile gloves were changed between handling individuals, and field equipment (nets, waders, boots) were disinfected with 10% bleach for 15 minutes between sites to prevent cross-contamination. All samples were kept on ice until transported to the lab, where they were refrigerated at 4 °C until extraction.

Twenty field sites were sampled in Alberta and Northwest Territories from April to July during 2015, 2016, and 2017 to assess ranavirus presence. Tissue samples were tested for FV3 from seven field sites across all three years (Table 3.1, Figure 3.1). Toe clips of adult frogs were collected while tadpoles were euthanized and stored in 95% ethanol. Toe-clippers were disinfected with 95% ethanol between individuals, and all equipment was disinfected between sites with 15% bleach for 15 minutes. All samples were kept in ethanol and stored at -20 °C until transportation and extraction. Samples were collected and processed by Joe-Felix Bienentreu at Laurentian University.

Table 3.1: Site locations and life stages of all collected samples, with breakdown of all samples positive for ranavirus**.**

Site	Date	Coordinates		Life Stage			FV3 prevalence	
		Latitude (°N)	Longitude (°W)	Tadpole	Meta	Adult	+/total	%
Ontario								
KEN	June 2016	44.57991	-78.42634	6	0	0	6/6	100%
MOA	Aug 2016	44.27409	-77.34493	7	0	0	1/7	14%
STL	Aug 2016	44.45036	-78.64189	7	0	0	2/7	29%
TIM	Aug 2016	46.53696	-80.94803	0	0	1	1/1	100%
Alberta								
Toadlet pond	2015	59.445	-112.362	0	4	15	13/25	52%
Toadlet pond	2016	59.445	-112.362	0	0	2	2/2	100%
Toadlet pond	2017	59.445	-112.362	25	0	2	8/27	30%
Wolf Creek	2015	59.927	-111.747	16	0	10	0/26	0%
Northwest Territories								
Antoinette's pond	2015	60.108	-112.263	4	31	10	6/45	13%
Dnp Wetlands	2015	60.034	-112.911	3	0	18	0/21	0%
Preble pond	2017	60.033	-113.189	5	0	0	0/5	0%
KM 190	2015	60.048	-113.137	30	7	10	21/47	45%
KM 190	2017	60.048	-113.137	12	0	18	12/30	40%
KM 196	2017	60.028	-113.027	58	0	8	55/66	83%

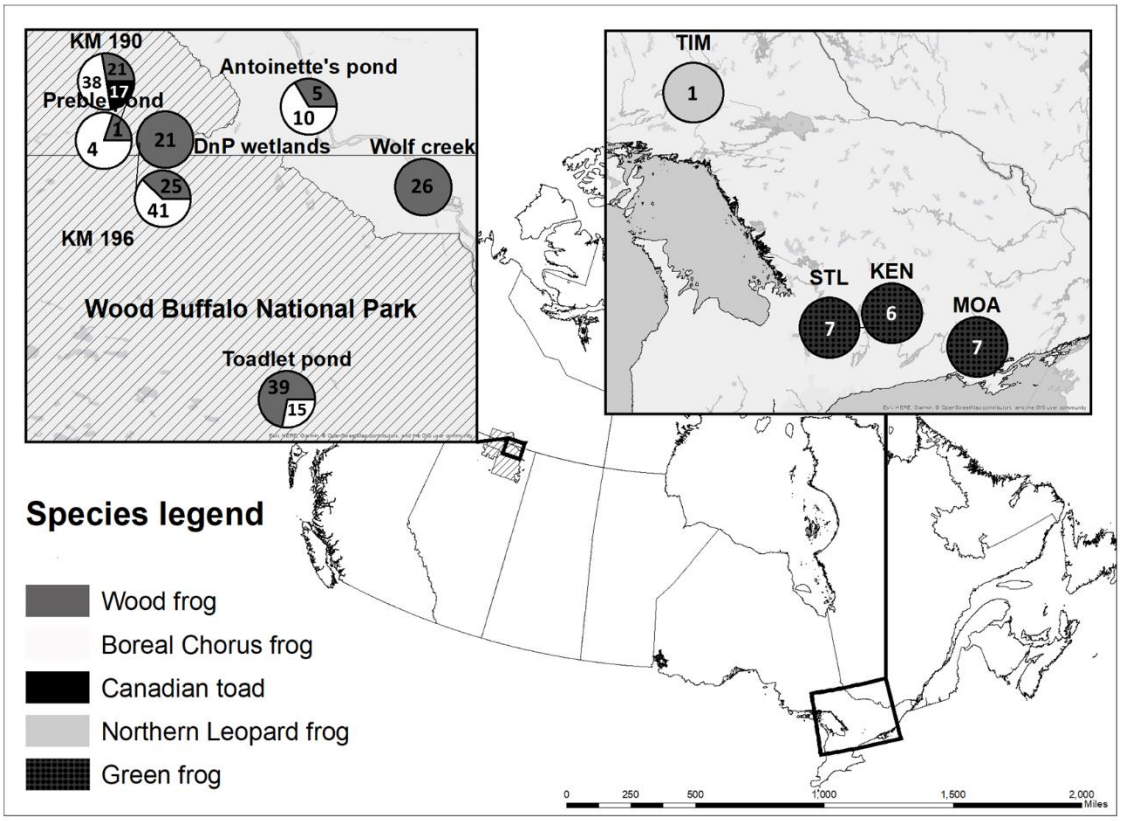

Figure 3.1: Map of sites across Ontario, Alberta, and Northwest Territories, Canada, including breakdown of total anuran species collected at each site between 2015 and 2017

3.2.2 Extraction

Tails of tadpoles (n=215) were clipped and toe clips (n=94) were put in tubes with 200 µL lysis buffer. All clippings (n=309) had 20 mg/mL proteinase K added and were incubated at 56 °C for 2 hours, vortexing every 30 minutes. Swabs were subsequently discarded using sterile forceps decontaminated in a 10% bleach solution and rinsed with deionized water. All samples were then extracted with a DNeasy Blood and Tissue kit (Qiagen Inc.) according to manufacturer's protocols.

3.2.3 PCR Amplification and Sequencing

Primers were newly designed to amplify the MCP of FV3 and the spotted salamander Maine isolate (SSME) (Table 3.2), excluding all other ranavirus isolates and species. Samples were run on conventional PCR targeting the major capsid protein gene (MCP), performed in 15 µL volume reactions consisting of 1X PCR buffer (Promega), 0.2 mmol/L dNTPs, 1.5 mM $MgCl_2$, 0.15 mg/mL Bovine Serum Albumin, 0.3 umol/L forward (5'-TCCACAGTCACCGTGTATCTT-3') and reverse (5'-TGCAGCAAACGGACACTT-3') primers, 0.2 U Taq polymerase (Promega), and 4 µL of template DNA. PCR conditions consisted of 5 minutes at 95 °C, then 38 cycles of 30 seconds at 95 °C, 30 seconds at 58 °C, and 2 minutes at 72 °C which were then followed by 2 minutes at 72 °C. Samples were amplified at the vIF-2α region with newly designed primers (Table 3.2) and were performed in 15 µL volume reactions identical as above except with 0.3 umol/L forward (5'-AACAAATGCAATGACTGTAAATG-3') and reverse (5'-ACACAAAGGGGCACAGTC-3') primers, and 3 µL template DNA. PCR conditions consisted of 5 minutes at 95 °C, then 35 cycles of 30 seconds at 95 °C, 30 seconds at 53 °C, and 90 seconds at 72 °C, followed by 2

minutes at 72 °C. Three positives of a FV3-like isolate cultured in epithelioma papulosum cyprini cells were included at concentrations of 200, 20, and 2 pfu/μL as well as a negative control. Amplified products were separated using gel electrophoresis on a 1.5% agarose gel, and visualized using ethidium bromide under ultraviolet light.

Amplified products were purified using ExoSAP (New England Biolabs) then sequenced using a Big Dye® Terminator version 3.1 cycle sequencing kit (Life Technologies), and run on an ABI 3730 sequencer.

Table 3.2: Primers used for DNA analysis. Primer positions were relative to the Frog Virus 3 genome (AY548484).

Primer	Location	Nucleotide sequence
MCP forward	97310 – 97330	5’ – TCC ACA GTC ACC GTG TAT CTT – 3’
MCP reverse	98061 – 98044	5’ – TGC AGC AAA CGG ACA CTT – 3’
vIF-2α forward	32947 – 32969	5’ – AAC AAA TGC AAT GAC TGT AAA TG – 3’
vIF-2α reverse	33195 – 33178	5’ – ACA CAA AGG GGC ACA GTC – 3’

3.2.4 BLAST and Phylogenetic Analysis

Completed sequences were aligned using ClustalW (Larkin *et al.* 2007) and manually verified for calling errors using MEGA7 (Kumar *et al.* 2016) using reference FV3 genes (MCP and vIF-2α) from GenBank Accession No. AY548484. MCP sequences were trimmed to 1,392 bp of the entire coding region, while vIF-2α sequences were left untrimmed due to the variable length of the gene found in various ranaviruses. Sequences were analyzed through Nucleotide Basic Local Alignment Search Tool (BLASTn) to determine sequence similarity. vIF-2α sequences were then trimmed to the reference sequence of best fit, and all sequences were then translated to determine the estimated protein sequences of unknown haplotypes.

Samples with <100% sequence homology to FV3 and SSME (Accession No. AY548484 and KJ175144 respectively) were aligned in MEGA7 (Kumar *et al.* 2016) to the MCP and vIF-2α of other FV3-like ranavirus isolates to determine variable nucleotide positions. Sequences compared to unknown samples (both MCP and vIF-2α) included FV3-like ranaviruses for MCP, along with CMTV-like ranaviruses for vIF-2α, and *Ambystoma tigrinum* virus (ATV) (AY150217) (Jancovich *et al.* 2003) as an outgroup (see Tables 3.3 and 3.4 for GenBank accession numbers). Nucleotide substitution model optimization was performed through MEGA7 for MCP and vIF-2α to determine the best fitting model for phylogenetic tree construction. For the MCP, the HKY+G model (Hasegawa *et al.* 1985) was the best fitting model, and for vIF-2α the HKY model (Hasegawa *et al.* 1985) was determined as best fit. Phylogenetic trees were constructed using maximum-likelihood methods in MEGA7 (Kumar *et al.* 2016), with 1,000 bootstrap replicates.

3.3 Results

A total of 127 tissue samples of 309 were positive for ranavirus and were fully sequenced at the major capsid protein (MCP) gene. 94 of the 127 samples fully sequenced at the vIF-2α gene due to low viral copy DNA. There was a total of five anuran species infected with ranavirus (Supplementary table S3.1): *Rana clamitans* (Green frog, n=9), *Rana pipiens* (Northern leopard frog, n=1), *Lithobates sylvaticus* (Wood frog, n=53), *Pseudacris maculata* (Boreal chorus frog, n=61), and *Anaxyrus hemiophrys* (Canadian toad, n=3). At the MCP, a previously undocumented haplotype, WBRV (referenced as Wood Buffalo ranavirus, as a matter of all three infected sites in Wood Buffalo National Park having this variant; 45 samples total) had high homology with FV3, with 99.3% sequence similarity with 9 nucleotide changes (Table 3.3). Out of the nine nucleotide changes, three were non-synonymous mutations (S235A, A238E, T290A). The vIF-2α region for the WBRV haplotype was truncated (231 bp), and there was a 99.6% homology to FV3 (AY548484) with one non-synonymous substitution (R29P) (Table 3.4).

The majority of sequences (82 samples, within all species except Canadian toad) had 100% similarity to the MCP of four FV3-like isolates (Table 3.3): FV3 sequence isolated in *Rana pipiens* from USA (Holopainen *et al.* 2009), SSME isolated in *Ambystoma maculatum* from USA (Morrison *et al.* 2014), FV3-RUK13 isolated in *Rana temporaria* in the UK, and PSRV-2009 isolated in *Scaphirhynchus albus* (pallid sturgeon). However, compared to the reference FV3 genome submitted to GenBank in 2004 (AY548484) (Tan *et al.* 2004), there was a 99.9% similarity with one nucleotide difference at position 648 between all sequences (Table 3.3). Interestingly, the vIF-2α region of samples from one site KEN (Ontario) had a band approximately 1,200 bp in length (Figure 3.2), which when trimmed to the coding region had a 99.8% sequence similarity to the eIF-2α protein of the Chinese giant salamander iridovirus

(GSIV) (Li *et al.* 2014) – also referred to as *Andrias davidianus* ranavirus (ADRV) – an isolate of the common midwife toad virus lineage (CMTV-like viruses) (Table 3.4, Supplementary table S3.1). Overall, there were three haplotypes found using these two genes (Figure 3.4).

A maximum likelihood phylogeny of the MCP (Figure 3.3) placed the new WBRV isolate outside the FV3 clade. However, the phylogenetic tree of the vIF-2α (Figure 3.4) clustered the WBRV isolate within with FV3 clade with high bootstrap value, providing a more reliable tree than the phylogenetic tree based on the MCP. Meanwhile, the samples from KEN with the CMTV-like vIF-2α gene clustered with SSME and FV3 when comparing the MCP, yet clustered with CMTV and GSIV when comparing the vIF-2α gene.

Table 3.3: Polymorphic sites of the entire MCP of 15 FV3-like ranaviruses with ≥98.5% sequence similarity to the reference FV3 (AY548484). Table includes three samples from this study (bolded): WBRV, an unknown haplotype discovered in Northwest Territories and Alberta, Canada; FV3/CMTV, a potentially recombinant isolate between FV3 and CMTV; and FV3 – CAN (Canadian isolate), which had no genetic variation across northern and southern provinces and territories.

Given name (isolate)	Accession Number	Country of origin	Species of origin	Variable nucleotide position - MCP																																																	
				11	12	18	20	39	42	90	171	186	249	261	268	279	292	297	306	327	414	432	443	460	579	612	648	660	681	703	711	713	783	816	833	867	868	889	893	913	989	1017	1023	1101	1174	1183	1200	1212	1278	1285	1324	1368	1380
FV3	**AY548484**	**USA**	***Rana pipiens***	T	A	T	C	C	C	G	G	C	G	C	G	T	G	C	C	C	C	G	C	A	C	C	C	C	G	T	T	C	A	T	C	G	A	C	T	T	T	T	A	G	C	C	C	T	T	A	A	C	C
FV3-CAN	**N/A**	**Canada**	**Many****																								G																										
FV3/CMTV	**N/A**	**Canada**	***Rana sylvaticus***																								G																										
FV3-RUK13	KJ538546	UK	*Rana temporaria*																								G																										
SSME	KJ175144	USA	*Ambystoma maculatum*																								G																										
FV3-PSRV	KF646249	USA	*Scaphirhynchus albus*																								G																										
FV3	FJ459783	USA	*Rana pipiens*																								G																										
FV3	DQ897669	Brazil	*Rana catesbeiana*					A									A	A									G																										
FV3 *Op*	MF360246	Netherlands / Nicaragua*	*Oophaga pumilio*																			A					G		A																	T			C	G			
STIV	EU627010	China	*Trionyx sinensis*																				T				G				C					A																	
RGV	JQ654586	China	*Rana grylio*																				T				G				C					A																	
STIV	DQ335253	China	*Trionyx sinensis*																				T	G			G				C					A			C														
RNR	MF359927	China	*Rana nigromaculatus*	A	T																		T				G				C					A								A									
HNV	AB500273	Japan	*Hynobius nebulosus*			A						T								A		T	T				G				C				T		G											C					
RCV	AB474588	Japan	*Rana catesbeiana*																				T				G				C				T		G															T	
RCV	FJ207464	Taiwan	*Rana catesbeiana*												A								T				G				C				T		G														G		
KRV	HM133594	South Korea	*Rana plancyi chosenica*																				T				G				C				T		G														G		
WBRV	**N/A**	**Canada**	**Many*****																							T	G			G	C	A	G	C			G			C		G											
BIV	AY187046	Australia	*Limnodynastes ornatus*				T		T	A									A			A				T	G	T			C						G	A				G	G					C	C	G			T
TFV	AF389451	China	*Rana tigrina rugulosa*								T		A	T		C		A			T				A		G				C		G		T		G				C	G	G		A		A	C	C	G			

* Reported in the Netherlands but imported from Nicaragua

** Species include: *Rana clamitans, Rana pipiens, Lithobates sylvaticus,* and *Pseudacris maculata*

*** Species include: *Lithobates sylvaticus, Pseudacris maculata,* and *Anaxyrus hemiophrys*

Abbreviations for isolate names were based on given names of sequences from Genbank. Several sequences share similar names however were sampled from different species or location. FV3: Frog virus 3; SSME: Spotted salamander Maine; STIV: Soft-shelled turtle iridovirus; RGV: *Rana grylio* virus; RNR: *Rana nigromaculata* ranavirus strain; HNV: *Hynobius nebulosus* virus; RCV: *Rana catesbeiana* virus; KRV: Korean ranavirus-1; WBRV: Wood Buffalo ranavirus; BIV: Bohle iridovirus; TFV: Tiger frog virus.

Table 3.4: Polymorphic sites of vIF-2α gene of 15 ranavirus isolates. Table includes three samples from this study (bolded): WBRV, an unknown haplotype discovered in Northwest Territories and Alberta, Canada; FV3/CMTV, a potentially recombinant isolate between FV3 and CMTV; and FV3 – CAN (Canadian isolate), which had no genetic variation across northern and southern provinces and territories. Sequences were compared to the truncated vIF-2α of FV3 (231 bp), therefore the complete extent of genetic variation is not seen within non-truncated samples.

Given name (isolate)	Accession number	Country of origin	Length (bp)	Variable nucleotide position - vIF-2α																																									
				1	2	3	6	7	8	9	10	11	12	13	14	15	18	19	21	23	24	25	26	27	28	31	44	45	49	62	74	90	100	146	150	153	158	159	160	161	166	167	172	184	192
FV3	**AY548484**	**USA**	**231**	**A**	**T**	**G**	**T**	**A**	**G**	**A**	**C**	**T**	**T**	**G**	**G**	**A**	**G**	**T**	**T**	**A**	**A**	**A**	**C**	**A**	**C**	**G**	**G**	**T**	**A**	**G**	**G**	**C**	**A**	**C**	**G**	**C**	**G**	**G**	**C**	**T**	**A**	**C**	**C**	**C**	**T**
SSME	KJ175144	USA	231																																										
FV3-CAN	**N/A**	**Canada**	**231**																																										
LMR	KM516757	Portugal	211	--	--	--																																							
RCV-Z2	MF187209	USA	231																																										
WBRV	**N/A**	**Canada**	**231**																																**G**											
STIV	DQ335253	China	200	--	--	--	--	--	--	--	--	--	--	--	--	--	--	--	--	--	--	--	--	--	--	A		C																	
RGV	JQ654586	China	200	--	--	--	--	--	--	--	--	--	--	--	--	--	--	--	--	--	--	--	--	--	--	A		C																	
BIV	AY187046	Australia	198	--	--	--	--	--	--	--	--	--	--	--	--	--	--	--	--	--	--	--	--	--	--	--	A	C					G												C
TFV	AF389451	China	200	--	--	--	--	--	--	--	--	--	--	--	--	--	--	--	--	--	--	--	--	--	--	A	A	C			A		G		A						G		A		C
CMTV	JQ231222	Spain	780	G	C	C	C	T	T	T	G	G	G	C	A	C	C	C	G	G		G	G	T	G	A	A	C					G			A	A	C	T	G	G			T	C
FV3 *Op*	MF360246	Netherlands/ Nicaragua*	780	G	C	C	C	T	T	T	G	G	G	C	A	C	C	C	G	G		G	G	T	G	A	A	C	C				G												
FV3/CMTV	**N/A**	**Canada**	**725**	**G**	**C**	**C**	**C**	**T**	**T**	**T**	**G**	**G**	**G**	**C**	**A**	**C**	**C**	**C**	**G**	**G**		**G**	**G**	**T**	**G**	**A**	**A**	**C**	**C**				**G**			**A**					**G**	**T**		**--**	**--**
GSIV	KF512820	China	780	G	C	C	C	T	T	T	G	G	G	C	A	C	C	C	G	G		G	G	T	G	A	A	C	C				G			A					G				C
ATV	AY150217	USA	780	G	C	C	C	T	T	T	G	G	G	C	A	C	C	C	G	G	G	G	G	T	G	A	A	C		A		T	G												

* Reported in the Netherlands but imported from Nicaragua

-- Gene sequences had fewer nucleotides than referenced FV3 sequence

FV3: Frog virus 3; SSME: Spotted salamander Maine; FV3-CAN; FV3 isolate found within Canada; LMR: *Lacerta monticola* ranavirus; RCV-Z2; *Rana catesbeiana* virus isolate Z2; WBRV: Wood Buffalo ranavirus; STIV: Soft-shelled turtle iridovirus; RGV: *Rana grylio* virus; FV3 *Op*: Frog virus 3 isolate *Op*/2015/Netherlands; BIV: Bohle iridovirus; TFV: Tiger frog virus; CMTV: Common midwife toad virus; FV3/CMTV: FV3-like isolate discovered in Ontario with CMTV-like vIF-2α gene; GSIV: Chinese giant salamander iridovirus; ATV: *Ambystoma tigrinum* virus.

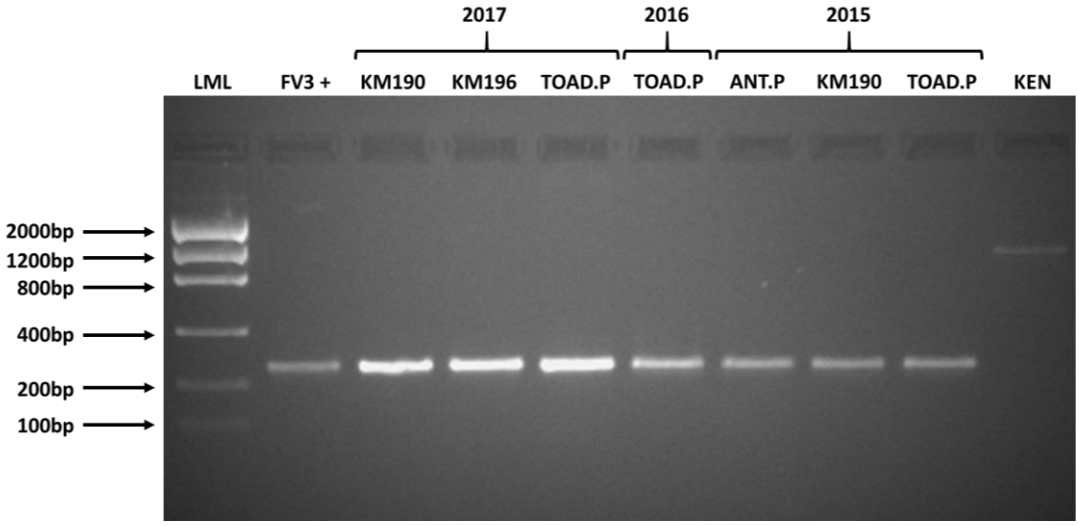

Figure 3.2: PCR amplification of the vIF-2α region of eight FV3-like samples sampled across Canada. LML: Low mass ladder; FV3+: Cultured FV3 positive control. Site abbreviations as follows: TOAD.P: Toadlet pond; ANT.P: Antoinette's pond. See Table 3.1 and Figure 3.1 for site locations

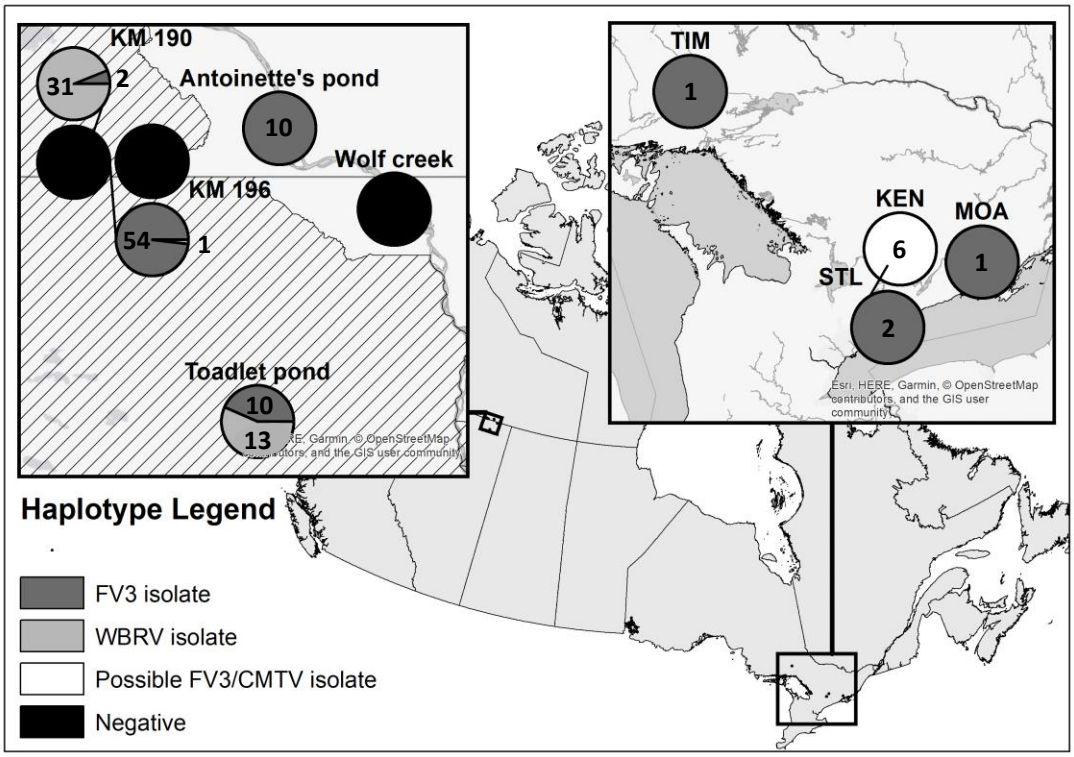

Figure 3.3: Map of haplotype frequencies across Ontario, AB, and NWT. Colors represent the different haplotypes in the MCP and vIF-2α genes, and numbers in the pie charts represent are the total samples infected with given isolate over three years.

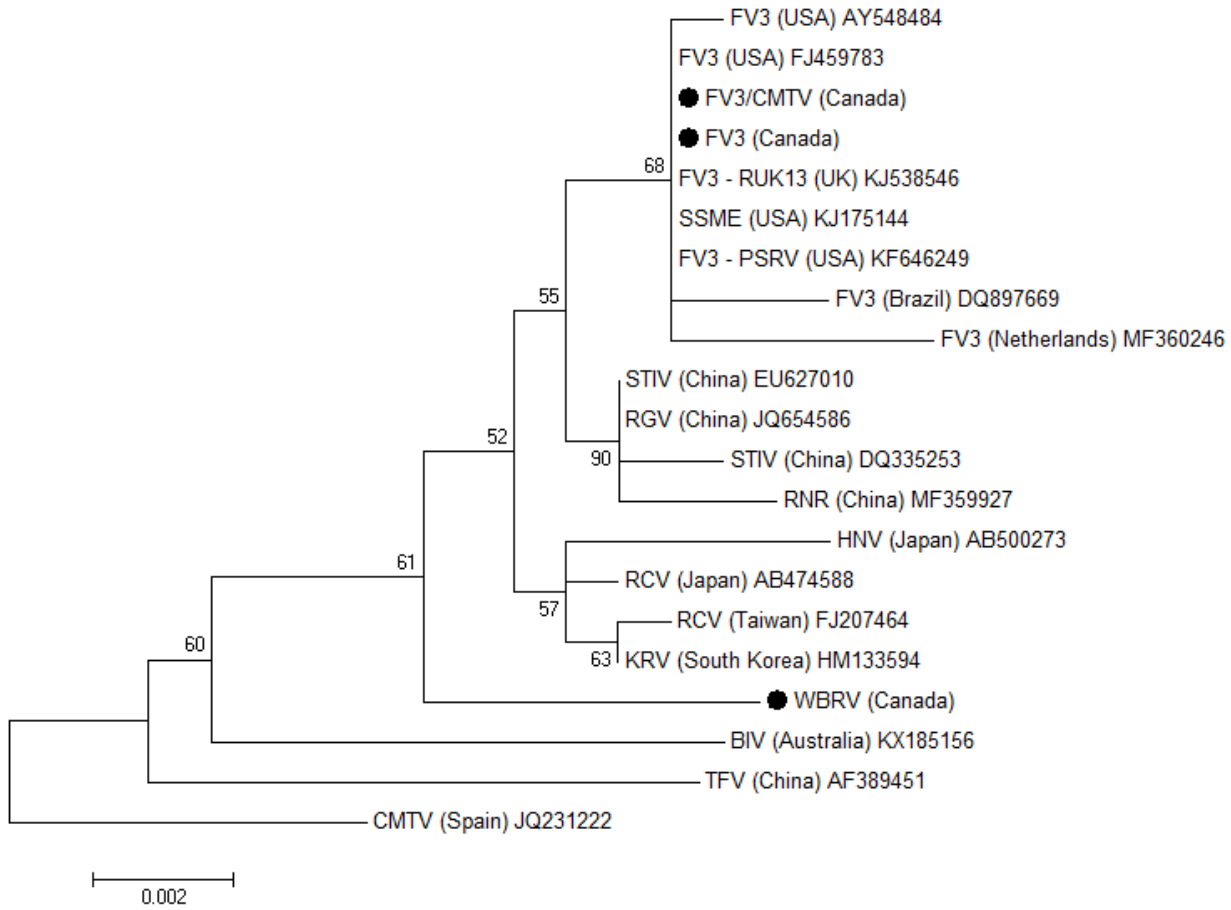

Figure 3.4: Maximum likelihood tree of the MCP of 20 FV3-like ranaviruses, with common midwife toad virus (CMTV) as an outgroup. The three samples found within this study are shown with a black circle. Sequences were named based on given names from genbank sequences. FV3: Frog virus 3; SSME: Spotted salamander Maine; STIV: Soft-shelled turtle iridovirus; RGV: *Rana grylio* virus; RNR: *Rana nigromaculata* ranavirus strain; HNV: *Hynobius nebulosus* virus; RCV: *Rana catesbeiana* virus; KRV: Korean ranavirus-1; BIV: Bohle iridovirus; TFV: Tiger frog virus; CMTV: Common midwife toad virus. See Table 3.3 for nucleotide polymorphisms.

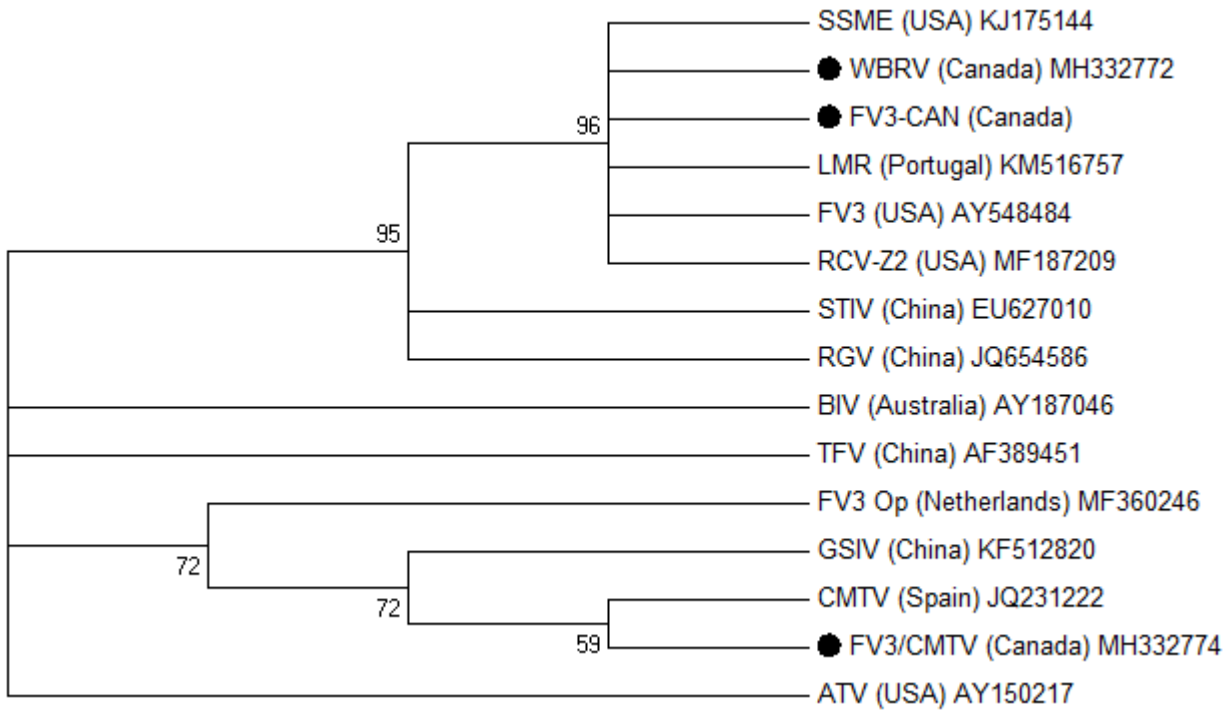

Figure 3.5: Maximum likelihood (ML) consensus tree of vIF-2α gene including eleven FV3-like ranavirus isolates, two CMTV-like isolates, and *Ambystoma tigrinum* virus (ATV) as an outgroup. Sequences with a black dot indicate samples sequenced during this study. LMR: *Lacerta monticola* ranavirus; SSME: Spotted salamander Maine; WBRV: Wood Buffalo ranavirus; FV3: Frog virus 3; FV3-CAN; FV3 isolate found within Canada; RCV-Z2; *Rana catesbeiana* virus isolate Z2; STIV: Soft-shelled turtle; RGV: *Rana grylio* virus; BIV: Bohle iridovirus; TFV: Tiger frog virus; FV3 *Op*: Frog virus 3 isolate *Op*/2015/Netherlands; GSIV: Chinese giant salamander iridovirus; iridovirus; FV3/CMTV: FV3-like isolate discovered in Ontario with CMTV-like vIF-2α gene; CMTV: Common midwife toad virus; ATV: *Ambystoma tigrinum* virus. See Table 3.4 for nucleotide polymorphisms.

3.4 Discussion

In this study, I sequenced the major capsid protein (MCP) and the putative viral homologue of eIF-2α (vIF-2α) to investigate the intraspecific genetic variability of FV3 across three Canadian regions over three years. Out of 127 tissue samples, there were a total of three FV3-like haplotypes: the FV3 isolate; a recombinant isolate that had the MCP of a FV3-like virus, but with a non-truncated vIF-2α gene of the common midwife toad virus (CMTV) lineage; and a novel isolate with nucleotide changes at both the MCP and vIF-2α, denoted as Wood Buffalo ranavirus (WBRV).

The FV3 isolate sequenced in this study showed no genetic variation found across Ontario, Alberta, and the Northwest Territories, and was present in four of the five sampled anuran species (minus Canadian toad) all at different life stages (Figure 3.3). These results showed that ranavirus in Canada was either FV3, or else a distant FV3-like, with a lack of intermediate haplotypes between the two. Likewise, this FV3 isolate clustered with FV3 isolates found in USA frogs, salamanders, and fish, as well as in frogs in the UK (Figure 3.4). The lack of variation across Canada, multiple countries, and taxonomic classes suggests that the virus may have moved rapidly over space and time, or that these markers are too conserved for this specific type of analysis.

Despite the lack of genetic variation across Canada and other countries at these two markers, insertion/deletions and structural rearrangements have been shown to be important sources of genetic variability in the FV3 genome (Morrison *et al.* 2014). The SSME isolate of FV3 has 100% sequence homology with FV3 at the MCP and vIF-2α, however there are multiple deletions, insertions, and rearrangements throughout the genome (Morrison *et al.* 2014). It is likely that other regions of the genome could show genetic variation across samples with the

FV3 haplotype across Canada, and that the markers selected for this study were too conserved. The lack of genetic diversity across provinces and territories is in contrast to what would be expected of viruses. Rabies virus for example is seen to have many genetic variants of the pathogen comparing on a global scale (Bourhy *et al.* 2008), as well as smaller geographic scales such as across Canada and across the Canada-US border (Nadin-Davis *et al.* 2017; Trewby *et al.* 2017). However, this variation could likely be due to rabies being a single-stranded RNA virus, which has a higher mutation rate compared to a double-stranded DNA virus, such as ranaviruses (Bourhy *et al.* 2008; Duffy *et al.* 2008; Jancovich *et al.* 2015a). Another notable DNA virus is herpesvirus, with a genome size ranging from 150 to 230 kb in length, has an estimated universal mutation rate of 10^{-9} substitutions/site/year, whereas RNA viruses have mutation rates around 10^{-2} to 10^{-5} substitutions/site/year (Drake & Hwang 2005; Shackelton *et al.* 2006; Duffy *et al.* 2008). Currently, the mutation rate in iridoviruses is unknown, preventing a clearer understanding to the lack of variability witnessed in our study (Ridenhour & Storfer 2008). However, due to its role in virulence, the vIF-2α gene may be under purifying selection, preventing deleterious mutations as already evidenced in *Ambystoma tigrinum* virus (ATV) (Ridenhour & Storfer 2008). The MCP may also be under selective forces, but there is currently no literature that supports this claim.

The lack of variation over time may also be due to host reservoirs carrying sublethal infections over winter and causing reinfection in the spring (Brunner *et al.* 2004; Allender *et al.* 2013a). Such events would need for only one individual to infect an entire habitat over multiple years, therefore the virus undergoes bottleneck then founder effect each season, however there is a lack of data supporting this scenario. Also, the lack of intermediate haplotypes seen in this study may be due to a lack of sampling between southern Ontario and northern

Alberta/Northwest Territories. A larger scope of variation at the MCP between FV3 and WBRV may be seen from sampling sites between these two extreme regions, should intermediates between these two haplotypes exist. The virus may also have high vagility across the landscape, causing the lack of observed genetic variation. Above all, the evolution rate of ranaviruses requires further study, and more variable markers are necessary to understand spatio-temporal movement of FV3.

Aside from the FV3 haplotype, the new WBRV isolate clustered within the FV3-like lineage of ranaviruses in the MCP phylogenetic tree (Figure 3.4), although it did not branch directly off from FV3 or SSME. Based on the low bootstrap values of clades for the MCP, we cannot definitively establish the relationship between these different clusters based on this gene alone. The phylogenetic tree based on the vIF-2α formed a cluster between FV3, SSME, and WBRV (Figure 3.5), with a higher bootstrap support. The inclusion of other genes, or even complete genomes should strengthen the phylogenetic analyses.

Over the span of three sampling years, the WBRV isolate was found at a total of three different field sites (Toadlet pond, KM 190, KM 196) and in three amphibian species, wood frog, boreal chorus frog, and Canadian toad. However, WBRV was only present in Toadlet pond in 2015, whereas in 2016 and 2017 the isolate found at that site was FV3 (Supplementary table S3.1). Also, the WBRV isolate was not found uniformly across all life stages within the same pond in 2017. At KM 190, the ten boreal chorus frog adults that tested positive for ranavirus were found to have the WBRV isolate, whereas the two wood frog tadpoles from the same site had the FV3 isolate. Likewise, at KM 196 the FV3 isolate was found within all 35 boreal chorus frog tadpoles and 19 wood frog tadpoles, while the one wood frog adult was found to have WBRV. Across both sites, it was found that only the adults had the WBRV isolate whereas the

tadpoles had the FV3 isolate, however, due to the small sample size of adults from KM 196 (n=1) and tadpoles from Toadlet pond (n=2) these results may not be representative of their entire ponds. This trend was also only observed in 2017, as in 2015 the viruses found were uniform across all their species and life stages. It is possible that the adult at KM 196 may have travelled from another waterbody where the WBRV isolate is widespread. However, the potential introduction of a new isolate in an environment where another FV3-like virus exists begs the question of viral competition within a waterbody. To further understand how many different viral isolates are within a single waterbody, future studies could use environmental DNA (eDNA) methods to sample the water and determine how many variants are within a site using metabarcoding (Valentini *et al.* 2016).

These two sites may also be evidence for virus variability between life stages and perhaps species, as the tadpoles at KM 196 were wood frogs and the adults were boreal chorus frogs. While the degree of virulence between the two isolates is unknown, it is likely that the isolate with higher infectability may out-compete the other virus. The vIF-2α gene between the FV3 strain and WBRV had little genetic variability, in that they were both the same length as the truncated version of the gene, and only had one synonymous nucleotide change between them. This suggests that virulence levels may be similar between both isolates. However, there are likely other genes that play roles in virulence as there is evidence that the SSME isolate has a lower virulence and mortality rate in frogs when compared to FV3, both of which have truncated vIF-2α genes with 100% sequence homology (Morrison *et al.* 2014). A complete phylogenomic analysis would be required to understand the extent of genetic variation between FV3, SSME, and the novel isolate WBRV.

Samples from KEN (Ontario) produced a MCP sequence that was identical to that of FV3 and SSME, however their vIF-2α sequences had a 99.9% homology to a CMTV-like ranavirus. FV3-like ranaviruses are known to have truncated versions of the gene whereas CMTV-like viruses have non-truncated genes. It is unlikely that there was co-infection of two ranavirus strains within this site, as there was no sign of double-banding of the vIF-2α on the gel during electrophoresis (Figure 3.2), despite primers for vIF-2α designed to bind to any ranavirus. Although studies of competition between ranavirus strains has yet to be observed, general parasite competition often selects the most virulent strains, leaving others for extinction (Antia *et al.* 1994; Brunner *et al.* 2015). Though, in 2017, a FV3 genome was sequenced from a strawberry poison frog (*Oophaga pumilio*) from the Netherlands (imported from and likely infected in Nicaragua) which had a non-truncated eIF-2α protein, and has a 99.7% homology to the samples from KEN (Table 3.4, Saucedo *et al.* 2017). There has been previous evidence for recombination of CMTV- and FV3-like viruses, where two isolates of ranavirus from epizootics in 1998 and 2006 from the same ranaculture facility were phylogenomically compared, and found that the isolate from 2006 had recombinant sequences from a CMTV-like ranavirus, with the major parent being a FV3-like ranavirus (Claytor *et al.* 2017). This recombinant virus was also found to have increased virulence compared to its FV3 counterpart, likely due to the CMTV-like genes acquired through recombination (Claytor *et al.* 2017). This study observed their recombinant in a facility within the United States, however our study is the first to document a CMTV-like virus within the wild. Also, CMTV-like viruses were previously assumed to not be native to North America, as they were previously found in regions of Europe and Asia (Balseiro *et al.* 2009; Geng *et al.* 2011; Chen *et al.* 2013; Price *et al.* 2017). It is possible that CMTV-like viruses are also present in North America and may have been for some

time, however, due to a lack of surveillance in an FV3 predominant region, its presence may have gone undetected. The lack of the N-terminal region in FV3-like ranaviruses causes the viruses to be less virulent than viruses with the complete gene (Majji *et al*. 2006), suggesting that this recombination may be positive selection towards higher virulence (Abrams *et al.* 2013).

To further investigate the extent of recombination at this field site, exploring the gene rearrangements of complete genomes can determine the alignment of unknown strains to known viruses and their lineages. Additionally, to explore the variation in virulence between isolates found throughout this study, a controlled experiment of infecting frogs at various life stages may provide insight on the unknown infectious behaviour of these identified strains.

Moreover, 33 positive samples did not produce a band nor a sequence for the vIF-2α gene. While there are ranaviruses that do not have the vIF-2α gene (grouper iridovirus and Singapore grouper iridovirus) (Song *et al.* 2004; Chen *et al.* 2011), it is unlikely that these samples have a deletion, and instead failed to amplify due to low viral copy DNA from the sample. Moreover, I sequenced samples from a total of seven regions in Alberta and NWT, yet three regions were negative for the virus. These results demonstrate that although there are two different FV3-like ranaviruses in this region, not all sites are infected with ranavirus.

In this study, I found a lack of genetic variation within FV3 at two regions across Canada. The haplotypes we found across all these regions were either uniformly FV3, or else an entirely novel isolate, with no intervening haplotypes. Evidence of intraspecific variation across Canada based on the MCP and vIF-2α was limited, however based on these two genes alone I found a novel ranavirus isolate closely related to FV3, as well as an isolate of FV3 that had a non-truncated version of vIF-2α, similar to ranaviruses of a separate lineage. The MCP is an excellent marker to identify and categorize pathogens within their appropriate lineage, and

demonstrates genetic variability across continents and taxonomic classes (Chinchar 2002; Holopainen *et al.* 2009; Duffus & Andrews 2013; Jancovich *et al.* 2015b; Stöhr *et al.* 2015; Claytor *et al.* 2017), and the length of the vIF-2α gene is often assessed to estimate virulence of new isolates (Essbauer *et al.* 2001; Majji *et al.* 2006; Stöhr *et al.* 2015), however these markers are not variable enough to demonstrate intraspecific variation across Canada. To further understand the relationships between FV3 samples across Canada, WBRV, and the recombinant, additional analyses should be performed, such as comparison of protein profiles and complete genome analysis (Tan *et al.* 2004; Majji *et al.* 2006; Jancovich *et al.* 2012; Cheng *et al.* 2014; Stöhr *et al.* 2015; Claytor *et al.* 2017). Comparison of complete viral genomes of apparently identical samples across the Canadian landscape are necessary to determine variable regions that could be used for evolutionary history and epidemiology of ranaviruses (Duffus *et al.* 2017).

3.5 Acknowledgements

I would like to thank Joe-Felix Bienentreu for allowing me to sequence and analyze the samples he collected in northern Canada, and Dr. David Lesbarrères for his support and sending additional ranavirus samples. I would also like to thank Dr. Sibelle Torres Vilaça for her endless help in the lab and phylogenetic analyses.

CHAPTER 4

SUMMARY

Monitoring invasive diseases and understanding mechanisms of their maintenance and spread are critical in evaluating threats to biodiversity and how to best manage and minimize their impact (Belant & Deese 2010). Disease monitoring can be applied on both spatial and temporal scales, using various molecular tools to assess fluctuations in presence and strain distribution. In my thesis, I attempted to utilize environmental DNA (eDNA) methods and phylogenetic analyses of FV3 variants to explore the spatial and temporal patterns of frog virus 3 (FV3) in the environment to make inferences on pathogen movement. Several challenges, both in the field and in the lab, were encountered, which somewhat limited both the spatial and temporal distributions of samples I was able to obtain to fully address the aforementioned questions. That said, this thesis was able to present several findings that have enhanced our understanding of FV3 and FV3-like viruses in Canada that will improve any future field studies of this pathogen.

In chapter 2, I used eDNA to study the spatio-temporal patterns of ranavirus presence from several water bodies in south-central Ontario. Results indicated that there was a slight trend where ranavirus was more likely to be detected in later months than earlier. This trend was seen on a finer geographic scale where I sampled 93 sites over 7,150 km^2, and a coarser scale where 33 sites were sampled over 73,100 km^2. There was also a lack of strong abiotic predictors that could estimate the likelihood of ranavirus presence and intensity within a site. It is unclear if a more rigorous and systematic temporal sampling of the water would have yielded stronger correlations, such as sampling biweekly over more months than just June, July, and August. It would be expected that the virus would be shed into the environment in higher densities during metamorphosis of different amphibians, as they are most vulnerable to this pathogen while they

are immunocompromised at this life stage (Rollins-Smith 1998; Carey *et al.* 1999; Green *et al.* 2002; Greer *et al.* 2008). While ranavirus was detected within 60-90% of waterbodies during 2017, leading to a conclusion that the virus is practically ubiquitous across the region, a large number of sample replicates did not yield positive FV3 results despite the development of a highly sensitive qPCR assay. Future investigations across broader sampling ranges and on more frequent sampling times may allow for finer-scale resolution of ranavirus presence, strengthening our confidence in the abundance of ranavirus.

This work was performed within a large collaborative group, and many of the processed samples were collected by other researchers. An associated, unforeseen challenge was that many of the samples collected by other researchers were targeting amphibian eDNA with the water samples. Given the nature of where amphibians live, other researchers preferred using coarser (1.45 µm pore size) filters to trap the eDNA to avoid clogging the filters with debris. FV3 is a relatively small virus and the efficiency of capturing the virus with 1.45 µm filters was very low. As such, there was a need to revert to collecting and processing my own samples with 0.2 µm filters from smaller volumes of non-turbid water (Hall *et al.* 2015). This greatly diminished the number and geographic extent of sampling and the potential to overlap host species presence and pathogen presence. Further, many of the water samples were from rather turbid waters with a lot of decaying plant material and other PCR inhibitors (Wilson 1997; Converse *et al.* 2009). These challenges were addressed in several ways including using a new extraction process using magnetic beads that repeatedly washed the DNA, and high-fidelity polymerases within an eDNA-based qPCR master mix (Kolby *et al.* 2015). We also used a different filtering technique for the fine-scale geographical analysis, where the water was filtered on site using Sterivex capsules (Chestnut *et al.* 2014; Spens *et al.* 2017). The volume of water from the capsule filters

varied from pond to pond, depending on plant material within the water, which may have brought on false negatives if volumes were lower than 250 mL: the maximum volume 0.2 µm filters can handle (Hall *et al.* 2015; Huver & Koprivnikar 2015). However, once inhibition was minimized, subsequent analyses of field samples were completed with relative ease.

While eDNA surveys have largely been lauded as cost-effectively providing higher sensitivities in detection for many species (Takahara *et al.* 2013; Rees *et al.* 2014; Turner *et al.* 2014; Wilson *et al.* 2014; Laramie *et al.* 2015; Boothroyd *et al.* 2016), and eDNA is likely the best way to provide active pathogen surveillance, this study demonstrates the real-world challenges to detecting a pathogen from stagnant water bodies. Perhaps five biological and three technical replicates (15 qPCR replicates per capsule sample site) could be decreased as per the results and discussion of chapter 2. The cost of testing one site with five biological samples in triplicate was about $126 CAN, whereas four biological samples would have been around $103 CAN. Omitting even one biological replicate would decrease the cost of processing, however the drawback would be losing detection in a few sites which only had detection in one capsule sample. On the other hand, the costs associated with the cellulose nitrate samples came out to approximated $50 CAN for 3 filters per site, each run in triplicate as recommended by standard qPCR operating procedures (Picco *et al.* 2007; Pilliod *et al.* 2014; Turner *et al.* 2014; Hall *et al.* 2015; Jane *et al.* 2015; Walker *et al.* 2017). This method was more cost effective as it was less expensive than sampling 10 specimen samples using traditional PCR techniques (around $62 CAN per site). Also, depending on the estimated population size of hosts, having only 10 specimen samples to estimate infection prevalence of ranavirus is very low, and usually require upwards of 30 specimen samples or more to be accurate (Gray, *et al.* 2015). It became clear that generic DNA extractions did not provide the DNA recovery or purification of PCR inhibitors

required to maintain the assay's sensitivity to detect FV3, and the cost of the Environmental Master Mix compared to Universal Master Mix also increased the cost per sample. In conclusion, despite marketing to suggest otherwise, eDNA is a labour intensive and relatively expensive endeavor. Further, the fluctuating amount of virus detected across sampling periods suggests more intense sampling would be required to better understand the presence and spread of the disease, further increasing costs.

In chapter 3, my initial goal was to scan for genetic variation within the MCP to determine if we could track the directional spread of the disease via phylogenetic relationships of the variants – similar to practices in tracking disease spread in other systems (Leitner *et al.* 1996; Bourhy *et al.* 2008; Wallace & Fitch 2008; Lemey *et al.* 2009). Despite finding that the virus is present in the water of most sampled sites as per chapter 2, I and collaborators were unable to obtain many live or recently dead animals with the virus. Our sample sizes and the spatial extent of our sampling was thus much smaller than initially anticipated. Part of the challenge is that visibly infected amphibians die quickly, and either rapidly disintegrate or are scavenged (Brunner *et al.* 2015), hence the sample size of only 10 in Ontario. The general lack of samples, while a concern, did not undermine the findings of a complete lack of genetic variation within the MCP of FV3 despite vast geographic distances between the sampled regions. It quickly became clear, that despite the genetic variation that exists within the MCP of FV3-like viruses on genebank, that there would not be enough variation at the MCP of Canadian FV3 samples for fine-scale phylogenetic analyses. The one interesting finding, however, was that the one other variant detected was found to not be FV3, but diverged by 9 nucleotides and was more closely related to Bohle iridovirus (BIV) and tiger frog virus (TFV), making it an FV3-like virus that had

not been previously documented. This variant was found in relatively high frequency in AB and NWT and collaborators are now planning to both culture and further describe this virus.

While the MCP is known to be highly conserved, there are many regions of the FV3 genome that have shown rearrangements and high levels of variability in repetitive segments (Morrison *et al.* 2014). The repeat markers unfortunately were deemed unsuitable for the phylogenetic analyses I wanted to perform. I also screened the genomes of multiple closely related FV3-like published variants and found a few regions that may have had enough variation to potentially be good molecular markers to track disease spread. ORF 65L and 66L had three different organizations within FV3-like ranaviruses, where SSME had a 757 bp deletion, deleting the entirety of 65L and most of 66L, and other FV3-like ranaviruses such as tiger frog virus and soft-shelled turtle iridovirus had a 139 bp insertion in 66L (Morrison *et al.* 2014). ORF 19 also had 52 bp substitutions between FV3 and SSME, along with a 27 bp insertion in SSME, suggesting that it may be a highly variable marker between closely related ranavirus isolates (Morrison *et al.* 2014). However, based on feedback from my collaborators and a restrictive timeline and budget, I was limited to focusing on a particular region of the FV3 genome associated with pathogenicity (Chen *et al.* 2011; Jancovich & Jacobs 2011; Grayfer *et al.* 2015). Specifically, vIF-2α size variants, as described in chapter 3, are associated with varying levels of pathogenicity. Fortunately, from this pathogenic marker, I found evidence for a possible recombinant between FV3 and common midwife toad virus (CMTV). I say 'possible' as the MCP primers would not have picked up a non-FV3-like ranavirus, however, based on the discussion in chapter 3, the lack of double-banding and evidence for recombinants in other studies supports our recombination claim (Claytor *et al.* 2017; Saucedo *et al.* 2017). In conclusion, while I was lucky to discover two possibly new isolates of FV3, I was limited by my

conserved molecular markers and from that, was unable to detect any kind of intraspecific variability, and in turn, unable to make inferences about pathogen movement. To improve these analyses, the addition of more variable markers may allow for increased resolution of variability within FV3. The markers mentioned above (ORF 19R, 65L/66L) are likely candidates to explore population variability, especially ORF 19R, where there are 28 variable nucleotides and a 27 bp insertion within a 960 bp segment of this marker.

While my research provided some context for the presence of ranavirus within the Kawartha region, other regions should be monitored for ranavirus using eDNA techniques to see if presence is similar across the landscape. A future study should be to perform eDNA sampling at sites on a latitudinal scale or across different ecozones of Canada, to test the epidemiological limits of ranavirus persistence in different habitats (D'Aoust-Messier *et al.* 2015). Although the ecozones and latitudes are greatly different between Ontario and Wood Buffalo National Park, sampling should encompass Canada as a whole, sampling far eastern and western regions, which may also uncover new FV3 haplotypes, either novel or intermediate between isolates found in my study. Sequencing should also be performed either on a genomic level, or at more variable markers to have a better judgement of spatio-temporal movement (Morrison *et al.* 2014). As mentioned previously in this chapter, markers such as ORF 19R, 65L, 66L should be explored as a phylogenetic and possibly phylogeographic markers, however at this point, genome analyses of samples collected in this study should take high priority, as they may highlight even more variable genetic markers to be tested on FV3 samples across the continent. Variable markers and samples from across the landscape would allow us to explore the historical evolution and distribution of ranavirus over time (Lemey *et al.* 2009; Trewby *et al.* 2017).

The discovery of a potential recombinant ranavirus within Canadian waters suggests an analysis should be performed to test the authenticity of the recombination. Aside from genome sequencing or long-range PCR, another proposal would be to demonstrate the recombination by designing primers set to amplify a region where the two viruses recombine, by use of previous recombinant genomes in the literature (Claytor *et al.* 2017; Saucedo *et al.* 2017).

Future work can combine sequencing with eDNA by use of metabarcoding, which simultaneously detects multiple taxa in eDNA samples without any prior knowledge of species that inhabit the water (Valentini *et al.* 2016). Metabarcoding would allow for the comparison of ranavirus presence with the presence of other species (amphibians, reptiles, plants, insects, other pathogens, etc.) and allow for biotic factors for model predictors. Biotic factors hold stronger predictive power as opposed to abiotic factors, such as taxonomic richness (Tornabene *et al.* 2017), and identifying a common host or temporal pattern of presence would move our understanding of ranavirus persistence further. Metabarcoding is also non-invasive, and requires minimal sampling in order to obtain the same amount of species as eDNA requires (Valentini *et al.* 2016). The next step in this realm of this research would be to combine sequencing with eDNA sampling. Metabarcoding may be used to sequence the virus within its waterbody, without the need for capturing infected individuals, and allow for phylogenetic analyses using water sampling. While metabarcoding is still up and coming in its field, the cost is currently non-comparable to our eDNA sampling costs, however, should the cost of metabarcoding be on par with traditional eDNA sampling, then cost would be more efficient as metabarcoding returns the DNA of all taxa within the pond (Valentini *et al.* 2016).

My research advanced our understanding on how a ranavirus maintains itself in its environment. Combining sequencing and eDNA allowed for various methods of tracking the

virus over space and time, leaving us now with new awareness of previously cryptic pathogens, and a more reliable tool for pathogen surveillance. With advancements in aquatic species monitoring, we now have an idea of how widespread and threatening ranaviruses are to amphibian biodiversity, leaving further avenues of research for understanding ranavirus movement.

REFERENCES

Abrams AJ, Cannatella DC, Hillis DM, Sawyer SL (2013) Recent host-shifts in ranaviruses: signatures of positive selection in the viral genome. *Journal of General Virology*, **94**, 2082–2093.

Allender MC, Bunick D, Mitchell M a (2013a) Development and validation of TaqMan quantitative PCR for detection of frog virus 3-like virus in eastern box turtles (*Terrapene carolina carolina*). *Journal of Virological Methods*, **188**, 121–5.

Allender MC, Mitchell MA, Torres T, Sekowska J, Driskell EA (2013b) Pathogenicity of frog virus 3-like virus in red-eared slider turtles (*Trachemys scripta elegans*) at two environmental temperatures. *Journal of Comparative Pathology*, **149**, 356–367.

Antia R, Levin BR, May RM (1994) Within-host population dynamics and the evolution and maintenance of microparasite virulence. *The American Naturalist*, **144**, 457–472.

Ariel E, Nicolajsen N, Christophersen MB *et al.* (2009) Propagation and isolation of ranaviruses in cell culture. *Aquaculture*, **294**, 159–164.

Balseiro A, Dalton KP, Del Cerro A *et al.* (2009) Pathology, isolation and molecular characterisation of a ranavirus from the common midwife toad *Alytes obstetricans* on the Iberian Peninsula. *Diseases of Aquatic Organisms*, **84**, 95–104.

Bataille A, Fong JJ, Cha M *et al.* (2013) Genetic evidence for a high diversity and wide distribution of endemic strains of the pathogenic chytrid fungus *Batrachochytrium dendrobatidis* in wild Asian amphibians. *Molecular Ecology*, **22**, 4196–4209.

Bayley A, Hill B, Feist S (2013) Susceptibility of the European common frog Rana temporaria to a panel of ranavirus isolates from fish and amphibian hosts. *Diseases of Aquatic Organisms*, **103**, 171–183.

Belant J, Deese A (2010) Importance of wildlife disease surveillance. *Human-Wildlife Interactions*, **4**, 165–169.

Boothroyd M, Mandrak NE, Fox M, Wilson CC (2016) Environmental DNA (eDNA) detection and habitat occupancy of threatened spotted gar (*Lepisosteus oculatus*). *Aquatic Conservation: Marine and Freshwater Ecosystems*, **1119**, 1107–1119.

Bourhy H, Reynes JM, Dunham EJ *et al.* (2008) The origin and phylogeography of dog rabies virus. *Journal of General Virology*, **89**, 2673–2681.

Boyle DG, Boyle DB, Olsen V, Morgan J a T, Hyatt a D (2004) Rapid quantitative detection of chytridiomycosis (*Batrachochytrium dendrobatidis*) in amphibian samples using real-time Taqman PCR assay. *Diseases of Aquatic Organisms*, **60**, 141–148.

Brenes R, Gray MJ, Waltzek TB, Wilkes RP, Miller DL (2014) Transmission of ranavirus between ectothermic vertebrate hosts (RE Paul, Ed,). *PLoS ONE*, **9**, e92476.

Bronnenhuber JE, Wilson CC (2013) Combining species-specific COI primers with environmental DNA analysis for targeted detection of rare freshwater species. *Conservation Genetics Resources*, **5**, 971–975.

Brunner JL, Beaty L, Guitard A, Russell D (2017) Heterogeneities in the infection process drive ranavirus transmission. *Ecology*, **98**, 576–582.

Brunner JL, Schock DM, Collins JP (2007) Transmission dynamics of the amphibian ranavirus *Ambystoma tigrinum* virus. *Diseases of Aquatic Organisms*, **77**, 87–95.

Brunner JL, Schock DM, Davidson EW, Collins JP (2004) Intraspecific reservoirs: complex life history and the persistence of a lethal ranavirus. *Ecology*, **85**, 560–566.

Brunner JL, Storfer A, Gray MJ, Hoverman JT (2015) Ranavirus Ecology and Evolution: From

Epidemiology to Extinction. In: *Ranaviruses: Lethal pathogens of ectothermic vertebrates* (eds Gray MJ, Chinchar V), pp. 71-104. Springer, San Diego.
Cameron AR, Baldock FC (1998) A new probability formula for surveys to substantiate freedom from disease. *Preventive Veterinary Madicine*, **34**, 1–17.
Carey C, Cohen N, Rollins-Smith L (1999) Amphibian declines: An immunological perspective. *Developmental and Comparative Immunology*, **23**, 459–472.
Chen Z, Gui J, Gao X *et al.* (2013) Genome architecture changes and major gene variations of *Andrias davidianus* ranavirus (ADRV). *Veterinary Research*, **44**, 1–13.
Chen G, Ward BM, Yu EK, Chinchar VG, Robert J (2011) Improved knockout methodology reveals that frog virus 3 mutants lacking either the 18K immediate-early gene or the truncated vIF2-{alpha} gene are defective for replication and growth in vivo. *Journal of Virology*, **85**, 11131–11138.
Cheng K, Jancovich JK, Burchell J *et al.* (2014) Isolation of a bohle-like iridovirus from boreal toads housed within a cosmopolitan aquarium collection. *Diseases of Aquatic Organisms*, **111**, 139–152.
Chestnut T, Anderson C, Popa R *et al.* (2014) Heterogeneous occupancy and density estimates of the pathogenic fungus *Batrachochytrium dendrobatidis* in waters of North America. *PLoS ONE*, **9**, e106790.
Chinchar VG (2002) Ranaviruses (family Iridoviridae): Emerging cold-blooded killers. *Archives of Virology*, **147**, 447–470.
Chinchar VG, Waltzek TB, Subramaniam K (2017) Ranaviruses and other members of the family Iridoviridae: Their place in the virosphere. *Virology*, **511**, 259–271.
Chinchar G V., Wang J, Murti G, Carey C, Rollins-Smith LA (2001) Inactivation of frog virus 3 and channel catfish virus by esculentin-2P and ranatuerin-2P, two antimicrobial peptides isolated from frog skin. *Virology*, **288**, 351–357.
Chinchar VG, Yu KH, Jancovich JK (2011) The molecular biology of frog virus 3 and other Iridoviruses infecting cold-blooded vertebrates. *Viruses*, **3**, 1959–1985.
Claverie J-M, Abergel C, Ogata H (2009) Mimivirus. *Current Topics in Microbiology and Immunology*, **328**, 89–121.
Claytor SC, Subramaniam K, Landrau-Giovannetti N *et al.* (2017) Ranavirus phylogenomics: Signatures of recombination and inversions among bullfrog ranaculture isolates. *Virology*, **511**, 330–343.
Converse RR, Blackwood AD, Kirs M, Griffith JF, Noble RT (2009) Rapid QPCR-based assay for fecal *Bacteroides* spp. as a tool for assessing fecal contamination in recreational waters. *Water Research*, **43**, 4828–4837.
Cooch EG, Conn PB, Ellner SP, Dobson AP, Pollock KH (2012) Disease dynamics in wild populations: modeling and estimation: a review. *Journal of Ornithology*, **152**, S485–S509.
Cullingham CI, Kyle CJ, Pond BA, Rees EE, White BN (2009) Differential permeability of rivers to raccoon gene flow corresponds to rabies incidence in Ontario, Canada. *Molecular Ecology*, **18**, 43–53.
Cunningham AA, Hyatt AD, Russell P, Bennett PM (2007) Experimental transmission of a ranavirus disease of common toads (*Bufo bufo*) to common frogs (*Rana temporaria*). *Epidemiology and Infection*, **135**, 1213–6.
D'Aoust-Messier AM, Echaubard P, Billy V, Lesbarrères D (2015) Amphibian pathogens at northern latitudes: Presence of chytrid fungus and ranavirus in northeastern Canada. *Diseases of Aquatic Organisms*, **113**, 149–155.

Daszak P, Cunningham AA, Hyatt AD (2000) Emerging infectious diseases of wildlife - threats to biodiversity and human health. *Science*, **287**, 443–449.
Daszak P, Cunningham AA, Hyatt AD (2001) Anthropogenic environmental change and the emergence of infectious diseases in wildlife. *Acta Tropica*, **78**, 103–116.
Daszak P, Cunningham AA, Hyatt A (2003) Infectious disease and amphibian population declines. *Diversity and Distributions*, **9**, 141–150.
Dejean T, Valentini A, Miquel C *et al.* (2012) Improved detection of an alien invasive species through environmental DNA barcoding: The example of the American bullfrog *Lithobates catesbeianus*. *Journal of Applied Ecology*, **49**, 953–959.
Drake JW, Hwang CBC (2005) On the mutation rate of herpes simplex virus type 1. *Genetics*, **170**, 969–970.
Duffus ALJ, Andrews AM (2013) Phylogenetic analysis of a frog virus 3–like ranavirus found at a site with recurrent mortality and morbidity events in Southeastern Ontario, Canada: partial major capsid protein sequence alone is not sufficient for fine-scale differentiation. *Journal of Wildlife Diseases*, **49**, 464–467.
Duffus ALJ, Garner TWJ, Davis AR, Dean AW, Nichols RA (2017) Phylogentic analysis of 24 ranavirus isolates from English amphibians using 2 partial loci. *Journal of Emerging Diseases and Virology*, **3**, 1–7.
Duffus ALJ, Waltzek TB, Stöhr AC *et al.* (2015) Distribution and host range of ranaviruses. In: *Ranaviruses: Lethal Pathogens of Ectothermic Vertebrates* (eds Gray MJ, Chinchar V), pp. 9–57. Springer, San Diego.
Duffy S, Shackelton LA, Holmes EC (2008) Rates of evolutionary change in viruses: patterns and determinants. *Nature Reviews Genetics*, **9**, 267–276.
Eaton HE, Metcalf J, Penny E *et al.* (2007) Comparative genomic analysis of the family Iridoviridae: re-annotating and defining the core set of iridovirus genes. *Virology journal*, **4**, 11.
Echaubard P, Leduc J, Pauli B *et al.* (2014) Environmental dependency of amphibian-ranavirus genotypic interactions: evolutionary perspectives on infectious diseases. *Evolutionary Applications*, **7**, 723–733.
Epstein B, Storfer A (2015) Comparative genomics of an emerging amphibian virus. *G3 - Genes, Genomes, Genetics*, **6**, 15–27.
Essbauer S, Bremont M, Ahne W (2001) Comparison of the eIF-2α homologous proteins of seven ranaviruses (Iridoviridae). *Virus Genes*, **23**, 347–359.
Fan J, Upadhye S, Worster A (2006) Understanding receiver operating characteristics (ROC) curves. *Canadian Journal of Emergency Medicine*, **8**, 19–20.
Fijan N, Sulimanovic D, Bearzotti M *et al.* (1983) Some properties of the Epithelioma papulosum cyprini (EPC) cell line from carp cyprinus carpio. *Annales de Virologie*, **134**, 207–220.
Fisher MC, Garner TWJ, Walker SF (2009) Global emergence of *Batrachochytrium dendrobatidis* and amphibian chytridiomycosis in space, time, and host. *Annual Review of Microbiology*, **63**, 291–310.
Forzán MJ, Jones KM, Ariel E *et al.* (2017) Pathogenesis of frog virus 3 (Ranavirus, Iridoviridae) infection in wood frogs (*Rana sylvatica*). *Veterinary Pathology*, 30098581668492.
Gantress J, Maniero GD, Cohen N, Robert J (2003) Development and characterization of a model system to study amphibian immune responses to iridoviruses. *Virology*, **311**, 254–

262.
García-Díaz P, Ross JV, Woolnough AP, Cassey P (2016) Managing the risk of wildlife disease introduction: pathway-level biosecurity for preventing the introduction of alien ranaviruses. *Journal of Applied Ecology*, **54**, 234-241.
Geng Y, Wang KY, Zhou ZY *et al.* (2011) First report of a ranavirus associated with morbidity and mortality in farmed Chinese giant salamanders (*Andrias davidianus*). *Journal of Comparative Pathology*, **145**, 95–102.
Goldberg CS, Pilliod DS, Arkle RS, Waits LP (2011) Molecular detection of vertebrates in stream water: A demonstration using rocky mountain tailed frogs and Idaho giant salamanders. *PLoS ONE*, **6**.
Goorha R, Murti K (1982) The genome of frog virus 3, an animal DNA virus, is circularly permuted and terminally redundant (genome structure/restriction endonuclease mapping/DNA replication). *Biochemistry*, **79**, 248–252.
Gosner K (1960) A simplified table for staging anuran embryos and larvae with notes on identification. *Herpetologica*, **16**, 183–190.
Granoff A, Came P, Rafferty K (1965) The isolation and properties of viruses from *Rana pipiens*: their possible relationship to the renal adenocarcinoma of the leopard frog. *Annals of the New York Academy of Sciences*, **5176**, 237–255.
Gray MJ, Brunner JL, Earl JE, Ariel E (2015) Design and analysis of ranavirus studies: surveillance and assessing risk. In: *Ranaviruses: Lethal pathogens of ectothermic vertebrates* (eds Gray MJ, Chinchar V), pp. 209-240. Spinger, San Diego.
Gray MJ, Lewis JP, Nanjappa P *et al.* (2015b) *Batrachochytrium salamandrivorans*: the North American response and a call for action. *PLoS Pathogens*, **11**, 1–9.
Gray M, Miller D, Hoverman J (2009) Ecology and pathology of amphibian ranaviruses. *Diseases of Aquatic Organisms*, **87**, 243–266.
Gray MJ, Miller DL, Hoverman JT (2012) Reliability of non-lethal surveillance methods for detecting ranavirus infection. *Diseases of Aquatic Organisms*, **99**, 1–6.
Gray MJ, Miller DL, Schmutzer AC, Baldwin CA (2007) Frog virus 3 prevalence in tadpole populations inhabiting cattle-access and non-access wetlands in Tennessee, USA. *Diseases of Aquatic Organisms*, **77**, 97–103.
Grayfer L, Edholm E, Andino FDJ, Chinchar VG, Robert J (2015) Ranavirus host immunity and immune evasion. In: *Ranaviruses: Lethal Pathogens of Ectothermic Vertebrates* (eds Gray M, Chinchar V), pp. 141–170. Springer, San Diego.
Green DE, Converse K a, Schrader AK (2002) Epizootiology of sixty-four amphibian morbidity and mortality events in the USA, 1996-2001. *Annals of the New York Academy of Sciences*, **969**, 323–339.
Greer AL, Berrill M, Wilson PJ (2005) Five amphibian mortality events associated with ranavirus infection in south central Ontario, Canada. *Diseases of Aquatic Organisms*, **67**, 9–14.
Greer AL, Briggs CJ, Collins JP (2008) Testing a key assumption of host-pathogen theory: density and disease transmission. *Oikos*, **117**, 1667–1673.
Gregory Chinchar V, Hick P, Ince IA *et al.* (2017) ICTV virus taxonomy profile: Iridoviridae. *Journal of General Virology*, **98**, 2–3.
Guy RA, Payment P, Krull UJ, Paul A, Horgen PA (2003) Real-Time PCR for quantification of *Giardia* and *Cryptosporidium* in environmental water samples and sewage. *Applied and Environmental Microbiology*, **69**, 5178–5185.

Hall EM, Crespi EJ, Goldberg CS, Brunner JL (2015) Evaluating environmental DNA-based quantification of ranavirus infection in wood frog populations. *Molecular Ecology Resources*, 423–433.
Harp EM, Petranka JW (2006) Ranavirus in wood frogs (*Rana sylvatica*): potential sources of transmission within and between ponds. *Journal of wildlife diseases*, **42**, 307–318.
Hasegawa M, Kishino H, Yano T (1985) Dating of the human-ape splitting by a molecular clock of mitochondrial DNA. *Journal of Molecular Evolution*, **22**, 160–174.
He JG, Lü L, Deng M *et al.* (2002) Sequence analysis of the complete genome of an Iridovirus isolated from the tiger frog. *Virology*, **292**, 185–197.
Holopainen R, Ohlemeyer S, Schütze H, Bergmann SM, Tapiovaara H (2009) Ranavirus phylogeny and differentiation based on major capsid protein, DNA polymerase and neurofilament triplet H1-like protein genes. *Diseases of Aquatic Organisms*, **85**, 81–91.
Huang Y, Huang X, Liu H *et al.* (2009) Complete sequence determination of a novel reptile iridovirus isolated from soft-shelled turtle and evolutionary analysis of Iridoviridae. *BMC Genomics*, **10**.
Hunter ME, Dorazio RM, Butterfield JSS *et al.* (2017) Detection limits of quantitative and digital PCR assays and their influence in presence–absence surveys of environmental DNA. *Molecular Ecology Resources*, **17**, 221–229.
Huver J, Koprivnikar J (2015) Development and application of an eDNA method to detect and quantify a pathogenic parasite in aquatic ecosystems. *Ecological Applications*, **25**, 991–1002.
Hyatt a D, Gould a R, Zupanovic Z *et al.* (2000) Comparative studies of piscine and amphibian iridoviruses. *Archives of virology*, **145**, 301–331.
James TY, Toledo LF, Rödder D *et al.* (2015) Disentangling host, pathogen, and environmental determinants of a recently emerged wildlife disease: lessons from the first 15 years of amphibian chytridiomycosis research. *Ecology and Evolution*, **5**, 4079–4097.
Jancovich J, Chinchar V, Hyatt A *et al.* (2012) Family Iridoviridae. In: *Virus Taxonomy: Ninth report of the International Committee on Taxonomy of Viruses* (eds King A, Adams M, Carstens E, Lefkowitz E), pp. 193–210. Elsevier, San Diego.
Jancovich JK, Jacobs BL (2011) Innate immune evasion mediated by the *Ambystoma tigrinum* virus eukaryotic translation initiation factor 2alpha homologue. *Journal of virology*, **85**, 5061–5069.
Jancovich JK, Mao J, Chinchar VG *et al.* (2003) Genomic sequence of a ranavirus (family Iridoviridae) associated with salamander mortalities in North America. *Virology*, **316**, 90–103.
Jancovich JK, Qin Q, Zhang Q, Chinchar VG (2015a) Ranavirus replication: molecular, cellular, and immunological events. In: *Ranaviruses: Lethal Pathogens of Ectothermic Vertebrates* (eds Gray MJ, Chinchar V), pp. 105–139. Springer, New York.
Jancovich JK, Steckler NK, Waltzek TB (2015b) Ranavirus Taxonomy and Phylogeny. In: *Ranaviruses: Lethal Pathogens of Ectothermic Vertebrates* (eds Gray MJ, Chinchar V), pp. 59–70. Springer, New York.
Jane SF, Wilcox TM, Mckelvey KS *et al.* (2015) Distance, flow and PCR inhibition: eDNA dynamics in two headwater streams. *Molecular Ecology Resources*, **15**, 216–227.
Jerde CL, Mahon AR, Chadderton WL, Lodge DM (2011) "Sight-unseen" detection of rare aquatic species using environmental DNA. *Conservation Letters*, **4**, 150–157.
Johnson PTJ, Lunde KB, Thurman EM *et al.* (2002) Parasite (*Ribeiroa ondatrae*) infection

linked to amphibian malformations inthe western United States. *Ecological Monographs*, **72**, 151–168.
Johnson JB, Omland KS (2004) Model selection in ecology and evolution. *Trends in Ecology and Evolution*, **19**, 101–108.
Keesing F, Belden LK, Daszak P *et al.* (2010) Impacts of biodiversity on the emergence and transmission of infectious diseases. *Nature*, **468**, 647–652.
Kiesecker JM, Blaustein a R, Belden LK (2001) Complex causes of amphibian population declines. *Nature*, **410**, 681–684.
Kolby JE, Smith KM, Berger L *et al.* (2014) First evidence of amphibian chytrid fungus (*Batrachochytrium dendrobatidis*) and ranavirus in Hong Kong amphibian trade. *PLoS ONE*, **9**.
Kolby JE, Smith KM, Ramirez SD *et al.* (2015) Rapid response to evaluate the presence of amphibian chytrid fungus (*Batrachochytrium dendrobatidis*) and ranavirus in wild amphibian populations in Madagascar (PLoS ONE). *PLoS ONE*, **10**, 1–21.
Kumar S, Stecher G, Tamura K (2016) MEGA7: Molecular Evolutionary Genetics Analysis Version 7.0 for bigger datasets. *Molecular Biology and Evolution*, **33**, 1870–1874.
Kutz S., Hoberg E., Polley L, Jenkins E. (2005) Global warming is changing the dynamics of Arctic host-parasite systems. *Proceedings of the Royal Society B: Biological Sciences*, **272**, 2571–2576.
Laramie MB, Pilliod DS, Goldberg CS (2015) Characterizing the distribution of an endangered salmonid using environmental DNA analysis. *Biological Conservation*, **183**, 29–37.
Larkin MA, Blackshields G, Brown NP *et al.* (2007) Clustal W and Clustal X version 2.0. *Bioinformatics*, **23**, 2947–2948.
Leitner T, Escanilla D, Franzén C, Uhlén M, Albert J (1996) Accurate reconstruction of a known HIV-1 transmission history by phylogenetic tree analysis. *Proceedings of the National Academy of Sciences*, **93**, 10864–10869.
Lemey P, Rambaut A, Drummond AJ, Suchard MA (2009) Bayesian phylogeography finds its roots. *PLoS Computational Biology*, **5**, e1000520.
Li W, Zhang X, Weng S *et al.* (2014) Virion-associated viral proteins of a Chinese giant salamander (*Andrias davidianus*) iridovirus (genus *Ranavirus*) and functional study of the major capsid protein (MCP). *Veterinary Microbiology*, **172**, 129–139.
Lodge DM, Turner CR, Jerde CL *et al.* (2012) Conservation in a cup of water: Estimating biodiversity and population abundance from environmental DNA. *Molecular Ecology*, **21**, 2555–2558.
Longcore JE, Pessier AP, Nichols DK (1999) *Batrachochytrium dendrobatidis* gen. et sp. nov., a chytrid pathogenic to amphibians. *Mycologia*, **91**, 219–227.
Majji S, LaPatra S, Long SM *et al.* (2006) *Rana catesbeiana* virus Z (RCV-Z): A novel pathogenic ranavirus. *Diseases of Aquatic Organisms*, **73**, 1–11.
Mao J, Hedrick RP, Chinchar VG (1997) Molecular characterization, sequence analysis, and taxonomic position of newly isolated fish iridoviruses. *Virology*, **229**, 212–220.
Martel A, Blooi M, Adriaensen C *et al.* (2014) Recent introduction of a chytrid fungus endangers Western Palearctic salamanders. *Science*, **346**, 630–631.
Martel A, Spitzen-van der Sluijs A, Blooi M *et al.* (2013) *Batrachochytrium salamandrivorans* sp. nov. causes lethal chytridiomycosis in amphibians. *Proceedings of the National Academy of Sciences*, **110**, 15325–15329.
Mazzoni R, De Mesquita AJ, Fleury LFF *et al.* (2009) Mass mortality associated with a frog

virus 3-like Ranavirus infection in farmed tadpoles *Rana catesbeiana* from Brazil. *Diseases of Aquatic Organisms*, **86**, 181–191.
McCallum H, Barlow N, Hone J (2001) How should pathogen transmission be modelled? *Trends in Ecology and Evolution*, **16**, 295–300.
Miller DL, Pessier AP, Hick P, Whittington RJ (2015) Comparative pathology of ranaviruses and diagnostic techniques. In: *Ranaviruses: Lethal Pathogens of Ectothermic Vertebrates* (eds Gray M, Chinchar V), pp. 171–208. Springer, San Diego.
Morrison EA, Garner S, Echaubard P *et al.* (2014) Complete genome analysis of a frog virus 3 (FV3) isolate and sequence comparison with isolates of differing levels of virulence. *Virology Journal*, **11**, 46.
Munro J, Bayley AE, McPherson NJ, Feist SW (2016) Survival of Frog Virus 3 in Freshwater and Sediment from an English Lake. *Journal of Wildlife Diseases*, **52**, 138–142.
Nadin-Davis S, Alnabelseya N, Knowles MK (2017) The phylogeography of Myotis bat-associated rabies viruses across Canada. *PLoS Neglected Tropical Diseases*, **11**, 1–23.
Nutz S, Döll K, Karlovsky P (2011) Determination of the LOQ in real-time PCR by receiver operating characteristic curve analysis: Application to qPCR assays for *Fusarium verticillioides* and *F. proliferatum*. *Analytical and Bioanalytical Chemistry*, **401**, 717–726.
O'Rourke DP (2007) Amphibians used in research and teaching. *ILAR journal / National Research Council, Institute of Laboratory Animal Resources*, **48**, 183–187.
Olson DH, Aanensen DM, Ronnenberg KL *et al.* (2013) Mapping the global emergence of *Batrachochytrium dendrobatidis*, the amphibian chytrid fungus. *PLoS ONE*, **8**.
Picco AM, Brunner JL, Collins JP (2007) Susceptibility of the endangered California tiger salamander, *Ambystoma californiense*, to Ranavirus infection. *Journal of Wildlife Diseases*, **43**, 286–290.
Pilliod DS, Goldberg CS, Arkle RS, Waits LP (2014) Factors influencing detection of eDNA from a stream-dwelling amphibian. *Molecular Ecology Resources*, **14**, 109–116.
Price SJ, Garner TWJ, Nichols RA *et al.* (2014) Collapse of amphibian communities due to an introduced ranavirus. *Current Biology*, **24**, 2586–2591.
Price SJ, Wadia A, Wright ON *et al.* (2017) Screening of a long-term sample set reveals two ranavirus lineages in British herpetofauna. *PloS one*, **12**, e0184768.
R Core Team (2017) *R: A Language and Environment for Statistical Computing.* R Foundation for Statistical Computing, Vienna, Austria. Available from http://www.R-project.org/.
Rees HC, Bishop K, Middleditch DJ *et al.* (2014) The application of eDNA for monitoring of the great crested newt in the UK. *Ecology and Evolution*, **4**, 4023–4032.
Reeve BC, Crespi EJ, Whipps CM, Brunner JL (2013) Natural stressors and ranavirus susceptibility in larval wood frogs (*Rana sylvatica*). *EcoHealth*, **10**, 190–200.
Ridenhour BJ, Storfer AT (2008) Geographically variable selection in *Ambystoma tigrinum* virus (Iridoviridae) throughout the western USA. *Journal of Evolutionary Biology*, **21**, 1151–1159.
Robert J, George E, De Jesús Andino F, Chen G (2011) Waterborne infectivity of the ranavirus frog virus 3 in *Xenopus laevis*. *Virology*, **417**, 410–417.
Rollins-Smith LA (1998) Metamorphosis and the amphibian immune system. *Immunological Reviews*, **166**, 221–230.
Romansic JM, Diez KA, Higashi EM, Johnson JE, Blaustein AR (2009) Effects of the pathogenic water mold *Saprolegnia ferax* on survival of amphibian larvae. *Diseases of Aquatic Organisms*, **83**, 187–193.

Roy BA, Kirchner JW (2000) EVOLUTIONARY DYNAMICS OF PATHOGEN RESISTANCE AND TOLERANCE. *Evolution*, **54**, 51–63.
Saucedo B, Hughes J, Beurden SJ Van *et al.* (2017) Complete genome sequence of frog virus 3, isolated from a strawberry poison frog (*Oophaga pumilio*) imported from Nicaragua into the Netherlands. *Genome Announcements*, **5**, 97–98.
Schloegel LM, Picco AM, Kilpatrick AM *et al.* (2009) Magnitude of the US trade in amphibians and presence of *Batrachochytrium dendrobatidis* and ranavirus infection in imported North American bullfrogs (*Rana catesbeiana*). *Biological Conservation*, **142**, 1420–1426.
Schock DM, Bollinger TK, Collins JP (2009) Mortality rates differ among amphibian populations exposed to three strains of a lethal ranavirus. *EcoHealth*, **6**, 438–448.
Serrao NR, Reid SM, Wilson CC (2017) Establishing detection thresholds for environmental DNA using receiver operator characteristic (ROC) curves. *Conservation Genetics Resources*, 1-8.
Shackelton LA, Rambaut A, Pybus OG, Holmes EC (2006) JC Virus evolution and its association with human populations. *Journal of Virology*, **80**, 9928–9933.
Shepard D (1968) A two-dimensional interpolation function for irregularly-spaced data. *Proceedings of the 1968 23rd ACM national conference*, 517–524.
Singh JS (2002) The biodiversity crisis: A multifaceted review. *Current Science*, **82**, 638–647.
Skerratt LF, Berger L, Speare R *et al.* (2007) Spread of chytridiomycosis has caused the rapid global decline and extinction of frogs. *EcoHealth*, **4**, 125–134.
Song WJ, Qin QW, Qiu J *et al.* (2004) Functional genomics analysis of Singapore grouper iridovirus: complete sequence determination and proteomic analysis, **78**, 12576–12590.
Speare R, Smith JR (1992) An iridovirus-like agent isolated from the ornate burrowing frog Limnodynastes ornatus in northern Australia. *Diseases of Aquatic Organisms*, **14**, 51–57.
Spens J, Evans AR, Halfmaerten D *et al.* (2017) Comparison of capture and storage methods for aqueous macrobial eDNA using an optimized extraction protocol: advantage of enclosed filter. *Methods in Ecology and Evolution*, **8**, 635–645.
Stallknecht DE (2007) Impediments to wildlife disease surveillance, research, and diagnostics. In: *Wildlife and Emerging Zoonotic Diseases: The Biology, Circumstances and Consequences of Cross-Species Transmission* (eds Childs J, Mackenzie J, Richt J), pp. 445–461. Springer.
Stark T, Laurijssens C, Weterings M, et al. (2014) Death in the clouds: ranavirus associated mortality in assemblage of cloud forest amphibians in Nicaragua. *Acta Herpetologica*, **9**, 125–127.
Stöhr AC, López-Bueno A, Blahak S *et al.* (2015) Phylogeny and differentiation of reptilian and amphibian ranaviruses detected in Europe. *PLoS ONE*, **10**, e0118633.
Strand DA, Holst-jensen A, Viljugrein H *et al.* (2011) Detection and quantification of the crayfish plague agent in natural waters : direct monitoring approach for aquatic environments. *Diseases of Aquatic Organisms*, **95**, 9–17.
Stuart SN, Chanson JS, Cox N a *et al.* (2004) Status and trends of amphibian declines and extinctions worldwide. *Science (New York, N.Y.)*, **306**, 1783–1786.
Takahara T, Minamoto T, Doi H (2013) Using environmental DNA to estimate the distribution of an invasive fish species in ponds. *PLoS ONE*, **8**.
Tan WG., Barkman TJ, Gregory Chinchar V, Essani K (2004) Comparative genomic analyses of frog virus 3, type species of the genus *Ranavirus* (family Iridoviridae). *Virology*, **323**, 70–84.

Thurmond MC (2003) Conceptual foundations for infectious disease surveillance. *Journal of Veterinary Diagnostic Investigation*, **15**, 501–514.
Tornabene B, Blaustein AR, Briggs CJ *et al.* (2017) The influence of landscape and environmental factors on ranavirus epidemiology in amphibian assemblages. , **33620**.
Trewby H, Nadin-Davis SA, Real LA, Biek R (2017) Processes underlying rabies virus incursions across US–Canada border as revealed by whole-genome phylogeography. *Emerging Infectious Diseases*, **23**, 1454–1461.
Turner CR, Miller DJ, Coyne KJ, Corush J (2014) Improved methods for capture, extraction, and quantitative assay of environmental DNA from Asian bigheaded carp (*Hypophthalmichthys spp.*). *PLoS ONE*, **9**, 1–20.
Une Y, Sakuma A, Matsueda H, Nakai K, Murakami M (2009) Ranavirus Outbreak in North American bullfrogs (*Rana catesbeiana*), Japan, 2008. *Emerging Infectious Diseases*, **15**, 1146–1147.
Valentini A, Taberlet P, Miaud C *et al.* (2016) Next-generation monitoring of aquatic biodiversity using environmental DNA metabarcoding. *Molecular Ecology*, **25**, 929–942.
Veldhoen N, Hobbs J, Ikonomou G *et al.* (2016) Implementation of novel design features for qPCR-based eDNA assessment. *PLoS ONE*, **11**, e0164907.
Waits LP, Paetkau D (2005) Noninvasive genetic sampling tools for wildlife biologists: a review of applications and recommendations for accurate data collection. *Journal of Wildlife Management*, **69**, 1419–1433.
Walker DM, Leys JE, Dunham KE *et al.* (2017) Methodological considerations for detection of terrestrial small-body salamander eDNA and implications for biodiversity conservation. *Molecular Ecology Resources*, **17**, 1223-1230.
Wallace RG, Fitch WM (2008) Influenza A H5N1 immigration is filtered out at some international borders. *PLoS ONE*, **3**, e1697.
Waltzek TB, Miller DL, Gray MJ *et al.* (2014) New disease records for hatchery- reared sturgeon I. Expansion of frog virus 3 host range into *Scaphirhynchus albus*. *Diseases of Aquatic Organisms*, **111**, 219–227.
Warne RW, Crespi EJ, Brunner JL (2011) Escape from the pond: stress and developmental responses to ranavirus infection in wood frog tadpoles. *Functional Ecology*, **25**, 139–146.
Wheelwright NT, Gray MJ, Hill RD, Miller DL (2014) Sudden mass die-off of a large population of wood frog (*Lithobates sylvaticus*) tadpoles in Maine, USA, likely due to ranavirus. *Herpetological Review*, **45**, 240–242.
Whitfield S, Geerdes E, Chacon I *et al.* (2013) Infection and co-infection by the amphibian chytrid fungus and ranavirus in wild Costa Rican frogs. *Diseases of Aquatic Organisms*, **104**, 173–178.
Wilson IG (1997) Inhibition and facilitation of nucleic acid amplification. *Applied and Environmental Microbiology*, **63**, 3741–3751.
Wilson CC, Wozney KM, Smith CM (2015) Recognizing false positives: Synthetic oligonucleotide controls for environmental DNA surveillance. *Methods in Ecology and Evolution*, 23–29.
Wilson C, Wright E, Bronnenhuber J *et al.* (2014) Tracking ghosts: combined electrofishing and environmental DNA surveillance efforts for Asian carps in Ontario waters of Lake Erie. *Management of Biological Invasions*, **5**, 225–231.
Xu K, Zhu DZ, Wei Y *et al.* (2010) Broad distribution of ranavirus in free-ranging *Rana dybowskii* in Heilongjiang, China. *EcoHealth*, **7**, 18–23.

Yap TA, Koo MS, Ambrose RF, Wake DB, Vredenburg VT (2015) Averting a North American biodiversity crisis. *Science*, **349**, 481–482.
Yutin N, Koonin E V (2012) Hidden evolutionary complexity of nucleo-cytoplasmic large DNA viruses of eukaryotes. *Virol J*, **9**, 161.
Zhang QY, Xiao F, Li ZQ *et al.* (2001) Characterization of an iridovirus from the cultured pig frog *Rana grylio* with lethal syndrome. *Diseases of Aquatic Organisms*, **48**, 27–36.

APPENDIX I

Supplementary Tables and Figures: Chapter 2

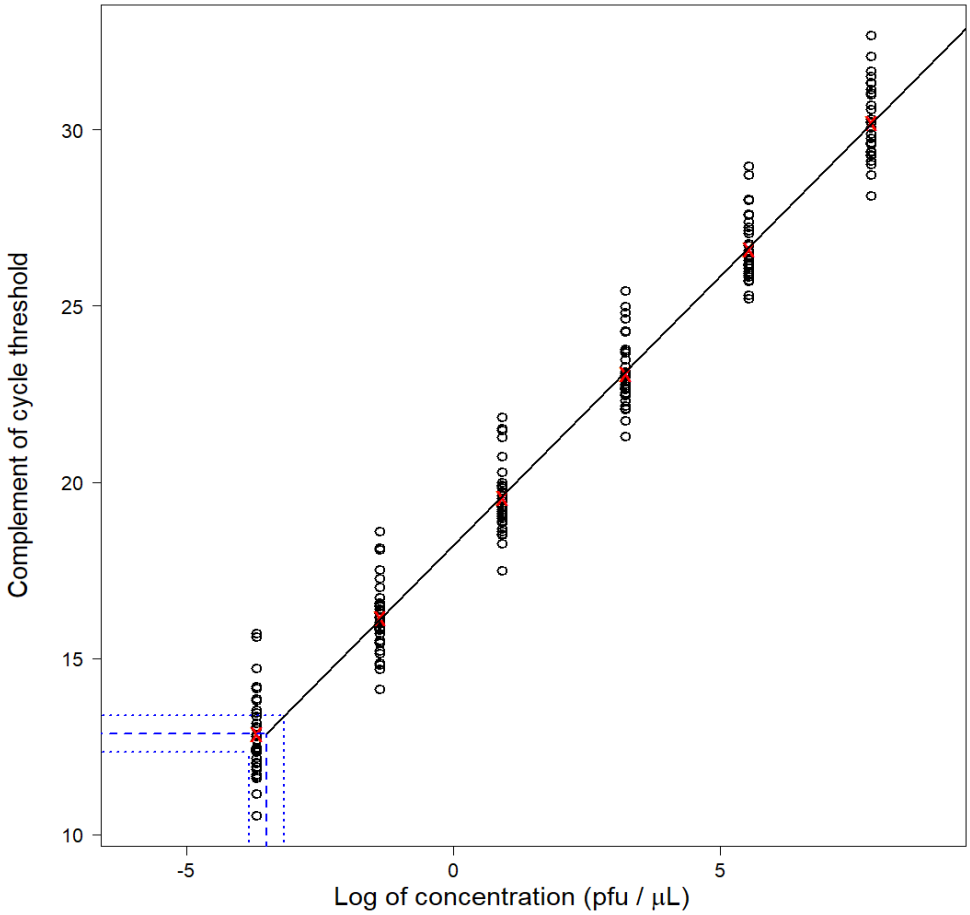

Supplementary Figure S2.1: qPCR-based limit of detection (LOD) assessment of low-concentration DNA. Standards consisted of cultured frog virus 3 in 10-fold serial dilutions from 10^4 to 10^{-1} plaque forming units (pfu/µL) run in duplicate. The y-axis consists of the log of the measured concentrations quantitative PCR cycle threshold (C_t). Red X denotes the average of respective replicates. The blue dashed line represents the concentration plateau, where the point of intersection between the linear standard concentrations (solid line) varies with instrumental response of concentration. The upper and lower 95% confidence limits are represented by the blue dotted lines.

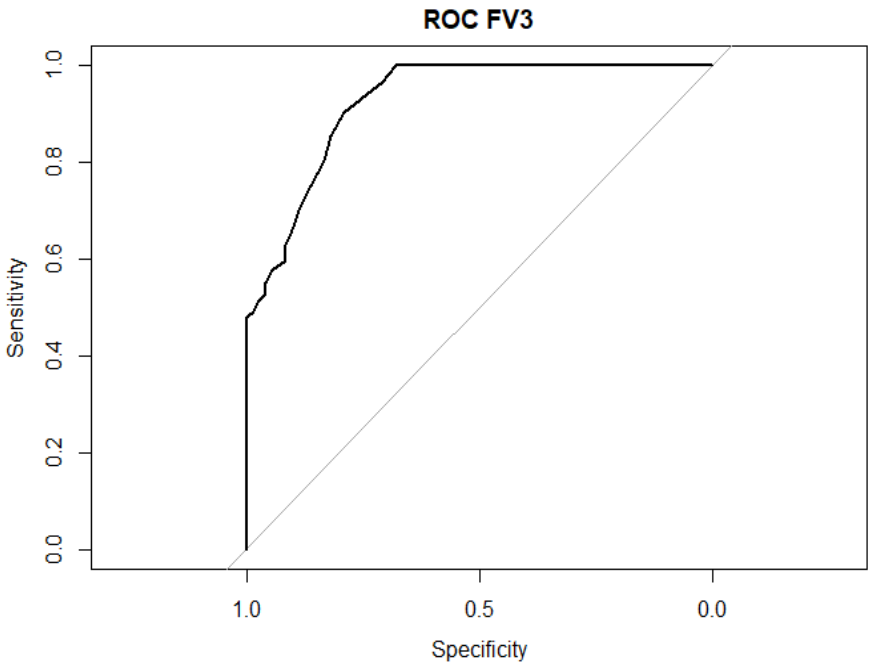

Supplementary Figure S2.2: Receiver operating characteristic (ROC) curve of specificity (x-axis) plotted against sensitivity (y-axis) based on environmental DNA samples tested with qPCR for detectable quantities of ranavirus eDNA from Sterivex capsule samples. The area under the curve (AUC) = 0.927. A total of 627 field samples and 72 negative controls were used to generate the curve.

APPENDIX II

Supplementary Tables and Figures: Chapter 3

Supplementary Table 1.1: Description of FV3-like samples taken across Canada between 2015-2017, including, sampling location, host species, host life stage, and number of samples with given classifications. Homology percentage of genes were based on isolate of highest similarity.

Sample code	Location	Year	Species	Life stage	# samples	Gene	% Homology	Isolate of highest similarity
AMW	Antoinette's pond, NWT	2015	*Lithobates sylvaticus*	Metamorphic	6	MCP	100%	FV3
						vIF-2α	100%	FV3
KAW	KM 190, NWT	2015	*Lithobates sylvaticus*	Adult	3	MCP	99.3%	WBRV (FV3)
						vIF-2α	99.6%	WBRV (FV3)
KTC	KM 190, NWT	2015	*Pseudacris maculata*	Tadpole	10	MCP	99.3%	WBRV (FV3)
						vIF-2α	99.6%	WBRV (FV3)
KTT	KM 190, NWT	2015	*Anaxyrus hemiophrys*	Tadpole	3	MCP	99.3%	WBRV (FV3)
						vIF-2α	99.6%	WBRV (FV3)
KTW	KM 190, NWT	2015	*Lithobates sylvaticus*	Tadpole	5	MCP	99.3%	WBRV (FV3)
						vIF-2α	99.6%	WBRV (FV3)
TAC	Toadlet pond, AB	2015	*Pseudacris maculata*	Adult	3	MCP	99.3%	WBRV (FV3)
						vIF-2α	99.6%	WBRV (FV3)
TAW	Toadlet pond, AB	2015	*Lithobates sylvaticus*	Adult	2	MCP	99.3%	WBRV (FV3)
						vIF-2α	99.6%	WBRV (FV3)
TMC	Toadlet pond, AB	2015	*Pseudacris maculata*	Metamorphic	2	MCP	99.3%	WBRV (FV3)
						vIF-2α	99.6%	WBRV (FV3)
TTW	Toadlet pond, AB	2015	*Lithobates sylvaticus*	Tadpole	6	MCP	99.3%	WBRV (FV3)
						vIF-2α	99.6%	WBRV (FV3)
KEN	Kennedy Drive, ON	2016	*Lithobates clamitans*	Tadpole	6	MCP	100%	FV3
						vIF-2α	99.9%	CGSIV
MOA	Frink Marsh, ON	2016	*Lithobates clamitans*	Tadpole	1	MCP	100%	FV3
						vIF-2α	100%	FV3
STL	Sturgeon road, ON	2016	*Lithobates clamitans*	Tadpole	2	MCP	100%	FV3
						vIF-2α	100%	FV3
TIM	Maley, ON	2016	*Lithobates pipiens*	Adult	1	MCP	100%	FV3
						vIF-2α	100%	FV3
TAW	Toadlet pond, AB	2016	*Lithobates sylvaticus*	Adult	2	MCP	100%	FV3
						vIF-2α	100%	FV3
KAC	KM 190, NWT	2017	*Pseudacris maculata*	Adult	10	MCP	99.3%	WBRV (FV3)
						vIF-2α	99.6%	WBRV (FV3)
KTW	KM 190, NWT	2017	*Lithobates sylvaticus*	Tadpole	2	MCP	100%	FV3
						vIF-2α	100%	FV3
K6AW	KM 196, NWT	2017	*Lithobates sylvaticus*	Adult	1	MCP	99.3%	WBRV (FV3)
						vIF-2α	99.6%	WBRV (FV3)
K6TC	KM 196, NWT	2017	*Pseudacris maculata*	Tadpole	35	MCP	100%	FV3
						vIF-2α	100%	FV3
K6TW	KM 196, NWT	2017	*Lithobates sylvaticus*	Tadpole	19	MCP	100%	FV3
						vIF-2α	100%	FV3
TTW	Toadlet pond, AB	2017	*Lithobates sylvaticus*	Tadpole	7	MCP	100%	FV3
						vIF-2α	100%	FV3
TTC	Toadlet pond, AB	2017	*Pseudacris maculata*	Tadpole	1	MCP	100%	FV3
						vIF-2α	100%	FV3